MONTHLY NOTICES

OF THE

ROYAL ASTRONOMICAL SOCIETY

Vol. 113 No. 5 1953

Published and Sold by the
ROYAL ASTRONOMICAL SOCIETY
BURLINGTON HOUSE
LONDON, W. 1

Price Thirteen Shillings and Sixpence

NOTICE TO AUTHORS

1. *Communications.*—Papers must be communicated to the Society by a Fellow. They should be accompanied by a summary at the *beginning* of the paper conveying briefly the content of the paper, and drawing attention to important new information and to the main conclusions. The summary should be intelligible in itself, without reference to the paper, to a reader with some knowledge of the subject; it should not normally exceed 200 words in length. **Authors are requested to submit MSS. in duplicate. These should be typed using double spacing and leaving a margin of not less than one inch on the left-hand side. Corrections to the MSS. should be made in the text and not in the margin.** Unless a paper reaches the Secretaries more than seven days before a Council meeting it will not normally be considered at that meeting. By Council decision, MSS. of accepted papers are retained by the Society for one year after publication; unless their return is then requested by the author, they are destroyed.

2. *Presentation.*—Authors are allowed considerable latitude, but they are requested to follow the general style and arrangement of *Monthly Notices*. References to literature should be given in the standard form, including a date, for printing either as footnotes or in a numbered list at the end of the paper. Each reference should give the **name and initials** of the author cited, irrespective of the occurrence of the name in the text (some latitude being permissible, however, in the case of an author referring to his own work). The following examples indicate the style of reference appropriate for a paper and a book, respectively :—

A. Corlin, *Zs. f. Astrophys.*, **15**, 239, 1938.
H. Jeffreys, *Theory of Probability*, 2nd edn., section 5.45, p. 258, Oxford, 1948.

3. *Notation.*—For technical astronomical terms, authors should conform closely to the recommendations of Commission 3 of the International Astronomical Union (*Trans. I.A.U.*, Vol. VI, p. 345, 1938). Council has decided to adopt the I.A.U. 3-letter abbreviations for constellations where contraction is desirable (Vol. IV, p. 221, 1932). In general matters, authors should follow the recommendations in *Symbols, Signs and Abbreviations* (London : Royal Society, 1951) except where these conflict with I.A.U. practice.

4. *Diagrams.*—**These should be designed to appear upright on the page, drawn about twice the size required in print and prepared for direct photographic reproduction except for the lettering, which should be inserted in pencil. Legends should be given in the manuscript indicating where in the text the figure should appear.** Blocks are retained by the Society for 10 years; unless the author requires them before the end of this period they are then destroyed.

5. *Tables.*—**These should be arranged so that they can be printed upright on the page.**

6. *Proofs.*—Costs of alterations exceeding 5 per cent of composition must be borne by the author. Fellows are warned that such costs have risen sharply in recent years, and it is in their own and the Society's interests to seek the maximum conciseness and simplification of symbols and equations consistent with clarity.

7. *Revised Manuscripts.*—When papers are submitted in revised form it is especially requested that they be accompanied by the original MSS.

Reading of Papers at Meetings

8. When submitting papers authors are requested to indicate whether they will be willing and able to read the paper at the next or some subsequent meeting, and approximately how long they would like to be allotted for speaking.

9. Postcards giving the programme of each meeting are issued some days before the meeting concerned. Fellows wishing to receive such cards whether for Ordinary Meetings or for the Geophysical Discussions or both should notify the Assistant Secretary.

MONTHLY NOTICES

OF THE

ROYAL ASTRONOMICAL SOCIETY

Vol. 113 No. 5

MEETING OF 1953 MAY 8

Professor H. Dingle, Vice-President, in the Chair

The election by the Council of the following Fellows was duly confirmed :—

Francis Parry Beech, National Provincial Bank, Ltd., Wolverhampton (proposed by W. M. Smart);

John Joseph Bennett, Windermere Hotel, South Kenton, Wembley, Middlesex (proposed by W. H. Julian);

Anthony McLoughlin, Ariston Gold Mines, Ltd., Prestea, Gold Coast, West Africa (proposed by S. W. R. Mottram);

Anthony Seymour Laughton, M.A., King's College, Cambridge (proposed by M. N. Hill);

Denzil Taylor Smith, B.Sc., F.G.S., Royal College of Science, South Kensington, London, S.W.7 (proposed by J. McG. Bruckshaw); and

Edmund Gardner Williams, M.A., F.R.I.C., 10 Glen Aber Park, Hough Green, Chester (proposed by R. M. Baum).

The election by the Council of the following Junior Member was duly confirmed :—

Herman Lawrence Helfer, Yerkes Observatory, Williams Bay, Wisconsin, U.S.A. (proposed by S. Chandrasekhar).

Eighty-four presents were announced as having been received since the last meeting, including :—

George G. Hoehne, *Practical celestial air navigation tables, Vol. II: Latitudes 20° to 39° north* (presented by D. H. Sadler);

P. J. van Rhijn, *Durchmusterung of Selected Areas of the special plan, Vols. I and II* (presented by the Kapteyn Astronomical Laboratory); and

Specola Vaticana, *Astrographic Charts* (presented by the Specola Vaticana).

After one paper had been read, the Meeting was adjourned until the return from Greenwich of the George Darwin Lecturer and members of Council who had attended the opening of the Octagon Room at the Royal Observatory by H.R.H. The Duke of Edinburgh. The Meeting was resumed under the chairmanship of the President, Dr J. Jackson.

Dr Edwin P. Hubble delivered the George Darwin Lecture on " The law of red shifts ".*

* Delivery of the MS. of this Lecture has been delayed by Dr Hubble's death. The text will appear in a later issue of *M.N.*

ADDITIONAL MEETING OF 1953 JULY 22

in the Stephenson Building of King's College,
Newcastle upon Tyne (University of Durham).

Dr J. Jackson, President, in the Chair

The President announced that this Additional Meeting was the sixth to take place outside the rooms of the Society in London. He expressed the thanks of the Society to the Vice-Chancellor of the University of Durham and the Professor of Engineering, by whose courtesy the meetings were being held in the Stephenson Building. The thanks of the Society were also extended to the Registrar of King's College, and to the Wardens of the University Halls, where accommodation had been provided for Fellows participating in the Meetings. In particular the President thanked the President (Professor G. R. Goldsbrough) and the Secretary (Mr Raymond Fallaw) of the Newcastle upon Tyne Astronomical Society, who had undertaken so many of the duties of organization of the Meetings and the associated activities.

One hundred and eighty-four presents were announced as having been received since the last Meeting, including :—

F. Baldet and G. d'Obaldia, *Catalogue générale des orbites des comètes* (presented by the Centre Nationale de Recherches Scientifiques);

International Seismological Summary (presented by the International Union of Geodesy and Geophysics);

S. Herrick, *Tables for rocket and comet orbits* (presented by the National Bureau of Standards); and

Atlas of magnetic declinations of Europe for epoch 1944–1945 (presented by the U.S. Army Map Service).

A number of Fellows signed the Admission Book. Papers were read by Dr F. D. Kahn, Dr R. Wilson and Mr D. G. Ewart. An account of a paper by Dr P. Swings, Dr A. McKellar and Mr K. N. Rao was given by Dr A. Hunter.

Other Meetings and activities in connection with the Society's visit to Newcastle upon Tyne included a reception on the evening of July 20 by the Vice-Chancellor of the University of Durham in the Hatton Gallery, where a special Exhibition had been arranged by the Professor and the Department of Fine Arts of the University. An Astronomical Colloquium on the Design of Astronomical Instruments was held on July 21, and on the evening of the same day a Public Lecture, entitled " The Origin of the Earth ", was given by Professor W. M. Smart at the Newcastle upon Tyne Royal Grammar School. A Geophysical Discussion was held on July 23. Visits to places of local interest included an excursion to the Roman Wall under the expert guidance of Professor I. A. Richmond; and another to Durham where the party was conducted over the Castle by the Master of University College, and over the Cathedral and its library by the Dean of Durham. The Chairman and Secretary of the Tyne Improvement Commission invited Fellows to tour the river in the Tyne Commissioners' launch; and Mr G. M. Sisson and the Directors of C. A. Parsons & Co. and Sir Howard Grubb, Parsons & Co. Ltd. welcomed a large party to tour their workshops and factories.

MEETING OF 1953 OCTOBER 9

Dr J. Jackson, President, in the Chair

The President announced that the deaths had taken place of two Associates of the Society—Dr Edwin P. Hubble and Professor Armin Leuschner. He paid a brief tribute to their memory, the Fellows standing. Referring to Dr Hubble, the President said :—

" As Dr Hubble delivered the George Darwin Lecture here only a few months ago the news of his sudden death has come to us as a shock. He will go down to history as one of the most distinguished astronomical observers of all time. His skill as an observer was matched by his foresight in selecting programmes, some dealing with problems which had been long outstanding, others with problems just coming to light. It was his good fortune, as well as that of our science, that the great telescopes required for these problems were available to him. His work on the nebulae will cause his name to be linked with that of Herschel, who preceded him by more than a century."

The election by the Council of the following Fellows was duly confirmed :—

Peter H. Dunkley Andrews, 183 Beehive Lane, Ilford, Essex (proposed by A. Hunter);

Goldwin Howland Biggar, B.Sc., Hydrographic Department of the Admiralty, Oxgate Lane, Cricklewood, London, N.W.2 (proposed by V. C. A. Ferraro);

George A. Davis, Jr., 15 Anderson Place, Buffalo City 22, New York, U.S.A. (proposed by Harlow Shapley);

Miss Guro Gjellestad, The University, Blindern, Oslo, Norway (proposed by S. Chandrasekhar);

Eric Robert Reginald Holmberg, Department of Operational Research, The Admiralty, Whitehall, London, S.W.1 (proposed by E. C. Bullard); and

Albert G. Wilson, Mount Wilson and Palomar Observatories, Pasadena 4, California, U.S.A. (proposed by F. Hoyle).

One hundred and sixty presents were announced as having been received since the last Meeting, including :—

Patrick Moore, *Guide to the Moon* (presented by the author); and
Kenneth Heuer, *The End of the World* (presented by the author).

ON THE RELATION BETWEEN DISTANCE AND INTENSITY FOR INTERSTELLAR CALCIUM AND SODIUM LINES

C. S. Beals and J. B. Oke

(Received 1953 February 16)

Summary

The results of spectrophotometric measurements of the intensities of the interstellar K and D lines carried out at the Dominion Astrophysical Observatory in the period 1928–1946 are presented in tabular form. The data relate to 1 055 medium-dispersion spectra of 182 stars, mostly of O and early B types, and include also measures of radial velocity for stellar and interstellar lines in most of the stars.

The interstellar intensities are correlated with stellar distance, a variety of criteria being used for estimating the latter, including trigonometric parallaxes, parallactic motions, luminosities of eclipsing binaries, spectroscopic absolute magnitudes, cluster parallaxes and galactic rotation effects. The various criteria are weighted according to the intrinsic reliability of each method and to the number of stars concerned. The distance–intensity relations best satisfying the observations are :

$$r = 34{\cdot}83K = 30{\cdot}75D,$$

where r is the distance in parsecs, K the equivalent width of the calcium K line in km/sec and D the mean equivalent width of the sodium lines D_1 and D_2 in km/sec. Distances assigned to individual stars by using these relations should rarely be more than 25 per cent in error. The scatter is attributed to irregularity in distribution of the discrete clouds of interstellar gas and to uncertainties in the distance estimates. The distance–intensity relations found are compared with those of other observers.

---

1. *Introduction.*—Ever since the first definite identification of gases in interstellar space it has been recognized that interstellar lines would be expected to increase in intensity with distance, and preliminary studies using eye estimates by Struve* and by Plaskett and Pearce† indicated that this was indeed the case. Since then, precise spectrophotometry of interstellar lines has been undertaken at a number of observatories, and graphs or equations relating distance to interstellar line intensity have been published by Williams‡, Merrill§, Sanford‖, Evans¶, van Rhijn** and Beals.†† The purpose of this paper is to present the results of observations of interstellar lines made at the Dominion Astrophysical Observatory during the period 1928–1946 and to compare them with the results of other observers in the hope of getting a reasonably clear picture of the relationship between the intensity of interstellar lines and the distances of the stars in whose spectra they appear.

* O. Struve, *Ap. J.*, **67**, 353, 1928.
† J. A. Pearce, *P. Dom. Ap. O.*, **5**, 167, 1935.
‡ E. G. Williams, *Ap. J.*, **79**, 280, 1934.
§ P. W. Merrill, *Ap. J.*, **86**, 28, 1937.
‖ R. F. Sanford, *Ap. J.*, **86**, 136, 1937.
¶ J. W. Evans, *Ap. J.*, **93**, 275, 1941.
** P. J. van Rhijn, *P. Groningen*, No. 50, p. 21, 1946.
†† C. S. Beals, *P. Dom. Ap. O.*, **6**, 333, 1937.

2. *Observational methods.*—The majority of the observations on which this study is based are of O and Bo stars, and although there are some objects of later type, very few of them are later than B2. This should minimize the effect of blends with stellar calcium lines which are often present as faint lines even in early B-type stars. Most of the spectra were of medium dispersion, 20 and 35 A per mm for *H* and *K* and 31 A per mm for the sodium *D* lines. A single prism was ordinarily used for the calcium lines, but three prisms were required to give comparable dispersion in the region of sodium *D*. A few spectra were secured with dispersions of 4·5 to 6·3 A per mm with three prisms at *K*, while a second-order grating, yielding dispersions of 5·0 to 7·0 A per mm, was used for some of the brighter stars in the *D* region. The calcium *H* line is almost always blended with Hε to some extent, and on single-prism spectrograms it is rare that the two lines are separated clearly enough to yield reliable interstellar intensities. If three-prism dispersion is used, especially if the hydrogen lines are broad and shallow, the calcium *H* line can be measured with sufficient precision, but on many of the single-prism spectra no attempt has been made to derive intensities for this line. The difficulties of measurement are illustrated in the tracing of BD 35° 3955 in Fig. 2.

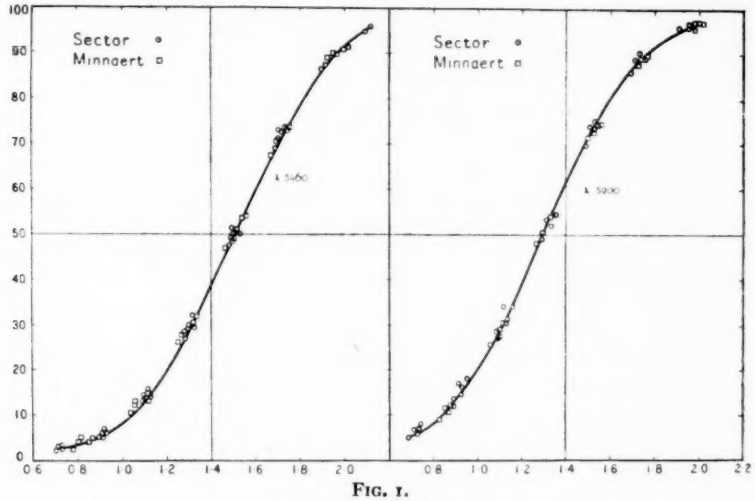

FIG. 1.

Ordinates: Deflection.
Abscissae: Log intensity.

The plates were calibrated by means of a neutral-tint wedge or a rapidly rotating sector placed close to the slit, and care was taken to see that the exposure times of the calibration and the stellar spectra were comparable. An account of the calibration of the wedge has been given elsewhere.* The sector was used for a majority of the plates. It was run at a speed of 100 revolutions per second, and numerous comparisons were made with other methods of calibration to test its validity as a calibration device. Some of these tests have already been published by Petrie and McKellar†, who compared the sector with a step-slit. Additional tests in a number of wave-length regions have been made by

* C. S. Beals, *P. Dom. Ap. O.*, **6**, 96, 1933.
† R. M. Petrie and A. McKellar, *Jour. R.A.S.Can.*, **31**, 130, 1937.

comparing the sector with a step-weakener calibrated by Professor Minnaert of Utrecht and loaned to the Dominion Astrophysical Observatory for a few months. Such tests for two wave-lengths in the visible region are illustrated in Fig. 1. Here are shown two calibration curves, each derived from five plates. Each plate had a sector and a step-weakener calibration impressed upon it. Separate curves were plotted for each plate and combined by displacing them

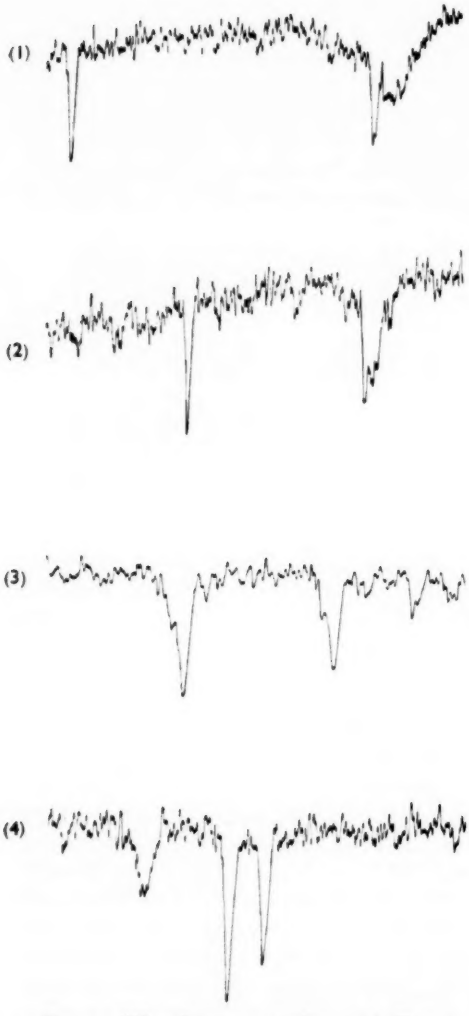

FIG. 2.—*Microphotometer tracings.* (1) *H and K, HD* 191201, (2) *H and K,* 35° 3955, (3) *Sodium D lines showing complex structure, HD* 37742, (4) *Sodium D lines with helium* D_3, *HD* 14818.

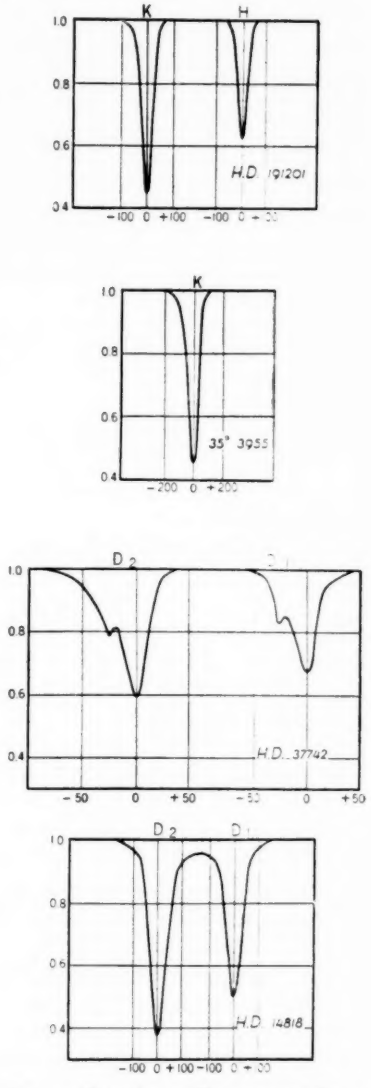

FIG. 3.—*Intensity profiles corresponding to the tracings of Fig.* 2.
Ordinates: Intensity.
Abscissae: Line width, km/sec.

horizontally till they coincided at the middle of the straight line portion of the curve. The squares represent the readings from the step-weakener, while the open circles are those from the sector. It will be seen that one curve represents both sets of points equally well. Similar tests were made for numerous other wave-length regions, and in no case was it possible clearly to distinguish a difference between the shapes of the calibration curves due to the two methods. The principal advantage of the sector is that its relatively large diameter of three inches makes it possible to divide the angles and to cut the steps in a sufficiently precise ratio, one to the other, so that in using the calibration it is not necessary to distinguish between the various steps, since all the steps will be equal. In so far as we are aware this is not possible with any other type of calibration device using steps.*

Most of the spectra were analysed with the Victoria microphotometer†, which has been described elsewhere, although some use was made of the Moll microphotometer at Ottawa modified to use a photoelectric cell as a sensitive element. Many of the tracings were reduced with the aid of the semi-automatic intensitometer‡ of the Dominion Astrophysical Observatory. Intensities were derived as equivalent widths in km/sec, and were obtained by integrating the area under the continuous spectrum by means of a planimeter. Specimen tracings and profiles are illustrated in Figs. 2 and 3.

3. *Observational data.*—The observational data refer to 182 stars. Calcium lines have been observed for 173 and sodium lines for 93. The total number of spectra was 1 055, making an average of 3·9 for each value of intensity. The number of stars for which both sodium and calcium have been observed is 84.

Radial velocities for practically all the stars and most of the calcium lines are available from the data of Plaskett and Pearce, although numerous additional measures have been made during the present study. Dr R. M. Petrie of Victoria has kindly supplied us with the velocities of a number of stars for which he has determined spectroscopic parallaxes. Many of the sodium line velocities have been measured by Mr John O'Connor of the Dominion Observatory.

The measures of intensity and radial velocity are collected in Table I. Column 1 contains the Henry Draper number or other designation of the star; columns 2 and 3 give the right ascensions and declinations; the magnitudes and spectral types of the stars are given together in column 4, while intensity data, equivalent widths in km/sec, with the number of plates for each star in brackets, are given in columns 5, 6, 7 and 8. The calcium and sodium interstellar velocities in km/sec, with the weighted means, are presented in columns 9, 10 and 11, while the stellar velocity is shown in column 12.

4. *Criteria of stellar distance.*—For such relatively distant objects as are involved in studies of interstellar matter there is a good deal of uncertainty about estimates of distance and it would appear reasonable to use as many different criteria of distance as possible in setting up a distance–intensity graph. The various criteria used in this paper are outlined under a number of separate headings below.

* E.g., in a step-slit the successive increments in width are so small that it is mechanically impossible to make them exactly equal.

† C. S. Beals, *M.N.*, **96**, 730, 1936.

‡ C. S. Beals, *Jour. R.A.S.Can.*, **38**, 65, 1944.

TABLE I

Star HD	R.A. 1900	Dec. 1900	Mag., Type	Interstellar line intensity Ca 3933	Ca 3968	Na 5889	Na 5896	Interstellar velocity Ca	Na	Mean	Stellar velocity
	h m	° ′									
108	00 00·9	63 07	7·36, O6fq	36·2 (13)	30·8 (1)	44·3 (9)	39·7 (9)	−20·4	−11·1	−15·7	−62·8
698	00 06·3	57 39	7·08, B6	19·8 (3)				−13·9			
886	00 08·1	14 38	2·87, B2s	34·3 (2)				− 0·1*		− 0·1	+ 5·0
1337	00 12·5	50 53	6·12, O8n	35·5 (10)		49·8 (6)	37·4 (6)	−22·8	−18·5	−22·4	−37·1
2083	00 20·0	71 15	6·94, Bo	25·3 (3)		35·6 (2)	24·4 (2)	−10·5	−06·2	−09·3	−05·2
2905	00 27·3	62 23	4·24, Bo	28·1 (3)		37·7 (1)	35·7 (1)	−16·4		−16·4	−04·7
3950	00 37·0	51 48	6·93, Bo	37·2 (2)				−14·6		−14·6	−92·5
5005	00 47·0	56 05	7·7, O6	53·5 (3)				−18·9		−18·9	−21·1
9311	01 26·6	60 10	7·26, B5	41·9 (1)				−32·3		−32·3	−38·1
9974	01 32·4	57 39	10, WN5	45·1 (3)	54·6 (3)			−26·0		−26·0	
10516	01 37·4	50 11	4·19, Bone	13·8 (3)				+02·8		+02·8	+01·4
11415	01 47·2	63 11	3·44, B5s	19·8 (2)				− 8·5*		− 8·5	− 8·1
12953	02 01·7	57 57	5·90, A2p	70·8 (3)		61·2 (1)	48·8 (1)	−38·4	−26·5	−34·4	
13841	02 09·8	56 34	7·21, B2s	55·0 (6)		67·2 (2)	53·5 (2)	−32·0	−22·1	−29·5	−39·4
13854	02 09·9	56 36	6·42, Bos	58·8 (7)		57·3 (3)	49·4 (3)	−27·5	−19·7	−25·9	−40·0
14134	02 12·1	56 40	6·66, B2s	68·4 (7)		66·3 (2)	57·2 (2)	−34·5	−20·0	−31·6	−43·4
14143	02 12·2	56 43	6·66, B1s	61·0 (9)		78·2 (2)	67·2 (2)	−33·1	−27·5	−32·2	−45·2
14489	02 15·3	55 23	5·22, A2p	69·4 (1)				−21·9		−21·9	
14633	02 16·7	41 02	7·7, O8	36·6 (13)	25·6 (1)	24·5 (1)	15·4 (1)	−14·7	+03·9	−12·6	−39·5
14818	02 18·2	56 10	6·24, B1s	60·8 (7)		53·5 (9)	45·0 (9)	−29·3	−13·0	−22·3	−47·0
14947	02 19·5	58 25	8·04, O5f	37·8 (2)				−26·3		−26·3	−53·7
14956	02 19·6	57 14	7·32, B1s	49·4 (6)				−25·7		−25·7	−30·3
15497	02 24·6	57 15	7·20, B7s	45·0 (1)				−36·7*		−36·7	−35·4
16691	02 35·5	56 28	8·4, O6f	52·5 (2)		50·9 (1)	53·4 (1)	−18·1	−24·3	−19·3	−40·8
17505	02 43·4	60 01	7·11, O7	47·5 (5)		44·5 (4)	38·9 (4)	−18·2	−05·6	−14·0	−16·8
19820	03 06·2	59 11	7·09, O8n	29·5 (2)		32·1 (1)	33·3 (1)	−14·6	−02·0	−13·7	−04·2
20365	03 11·5	49 51	5·30, B3	18·3 (1)				− 4·4*		− 4·4	− 5·1
20418	03 12·0	49 43	5·08, B3	10·7 (1)				+ 3·5*		+ 3·5	+ 3·0
21389	03 21·9	58 32	4·76, Aop	61·8 (4)				−06·4		−06·4	
21428	03 22·2	49 10	4·67, B5	16·8 (2)				−10·2*		−10·2	− 0·8
22253	03 29·9	56 23	6·79, B1n	15·5 (2)				−05·4		−05·4	+04·8
23180	03 38·0	31 58	3·94, B2	10·9 (8)				+12·4		+12·4	+18·5
23675	03 41·9	52 21	6·76, Bo	30·0 (2)		37·3 (2)	33·8 (2)	+00·1	+00·3	+00·1	−01·9
24398	03 47·8	31 35	2·91, B1s	24 (1)		21·8 (2)	10·9 (2)	+02·9	+25·2	+17·8	+21·0
24431	03 48·1	52 21	6·70, O8	29·0 (3)		43·3 (1)	33·5 (1)	−02·3		−02·3	−08·6

*Believed blended with stellar line.

24760	03 51·1	39 43	2·96, B2	6·1 (1)				+ 9·1			− 6·0
24912	03 52·5	35 30	4·05, O7n	12·4 (22)	05·5 (3)	20·0 (13)	15·9 (13)	−14·5	+12·6	−10·0	+67·4
25443	03 57·4	61 48	6·75, Bo			33·4 (1)	26·6 (1)	−04·0	−01·3	−03·1	−01·6
25638	03 59·4	62 04	7·04, Bon	23·0 (3)				−07·4		−07·4	+11·0
25639	03 59·1	62 04	7·07, Bon	27·0 (1)				−08·2		−08·2	−12·8
25833	04 00·6	33 11	6·61, B3	18·3 (2)				+11·7		+11·7	+15·8
25940	04 01·4	47 27	4·03, B3e	9·1 (1)				+ 4·9*		+ 4·9	+ 4·0
28446	04 24·1	53 42	5·42, B1	20 (1)				+01·3		+01·3	
29376	04 32·5	07 07	6·89, B5	27·4 (6)				+21		+21	+38·2
29763	04 36·2	22 46	4·33, B5n	19·0 (1)				+17·0*		+17·0	+13·6
30614	04 44·1	66 10	4·38, O9se	28·5 (5)		32·7 (10)	27·8 (10)	−06·0	−05·7	−06·0	+06·0
30836	04 45·9	05 26	3·78, B2s	16·0 (7)	18·2 (1)	15·6 (1)	6·2 (1)	+16·3*	+24·1	+20·9	+23·3
31237	04 49·0	02 17	3·87, B2s	15·6 (7)		20·3 (1)	10·9 (1)	+ 8·1*	+23·1		+24·2
33328	05 04·4	−08 53	4·34, B3n					+12			+ 3·0
34078	05 09·7	34 12	5·81, O9ss	12·1 (1)				+12·8		+12·8	+59·3
34333	05 11·6	36 31		27·4 (6)				+12·7			
34656	05 14·0	37 20	6·71, O6se	20·3 (4)	11·5 (1)	35·6 (1)	29·3 (1)	+03·6	+05·8	+04·2	−00·4
35039	05 16·7	−00 29	4·65, B3	14·5 (2)				+10·4*		+10·4	+28·8
35411	05 19·4	−02 29	3·44, Bo	9·9 (2)				+10·8*		+10·8	+19·5
35468	05 19·8	06 16	1·70, B2s	8·4 (2)				+21·6*		+21·6	+18·0
35715	05 21·6	03 00	4·66, B2	7·6 (3)				+19·7		+19·7	+12·0
35921	05 23·0	35 18	6·71, O9	26·5 (2)				+07·4		+07·4	−18·9
36267	05 25·4	05 52	4·32, B4n	9·1 (2)				+19·0*			+20·7
36486	05 26·9	−00 22	2·48, Bo	3·5 (9)	1·8 (6)	6·5 (1)	4·6 (1)	+15·7	+16·0	+15·7	+19·9
36822	05 29·3	09 25	4·53, Boss	18·3 (2)				+16·5			+33·2
36861	05 29·6	09 52	3·66, O8s	17·6 (6)		18·2 (6)	14·0 (6)	+13·3	+24·8	+16·2	+34·8
37043	05 30·5	−05 59	2·87, O8s	5·7 (7)	3·5 (4)	7·2 (5)	5·4 (5)	+29·9	+10·2	+26·0	+21·5
37128	05 31·1	−01 16	1·75, Bo	9·1 (10)	4·4 (7)	17·0 (9)	10·5 (9)	+18·5	+17·4	+18·1	+25·8
37468	05 33·7	−02 39	3·78, Bo	6·3 (1)				+16·3		+16·3	+27·8
37742	05 35·7	−02 00	2·05, Bon	8·2 (6)	4·5 (4)	16·2 (9)	10·8 (9)	+11·2	+22·0	+13·8	+19·0
37756	05 35·8	−01 11	5·00, B3	12·2 (3)				+13·9			+26·1
41161	05 58·2	48 15	6·51, O9n	19·2 (5)	15·8 (3)	29·5 (2)	23·8 (2)	+09·2	+06·2	+08·4	+05
41398	05 59·8	28 56	7·45, Bo	45·5 (1)				+06·0		+06·0	+17·1
42088	06 03·7	20 31	7·40, O6	19·9 (1)	16·1 (1)			+09·7		+09·7	+24·1
42560	06 06·3	14 14	4·35, B3nn	15·2 (2)				+10·0*			+24·0
43818	06 13·2	23 30	7·03, Bos	26·2 (2)		32· (1)	35· (1)	+12·5	+07·2	+11·2	+18·2
45542	06 23·0	20 17	4·06, B5ne	19·8 (2)				+18·0*		+18·0	+38·4
45910	06 27·2	05 57	6·70, B3eq	25·6 (3)		59·5 (1)	43·0 (1)	+20		+20	
46149	06 26·6	05 06	7·66, O8	19·3 (1)				+17·1		+17·1	+38·9

* Believed blended with stellar line.

TABLE 1 (*cont.*)

Star HD	R.A. 1900	Dec. 1900	Mag., Type	Interstellar line intensity Ca 3933	Ca 3968	Na 5889	Na 5896	Interstellar velocity Ca	Na	Mean	Stellar velocity
	h m	° ′									
46150	06 26·6	05 00	6·80, O6	23·3 (3)	16·4 (1)	26·2 (1)	33·1 (1)	+18·5	+23·9	+19·8	+35·9
46223	06 27·0	04 53	7·14, O8	22·4 (2)	16·2 (1)	36·2 (1)	25·1 (1)	+16·4	+24·4	+17·7	+42·2
46966	06 31·1	06 10	7·3, O8	29·9 (3)		37·2 (1)	26·5 (1)	+14·0	+30·2	+16·3	+42·3
47129	06 32·0	06 13	6·06, O8e	26·4 (6)		36·1 (2)	36·1 (2)	+16·0		+16·0	+23·9
47432	06 33·5	01 42	6·13, Bo	23·6 (4)	15·1 (1)			+21·6		+21·6	+49·0
47755	06 35·1	09 53	8·12, B4	24·4 (4)							
47839	06 35·5	09 59	4·68, O7s	17·4 (9)	8·3 (3)	16·8 (3)	10·0 (3)	+13·6	+17·2	+14·5	+33·4
48099	06 36·6	06 27	6·20, O7	30·4 (4)		47·4 (3)	39·0 (3)	+14·3	+09·3	+12·6	+30·8
48434	06 38·3	04 02	5·78, Bo	25·1 (3)		40·6 (2)	34·8 (2)	+19·2	+23·0	+20·3	+34·5
54662	07 04·6	−10 11	6·20, O7	19·4 (6)	11·4 (1)			+29·5		+29·5	+63·0
55879	07 09·7	−10 08	5·99, O9s	11·3 (3)				+28·6		+28·6	+31·9
60848	07 31·4	17 07	7·7, O7ne	17·3 (1)				+13·1	+15·8	+13·5	+28·1
91316	10 27·5	09 49	3·85, Bos	7·8 (18)	3·0 (13)	11·6 (17)	5·7 (17)	+07·4	−02·2	+05·3	+42·2
104337	11 55·7	−19 06	5·28, B3	7·6 (2)				−12·9*		−12·9	+ 1·7
109387	12 29·2	70 20	3·88, B5e	3·8 (2)				−11·5		−11·5	−11·4
116658	13 19·9	−10 38	1·21, B2	2·3 (2)				+13·9*		+13·9	+ 1·6
144217	15 59·6	−19 32	2·90, B2	3·0 (1)				−13·0		−13·0	− 9·3
144218	15 59·6	−19 32	5·06, B3	9·1 (2)				−23·9*		−23·9	− 4·3
149757	16 31·7	−10 22	2·70, Bonn	7·0 (9)	4·2 (6)	13·2 (5)	11·6 (5)	−10·8		−10·8	−18·9
149881	16 32·4	14 40	6·59, B2	28·9 (7)				−16·3		−16·3	+18·2
166182	18 04·4	20 48	4·32, B2s	18·4 (4)		13·3 (2)	8·1 (2)	−19·9	−24·2	−20·9	−13·0
168957	18 17·3	25 01	6·86, B3e	25·8 (4)				−17·2		−17·2	−41·2
169454	18 19·6	−14 02	6·84, Bo	65·1 (6)				−01·0	+22·6	+03·7	
170650	18 25·5	23 48	5·72, B5			15·0 (1)	12·8 (1)	−18·7	−09·3	−17·5	−17·3
175227	18 49·3	24 09	8·4, B5, B4	10·7 (5)				−21·1		−21·1	
180554	19 11·9	21 13	4·60, B5n	16·0 (2)				−14·0*		−14·0	−17·4
181987	19 17·5	25 23	7·3 to 8·3, B4, B6	16·8 (3)				−25·6*		−25·6	−15·1
183143	19 23·0	18 05	6·93, B8s			43·5 (3)	34·3 (3)		+03·4	+03·4	+13·0
184915	19 31·5	−07 15	5·04, Bon	18·0 (2)	7·4 (2)	21·6 (4)	15·7 (4)	−05·1	−16·2	−08·8	−22·5
185859	19 36·1	20 15	6·44, Bo	33·2 (4)		28·0 (2)	19·8 (2)	−05·2	−00·2	−03·5	+05·6
186745	19 41·2	23 41	7·0, B8	54·9 (1)				−13·8		−13·8	
186980	19 42·4	31 52	7·28, O8	27·2 (4)		43·1 (4)	43·1 (4)	−13·5	−07·2	−11·0	+04·2
187459	19 45·0	33 12	6·35, Bon	25·9 (4)		35·1 (3)	24·6 (3)	−12·3	+03·6	−09·9	−10
187879	19 47·2	40 20	5·62, B2	9·1 (3)				−17·4			− 6·2

* Believed blended with stellar line.

188001	19 47·9	18 25	6 29, O7f	26·4 (4)	24·0 (1)	29·1 (8)	29·1 (8)	−05·0	−05·9	−05·4	+11·1
188209	19 49·0	46 47	5·51, O8s	26·9 (4)		35·2 (3)	32·2 (3)	−07·3	−13·1	−09·0	−04·7
190066	19 58·1	21 52	6·55, Bos	30·3 (2)		32·1 (2)	28·4 (2)	−05·1	−02·2	−04·3	+16·1
190429N	19 59·8	35 45	7·2, O5nf	52·4 (7)		79·7 (3)	80·0 (3)	−14·8	−01·1	−12·1	−16·7
190429S	19 59·8	35 45	7·5, O9n	47·8 (5)		53·3 (1)	51·0 (1)	−14·5	−01·4	−13·0	−05·8
190603	20 00·7	31 56	5·69, Boss	43·7 (5)		45·6 (5)	41·4 (3)	−13·8	−09·2	−12·9	+18·0
190864	20 01·9	35 19	8·2, O6f	56·3 (3)				−14·3		−14·3	+02·8
190918	20 02·2	35 31	7·01, O9, WN5	49·2 (5)	29·0 (3)	55 (1)	44 (1)	−16·7	+02·5	−10·9	−10·2
190919	20 02·2	35 24	7·30, B1s	45·2 (3)		57·3 (1)	28·9 (1)	−15·2		−15·2	−21·6
+35°3955	20 02·2	35 31	7·8, B1	46·9 (3)				−14·8		−14·8	−08·8
190967	20 02·4	35 06	7·9, B1	45·0 (5)				−14·1		−14·1	
191201	20 03·6	35 26	7·12, Bo	32·6 (5)	16·6 (2)	55·8 (2)	51·4 (2)	−13·3	+00·8	−12·4	−05·4
191566	20 05·5	35 11	8·7, B2	42·5 (1)				−17·5		−17·5	−45
191765	20 06·5	35 53	7·80, WN6	37·3 (8)	28·3 (7)			−14·3		−14·3	
+35°4000	20 06·5	35 54	8·6, B4	33·0 (1)				−12·0		−12·0	
191877	20 07·0	21 35	6·11, Bo	25·1 (3)	11·2 (1)	32·3 (3)	24·3 (3)	−06·2	−00·0	−05·0	−18·4
192103	20 08·1	35 54	7·94, WC9	41·0 (6)	30·2 (5)	64·6 (1)	47·5 (1)	−21·1		−16·5	
192163	20 08·4	38 03	7·44, WN6	36·2 (9)	29·7 (8)	44·1 (1)	26·0 (1)	−17·4	−10·9	−16·6	
192281	20 09·0	39 58	7·47, O5n	36·5 (6)	27·3 (4)	46·1 (3)	38·9 (3)	−13·1	−05·0	−11·1	−59·7
192422	20 09·7	38 28	7·10, Bos	43·0 (3)	31·7 (1)	45·5 (3)	37·0 (3)	−06·2	−01·0	−04·0	−01·7
192445	20 09·8	36 02	7·12, B3ne	21·7 (3)		31·1 (2)	26·4 (2)	−07·7	+01·5	−05·4	+03·6
192539	20 10·3	31 41	7·38, B2s	29·6 (3)				−08·6		−08·6	−23·3
192639	20 10·8	37 03	7·02, O7sf	27·4 (5)		35·8 (4)	29·1 (4)	−14·9	−04·2	−10·6	−02·3
192641	20 10·8	36 21	7·94, WC9	27·3 (8)	23·6 (4)	28·8 (1)	32·8 (1)	−15·2	+03·7	−12·1	
193009	20 12·9	32 04	7·02, Boe	26·0 (3)	12· (1)			−08·7		−08·7	−21·7
193077	20 13·3	37 07	7·97, WN6	31·1 (5)	22·5 (4)			−19·6		−19·6	
193183	20 13·8	37 55	7·12, B2s	42·7 (3)				−16·6		−16·6	−00·1
193237	20 14·1	37 43	4·88, B1q	35·0 (12)		29·1 (14)	26·8 (14)	−14·8		−14·8	
193322	20 14·6	40 25	5·82, O8	39·6 (4)		45·3 (1)	36·6 (1)	−12·4	−11·2	−12·3	−06·4
193514	20 15·5	38 57	7·29, O8	36·9 (3)	16·7 (1)	33·3 (3)	27·3 (3)	−15·2	−12·6	−14·2	−19·5
193536	20 15·6	46 00	6·28, B2	27·4 (3)				−11·1		−11·1	− 8·9
193576	20 15·8	38 25	8·04, O6+WN5·5	28·2 (21)				− 8·6		− 8·6	
228911	20 15·8	40 00	8·7, B3	28·2 (6)				−16·3		−16·3	
193611	20 16·0	38 01	9·2, Bo	38·1				− 9·9		− 9·9	
193793	20 17·1	43 32	6·83, O5+WC8	50·5 (10)	27·6 (2)	65·4 (4)	56·7 (4)	−20·7	−21·6	−20·9	+01·7
194279	20 19·7	40 26	7·05, Bos	61·0 (3)				−22·6		−22·6	−30·2
194839	20 22·8	41 03	7·45, B2s	41·5 (3)				−18·8		−18·8	−21·1
195592	20 27·2	43 59	7·15, Bos	44·5 (4)				−18·0		−18·0	−23·5
197345	20 38·0	44 55	1·33, A2p			42·1 (5)	32·7 (5)	−10·2		−10·2	

• Believed blended with stellar line.

TABLE I (*cont.*)

Star HD	R.A. 1900	Dec. 1900	Mag., Type	Interstellar line intensity Ca 3933	Ca 3968	Na 5889	Na 5896	Interstellar velocity Ca	Na	Mean	Stellar velocity
	h m	° ′									
197911	20 41·6	62 51	8·7, B5	32·8 (5)				−18·5		−18·5	
198478	20 45·5	45 45	4·89, B2s	40·8 (2)		29·3 (6)	26·0 (6)	−07·6	−13·6	−12·3	−06·6
198639	20 46·6	43 41	5·07, A5			21·9 (1)	17·2 (1)		−14·7	−14·7	
198846	20 48·1	34 17	Var., O9nn	28·9 (6)		43·6 (3)	39·5 (3)	−09·7	−18·0	−10·2	−56·8
199140	20 50·1	28 08	6·44, B3	26·3 (16)				− 4·9		− 4·9	
199478	20 52·4	47 02	5·76, B8p			38·6 (2)	28·6 (2)		+00·4	+00·4	
199579	20 53·1	44 33	6·01, O6	23·3 (4)		53·1 (1)	48·4 (1)	−11·3.	−17·1	−11·5	−05·8
202214	21 09·3	59 35	5·65, O9s	26·9 (4)	9·8 (1)	30·4 (6)	26·0 (6)	−18·8	−15·4	−18·0	−16·1
202904	21 13·8	34 29	4·42, B3ne	5·3 (2)				−19·3*		−19·3	+ 3·5
203064	21 14·8	43 31	5·06, O8nn	25·5 (7)	20·1 (4)	19·2 (10)	15·3 (10)	−13·7	−10·4	−13·0	+03·6
203374	21 16·7	61 25	6·64, Bone	27·0 (1)		37·0 (2)	34·8 (2)	−16·7	+13·9	−16·7	−07·0
204116	21 21·4	54 57	7·96, Bon	33·6 (2)		44·1 (2)	20·7 (2)	−11·5	−01·4	−08·1	−22·6
204172	21 21·7	36 14	5·84, Bo	23·1 (2)		23·2 (3)	22·5 (3)	−10·8	−14·6	−12·1	+02·8
205196	21 28·6	57 04	7·36, Bos	20·8 (1)		27·2 (1)	23·4 (1)	−19·6	−09·1	−16·1	−12·8
206267	21 35·9	57 02	5·64, O6n	26·3 (2)		42·5 (1)	31·2 (1)	−18·5	+04·3	−17·5	−08·0
206773	21 39·3	57 17	6·98, Bonne			46·2 (1)	29·6 (1)	−19·0		−19·0	−21·6
207198	21 42·2	61 59	5·97, O9s	22·7 (3)		38·5 (4)	30·7 (4)	−20·5	−11·5	−17·2	−20·5
207260	21 42·6	60 40	4·46, A2p			42·5 (1)	29·4 (1)		−17·7	−17·7	
209339	21 57·6	62 00	6·48, Bo	18·9 (3)				−12·7		−12·7	−20·7
209481	21 58·7	57 31	5·50, O9n	20·1 (5)		47·0 (9)	37·8 (9)	−10·9	−06·7	−10·1	−17
209975	22 02·1	61 48	5·17, O9	21·0 (4)		35·8 (5)	30·7 (5)	−12·6	−06·9	−11·2	−12·8
210839	22 08·1	58 56	5·19, O6ne	24·4 (14)	22·6 (5)	41·1 (9)	35·8 (9)	−13·0	−16·5	−13·7	−74·3
211853	22 15·0	55 37	9·0, O7+WN7	64·4 (1)	59·4 (1)			−29·7		−29·7	−33
212455	22 19·3	54 44	8·4, B3	81·2 (1)				−13·5	−29·8	−21·6	−54·7
214240	22 31·8	49 33	6·2, B4	38·1 (2)				−18·9		−18·9	−15·1
214419	22 32·9	56 23	8·92, WN7	42·3 (4)	35·5 (4)			−20·0		−20·0	
214680	22 34·8	38 32	4·91, O9s	18·1 (4)		27·4 (5)	19·0 (5)	−17·8	−07·1	−14·7	−09·5
216014	22 44·2	64 32	6·83, Bo	47·4 (10)		54·9 (3)	37·7 (3)	−26·3	−22·0	−25·7	−23·1
216411	22 47·6	58 28	7·16, Bos	51·9 (5)		51·8 (2)	33·6 (2)	−22·4	−21·9	−22·3	−43·8
217297	22 54·7	63 10	7·36, Bo	30·1 (4)		35·1 (3)	32·4 (3)	−11·4	+09·3	−04·5	−10·1
218066	23 00·0	62 51	7·8, B5	35·1 (3)				−15·6		−15·6	
218440	23 03·0	59 13	6·28, B3	17·5 (3)				− 9·8		− 9·8	− 7·4
218915	23 06·7	52 31	7·06, O9s	37·9 (4)		53·9 (2)	36·5 (2)	−26·3	−10·4	−22·8	−72·0
221253	23 25·4	58 00	4·89, B3	22·1 (2)				−11·5*		−11·5	−14·8
224055	23 49·7	61 17	7·16, B8s			71·6 (1)	54·3 (1)		−09·3	−09·3	−42·7
224151	23 50·5	56 35	6·05, Bo	33·5 (6)	33·1 (2)			−21·0		−21·0	−26·7

*Believed blended with stellar line.

Trigonometric parallaxes. While trigonometric parallaxes are available for quite a number of early-type stars* a good deal of caution is necessary in their use. For most of the stars the parallaxes are of the same order as their probable errors, while a further indication of the uncertainty of such measures is the existence of many negative parallaxes. It was recognized therefore that trigonometric parallaxes would be significant only for nearby stars with relatively weak lines. In a first attempt to use such parallaxes a list of 27 stars was drawn up, all with interstellar *K* line intensities less than 20 km/sec. These stars were divided into two groups with intensities in the range 0 to 10 and 10 to 20 km/sec respectively. The mean trigonometric parallax for the first group was $+0''.012$, while that of the second was $-0''.0003$. This suggested that it was probably useless to try to utilize the trigonometric parallaxes to fix more than one point on the distance–intensity graph. It was accordingly decided to use the trigonometric parallaxes only for stars with intensities of 12 or less and to average the parallaxes regardless of sign, resulting in a single point on the graph.

This has been done and the resulting values for calcium and sodium are given in Tables IV and V. The basis of selection for the stars has been a calcium intensity of 12 or less and since some of the sodium lines are stronger than calcium this accounts for the higher average sodium intensities. The mean distance of 154 parsecs for calcium is based on 19 stars, while that of 167 parsecs for sodium is based on 6. This close agreement must be regarded as probably fortuitous and both of the points have been given low weight.

Parallactic motions. While it is theoretically possible to utilize both the tau and the upsilon components of proper motion to compute the distances of stars it has been shown by Russell† and by Plaskett and Pearce‡ that more reliable results are obtained from the upsilon components and they have been used here. The proper motions have been taken from the Albany *General Catalogue* and Mrs Dorothy Edmonds of the Dominion Astrophysical Observatory has very kindly computed the upsilon components. For the distant O- and B-type stars the probable errors are quite large and some of the more distant stars with stronger lines have been excluded from the calculation. For calcium, only lines with intensities less than 40 have been used, while for sodium, with somewhat stronger lines, the limit has been set at 50.

A total of 104 calcium stars have been used, divided into three approximately equal groups, while 59 stars are available for sodium.

The usual formula

$$\pi_v = \frac{4{\cdot}738\ \overline{v \sin D}}{\overline{V_0}\ \overline{\sin^2 D}}$$

has been used in deriving distances for the various groups. The stars of the h and χ cluster in Perseus have been excluded from the data by the intensity criterion and it is not considered that other cluster stars have seriously interfered with the solutions.

The results are given in Tables IV and V. It will be seen that the mean intensities range from 10 to 35 while the mean distances are from 200 to 1 000 parsecs, covering a reasonable proportion of the distance–intensity range.

* Louise F. Jenkins, *Gen. Cat. Trig. Parallaxes*, Yale University Observatory, 1952.

† H. N. Russell, *Ap. J.*, **54**, 140, 1921.

‡ J. S. Plaskett and J. A. Pearce, *P. Dom. Ap. O.*, **5**, 203, 1931.

Eclipsing binaries. Objects of this type for which absolute dimensions are available as a result of spectroscopic and photometric studies afford distances for eleven stars listed in Table II. We are indebted to Dr R. M. Petrie for help in selecting this list. In deriving the calculated absolute magnitudes from radii

TABLE II

Eclipsing binaries

Star HD	Spectral type	App. mag. m	Abs. mag. M	Int. K	Int. D	Dist. r (ps)
1 337	O8·5*	6·1	−6·2	35·2	43·6	2 630
19 820	O8	7·4	−4·9	29·5	32·7	1 030
25 833	B3	6·6	−2·1	18·3	...	390
34 333	B3	7·8	−5·6	27·5	...	3 160
175 227	B5	8·5	−1·2	10·7	...	690
181 987	B3	7·1	−3·1	16·8	...	740
193 576	O6WN5·5	8·0	−5·9	28·2	...	2 840
193 600	Bo·5	9·2	−4·5	38·1	...	2 630
198 846	O9·5	7·1	−4·4	28·1	41·6	1 460
216 014	B3	6·8	−3·6	32·6	46·3	510
218 066	B3	7·8	−2·8	35·1	...	1 010

* Unless otherwise indicated the two components are assumed to be of the same type.

Calcium		Sodium	
Two groups		One group	
Int. K	r	Int. $\frac{D_1+D_2}{2}$	r
15·3	610	41·1	1410
31·8	1910		

and spectral types the temperature scale recently published by Beals*, smoothed for uniformity, has been used for the O-type stars, while Kuiper's† scale has been used for stars later than Bo. To correct the apparent magnitudes for space absorption we have followed Stebbins, Huffer and Whitford‡ in using the relationship

$$m_0 = m - 7E_1,$$

where m is the observed apparent magnitude, E_1 is the colour index of Stebbins and Whitford and m_0 is the apparent magnitude corrected for space absorption. This relationship has been derived from the observational results of a number of workers, including not only Stebbins and Whitford but also Rudnick, Hall and Greenstein, indicating that selective absorption in space is closely proportional to the inverse first power of the wave-length (λ^{-1} law). In certain instances, such as the Wolf-Rayet binary HD 193 576, or other stars where the colour indices are not available or are of doubtful interpretation, it is assumed that the general absorption amounts to 0·8 magnitudes per thousand parsecs.

* C. S. Beals, *Jour. R.A.S.Can.*, **44**, 221, 1950.

† G. P. Kuiper, *Ap. J.*, **88**, 429, 1938.

‡ J. Stebbins, C. M. Huffer and A. E. Whitford, *P. Washburn O.*, **15**, Part 5, 1934; *Ap. J.*, **90**, 213, 1939; *Ap. J.*, **91**, 20, 1940.

The calcium stars of Table II have been divided into two groups, those with intensities less than 20 km/sec and those with intensities over 20; three stars being in the first group and eight in the second. Only four of the stars have measured sodium lines and since these intensities are all over 20 they have been used to define a single point on the curve. Actual values are given at the bottom of Table II and in Tables IV and V. The relatively large deviation of individual stars from a smooth distance–intensity relation will be discussed in a later paragraph.

Spectroscopic absolute magnitudes. At the time these data were being prepared we were in communication with Dr W. W. Morgan of the Yerkes Observatory and Dr R. M. Petrie of the Dominion Astrophysical Observatory, both of whom had derived spectroscopic absolute magnitudes for a considerable number of early-type stars. Both Dr Morgan and Dr Petrie very kindly offered to place relevant parts of their data at our disposal in advance of publication. Morgan's list included 102 of our stars. For 97 of these, calcium line intensities had been measured, while there are sodium lines for 59. Dr Petrie provided absolute magnitudes for 53 stars. While a few of these were on our original list, a majority of the calcium lines had been measured by Dr Petrie himself and he has kindly allowed us to add this material to our Table I.

Dr Morgan informs us that the zero point of his calibration depends on two independent sources:

(1) The main sequence B2 and B3 stars in the Scorpio–Centaurus cluster as re-discussed by Blaauw (*Groningen Pub.* No. 52).

(2) Mean parallaxes determined from upsilon components for a group of main sequence B3 stars not members of any cluster and scattered over the sky; also unpublished results of Blaauw on a similar calibration of B2, B3 and B5 stars from upsilon components.

The standard luminosities for stars of other types and those brighter than the main sequence have been determined from certain clusters, principally the Orion aggregate and the Double Cluster in Perseus, by use of the calibrated main sequence B2 and B3 stars.

Dr Petrie writes that he has used the following material for the calibration of his absolute spectroscopic magnitudes:

(1) The galactic clusters h and χ Persei, the Perseus stream, the Pleiades, the Orion cluster, Messier 35, IC 4665, NGC 6633 and the Scorpio–Centaurus stream.

(2) Visual binaries in which the fainter component is of spectral type B9 or later.

(3) Eclipsing binaries for which reliable absolute magnitudes could be calculated from the combination of photometric and spectroscopic orbits.

For Petrie's stars we have used the photoelectric colour indices of Stebbins, Huffer and Whitford to correct the apparent magnitudes for general absorption in the manner already discussed under spectroscopic binaries. In spite of the uncertainties involved in this method, it is probably the best that can be done at the present time.

Morgan has himself corrected the apparent magnitudes of his stars by a method which is similar except that he used a revised table of colours available at Yerkes which is slightly different from that of Stebbins and his group.

In order to derive mean distances, the stars have been divided into the following intensity groups: 0 to 15, 15 to 30, 30 to 50 and over 50. The results are given in Tables IV and V. The data of Morgan and Petrie have been combined strictly according to the numbers of stars. While there are quite large systematic differences between them, we feel that a discussion of such differences should await publication of individual parallaxes.

Galactic clusters. Estimates of the distances of galactic clusters are based on spectroscopic parallaxes and on considerations of apparent diameter. Trumpler* has discussed both methods in considerable detail and has shown that there is reasonable agreement between them. Later studies by Zug, Rieke, Bidelman and others† have been based mainly on spectroscopic parallaxes.

TABLE III

Galactic clusters

Cluster	Distance parsecs	Int. K	No. of stars	Int. D	No. of stars
h and χ Per	1 900	58·9	(6)	59·5	(2)
IC 1848	1 610	47·5	(1)	41·7	(1)
NGC 1444	3 340	30·0	(1)	35·6	(1)
NGC 1502	1 450	24·0	(2)	...	
NGC 2244	1 340	22·3	(3)	30·2	(3)
NGC 2264	450	17·4	(1)	13·4	(1)
NGC 2353	760	11·3	(1)	...	
NGC 6871	1 340	46·2	(8)	55·6	(2)
NGC 6910	2 200	61·0	(1)	...	
AN 37	730	26·3	(1)	36·8	(1)

Calcium Three groups		Sodium Three groups	
Int. K	r	Int. $\frac{D_1+D_2}{2}$	r
14·4	605	13·4	450
25·7	1715	34·2	1803
52·9	1750	51·4	1616

Although a number of the stars in the present study appear to be members of clusters, there is some question as to how much use should be made of cluster distances based on spectroscopic parallaxes. The distances of numerous individual stars have already been derived by this method and there is some doubt whether the same method should indirectly be used over again. The matter turns on the question of the similarity in spectral type between the stars in Table I whose distances have been directly found by spectroscopic methods and the stars used in the original determinations of cluster distance. We have had the benefit of discussions of this question with Dr R. J. Trumpler and Dr R. M. Petrie. They point out that the spectroscopic determinations of cluster distance are, in general, based on later spectral classes than the stars of Table I and that, therefore, the distances of the clusters may be regarded as independently determined. It accordingly appears that the inclusion of such distances should be a valuable addition to the data and we have proceeded accordingly. In Table III

* R. J. Trumpler, *L.O.B.*, **14**, 154, 1930.

† R. S. Zug, *L.O.B.*, **16**, 119, 1933. C. A. Rieke, *Harv. Circ.*, 397, 1935. W. P. Bidelman, *Ap. J.*, **98**, 61, 1943.

are given the values of distance and interstellar line intensity for individual clusters, together with the number of stars involved for each cluster. For the most part Trumpler's data have been used but some results of Zug, Mrs Rieke and Bidelman have been included. The values of cluster distance based on spectroscopic parallaxes have been given somewhat greater weight than those estimated from cluster diameter. It is never possible to be certain that a given star is not a foreground or background object but it is hoped that the assignments of stars to particular clusters are, in general, correct. The clusters have been divided into three groups, as shown in Tables IV and V, with intensity ranges 0–20, 20–40 and over 40.

Galactic rotation. The velocity of stars or of interstellar matter due to the motion of rotation of the Galaxy is related to the distance by the well-known equation*

$$v = \bar{r} A \sin 2(l - l_0) \cos^2 b.$$

Here v is the velocity of the star or group of stars with the solar motion removed, r is the distance in parsecs, A the constant of galactic rotation (here assumed to be 0·017 km/sec per parsec), l is the galactic longitude of the star and l_0 the longitude of the galactic centre (assumed to be 325° following Plaskett and Pearce), while b is the galactic latitude. For interstellar matter it is necessary to use twice the velocity since the centre of the absorbing column may be assumed to be located at half the stellar distance.

Fortunately the stars of the present list are well distributed in galactic longitude, extending from 346° to 192°, so that approximately half of the double-wave cycle in radial velocities is well covered. Radial velocities are available for all the stars, so that the distance estimates from galactic rotation are more representative of the data as a whole than those of other methods.

The stars were divided into distance groups by a graphical method designed to combine fairly equal-sized groups with reasonable ranges of intensity. Calcium intensities were plotted against sodium for all the stars in the table and a smooth curve drawn through the points. For stars with calcium or sodium only the points were plotted on the curve. The division into groups was accomplished by drawing lines normal to the curve on the basis of the general distribution of the points in intensity and distance, the stellar and interstellar velocities being treated separately. After discussions with Dr Petrie it was decided to exclude from the solutions a considerable number of stars with weak lines in which the presence of interstellar calcium was doubtful. In deriving final values of distance, those calculated from velocities by interstellar lines have been given twice the weight of those using the stellar velocities. The results are shown in Tables IV and V.

5. *Weights of the observations.*—In choosing weights for the various points used in defining the distance–intensity relationship both the methods of distance determination and the numbers of stars are considered.

For the trigonometric parallaxes we may note that for stars only a few hundred parsecs distant the probable errors are of the same general order as the quantity to be measured. It has, therefore, been found necessary to limit this method to stars with relatively weak lines and even with this restriction the distances derived have only statistical value. It is probable that the weak lines of the nearer

* J. S. Plaskett and J. A. Pearce, *P. Dom. Ap. O.*, **5**, 175, 1931.

stars are measured with less accuracy than the stronger lines but this factor is scarcely important enough to influence the weighting. In spite of the fundamental character of trigonometric parallaxes their large probable errors necessitate low weight and a weight of 1 has accordingly been assigned to this method.

TABLE IV

Distance–intensity graph for calcium

Method of distance measurement	Group number	No. of stars	Interstellar *K* line intensity	Distance parsecs	Weight
Trigonometric parallaxes	1	19	7·0	154	19
Parallactic motions	1	34	9·8	210	119
	2	35	20·7	464	105
	3	35	30·4	1 095	88
Eclipsing binaries	1	3	15·3	610	9
	2	8	31·8	1 910	24
Spectroscopic parallaxes	1	28	8·0	295	56
	2	67	26·0	860	134
	3	29	37·9	1 190	58
	4	12	59·2	1 830	24
Galactic clusters	1	2	14·4	605	3
	2	7	25·7	1 715	11
	3	16	52·9	1 750	24
Galactic rotation	1	16	7·4	233	32
	2	35	20·3	519	87
	3	39	28·4	789	117
	4	31	39·2	1 782	109
	5	14	57·3	2 069	56

Parallactic motions, as indicated by the upsilon components of proper motion, depend on astronomical measurements of the same character as trigonometric parallaxes, but their larger base lines give them considerably higher weight. The method is, for obvious reasons, more definitive for near than distant stars. After a consideration of various factors, including the relatively small peculiar motions of the O- and B-type stars, it has been decided to assign a general weight of 3 to this method with the proviso that the nearer groups in Tables IV and V shall receive weights of 3·5 and the more distant a weight of 2·5.

The use of eclipsing binaries as indicators of distance has special advantages, chief of which are the fundamental character of the theory involved and the fact that, apart from the effects of general space absorption, the distance of near and distant stars are obtained with comparable accuracy. Errors in the determination of orbital elements and assumptions concerning the relationship between effective temperature and spectral type introduce uncertainties of unknown amount into the calculations, however, and it must also be acknowledged that the influence of general absorption by solid particles in space is not too definitely known. Considering all these factors it has been decided to give this method a weight of 3, equal to that of parallactic motions.

The method of spectroscopic parallaxes, at least in the present state of astrophysical knowledge, is derivative rather than fundamental and depends on a variety of methods, including the three described above. The broadness of its base is in its favour, but the systematic differences mentioned earlier in this paper between such senior investigators as Morgan and Petrie are an indication of its uncertainties. In consideration of these factors it has been decided to give this method a weight of 2.

TABLE V

Distance–intensity graph for sodium

Method of distance measurement	Group number	No. of stars	Interstellar *D* line intensity*	Distance parsecs	Weight
Trigonometric parallaxes	1	6	10·2	167	6
Parallactic motions	1	30	19·0	377	105
	2	29	35·5	747	73
Eclipsing binaries	1	4	41·1	1 410	12
Spectroscopic parallaxes	1	9	10·9	392	18
	2	20	22·4	885	40
	3	29	36·4	1 190	58
	4	6	60·0	1 884	12
Galactic clusters	1	1	13·4	450	2
	2	5	34·2	1 803	8
	3	5	51·4	1 616	8
Galactic rotation	1	7	10·6	260	14
	2	23	23·5	560	57
	3	29	34·2	840	87
	4	20	43·3	1 490	70
	5	9	58·9	2 300	36

* The interstellar line intensity used here is $\frac{D_1+D_2}{2}$.

As has already been mentioned, the use of cluster distances is dependent upon estimates of diameter and on the spectroscopic parallaxes of stars of later type than those considered here. Discussions with Dr Trumpler, who is mainly responsible for the use of diameters in the estimation of distance, indicate that this method is none too reliable. The use of spectroscopic parallaxes at second hand and the fact that there is always the possibility that a given object is a foreground or background star would appear to place this method in a lower rank than that of spectroscopic parallaxes proper. It has accordingly been decided to give this method a weight of 1·5.

The method of galactic rotation is free from most of the disadvantages mentioned in connection with the other methods. The theory appears to be well established and has been confirmed by extensive observations, at least for stars with distances less than 2 000 parsecs. Within reasonable limits it is applicable to stars of various distances. It is actually more definitive for distant objects, partly because of the greater ease of separating the galactic rotation effects from peculiar motions and partly because for interstellar lines the averaging effect may be

regarded as more complete for long than for short optical paths. Although in the initial determination of the constant A the effects of general absorption must be considered, the method is less likely than others to lead to serious errors due to this cause when dealing with restricted groups of stars. The principal disadvantages are the lack of observations in the Southern Hemisphere, interfering somewhat with the statistical average for each group of stars, and the existence of peculiar or group motions which are not in accord with the theory. In spite of these disadvantages we were at first inclined to feel that this method superseded the others and originally it was assigned a weight of 4. A study of the solutions, however, showed that many of the stars near the null points of galactic rotation made a negligible contribution to the result, while it was apparent that a few large residuals could have a serious effect on the calculations of mean distance. The method of galactic rotation has accordingly been assigned a general weight of 3, equal to that of eclipsing binaries and parallactic motions. The various groups have, however, been weighted according to distance, beginning with the nearest as follows : 2, 2·5, 3, 3·5, 4.

The weights of the various groups in Tables IV and V have been computed on the basis of the above discussion, the weight assigned to the method being multiplied in each case by the number of stars involved. A preliminary study of the data indicated that the scatter of the points was too great to make it possible to distinguish between a straight line and a curve for the distance–intensity graph. It was accordingly decided to assume a straight line and solve for the slope by a least-squares method, assuming the line to pass through the origin. This has been done for calcium and sodium with the following results, which are illustrated graphically in Figs. 4 and 5 :

$$r = 34{\cdot}83\ K,$$

$$r = 30{\cdot}75\ D,$$

r being in parsecs, K being the equivalent width of the K line in km/sec and D being the average intensity of D_1 and D_2 expressed in the same units. If the equivalent widths are given in angstroms the coefficients become 2660 and 1566 respectively. It should perhaps be mentioned that quite large differences in the system of weighting will lead to essentially the same result.

The scatter of the points about the lines in Figs. 4 and 5 is larger than had been expected, and it is difficult to be sure whether it is due mainly to uncertainties in the measurement of distance or to the irregular distribution of interstellar gas. Of special interest in this connection is the poor fit on the curve of the points due to spectroscopic binaries. Here we would normally expect the absolute magnitudes to be reliable and yet it is clear from a study of Table II that individual stars deviate widely from the distance–intensity graph. It seems extremely unlikely that errors in the determination of spectroscopic elements combined with uncertainty in the relation between spectral type and temperature could be the cause of such major deviations. If this conclusion is correct there remain only two other possible sources : (1) irregular distribution of the material (presumably solid particles) producing general space absorption, and (2) irregular distribution of interstellar gas.

Turning first to (1) we may note that many photographs of the sky give evidence of extreme irregularities in the distribution of absorbing material. In spite of this, however, it was hoped that the use of the equation

$$m_0 = m - 7E$$

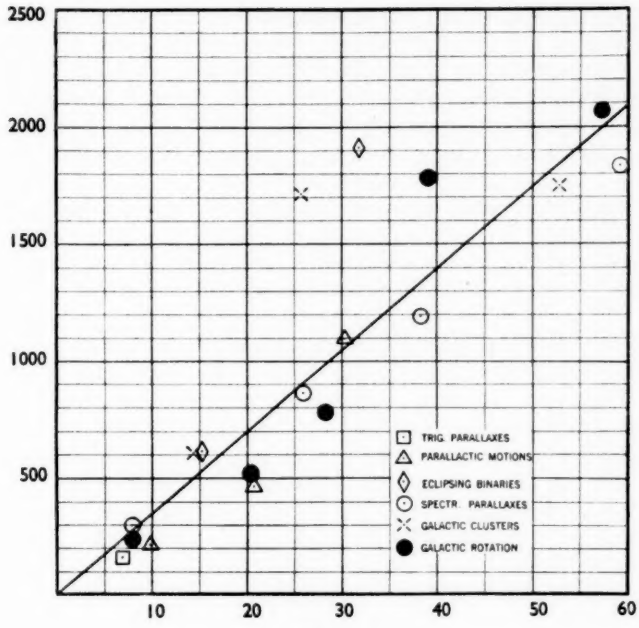

FIG. 4.
Ordinates: Distance, parsecs.
Abscissae: Calcium intensity (K).

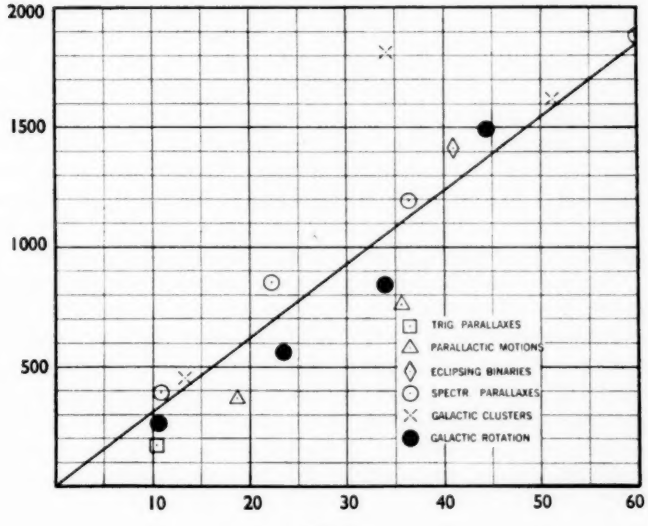

FIG. 5.
Ordinates: Distance, parsecs.
Abscissae: Sodium intensity $\left(\frac{D_1+D_2}{2}\right)$.

would lead to valid corrections to the apparent magnitudes for space absorption, since it is based on the idea of integrated optical thickness rather than on assumptions as to the correlation of general absorption with distance. Although it is an empirical rather than a theoretical relation it implies that the reddening properties of absorbing material are the same in different parts of space. Such an inference is supported by the excellent observational material of Stebbins and Whitford and other workers, but there can be no certainty that it applies for each individual star. If it does not, then some of the estimated distances may be in error due to this cause.

With regard to (2), the work of Stebbins and Whitford and others indicates that there is no close correlation between space reddening and interstellar line intensity. Thus the patchy character of the material causing general absorption does not in itself indicate a similar irregularity of distribution of interstellar gas. However, high-dispersion spectrograms of early-type stars clearly indicate the existence of clouds of interstellar gas* with radial velocities which may differ from one another by as much as 60 km/sec. It is thus quite certain that the atoms of interstellar gas are not distributed in an even, uniform manner throughout the Galaxy. The data on radial velocity suggest that the distribution of discrete gas clouds approximates to uniformity since the mean residual velocity due to galactic rotation for interstellar lines is half that of the stars in whose spectra they appear. Examination of the data shows that this relationship does not hold in all cases for individual stars or groups of stars, and this may be due to peculiar motions of the stars or the clouds, or to lack of uniformity in the distribution of the clouds. Lack of uniformity of distribution, if sufficiently drastic, would interfere with the validity of the distance–intensity relation and could cause the type of scatter which has been observed in Figs. 4 and 5.

This discussion could be pursued at considerable length but it is apparent that there is only one conclusion, namely, that it is impossible to apportion the origin of the scatter of points on the graph as between irregularity of distribution of interstellar gas and other causes. It is therefore necessary to assume that distances of individual stars determined from interstellar lines are subject to considerable errors. If it be supposed that all the scatter is due to irregular distribution of gas, the graphs suggest that maximum errors of the order of 50 per cent may be expected, although in general they should not be more than half this amount. Errors of this magnitude may, however, be regarded as moderate when compared with other means of deriving the parallaxes of individual stars, and we believe that there can be no doubt of the value of interstellar line intensities as a general indication of stellar distance. Where groups of stars are involved, the use of the graphs of Figs. 4 and 5 should give reliable values of mean parallax, while for isolated peculiar objects such as novae the immediate indication of distance and absolute magnitude given by the interstellar lines is invaluable.

6. *Comparison with other observers.*—Comparisons of interstellar line intensities obtained at different observatories have usually indicated quite substantial systematic differences, though the reasons for these differences are obscure. Merrill, Sanford, Wilson and Burwell† have published graphs and tables

* C. S. Beals, *M.N.*, **96**, 661, 1936; *Ap. J.*, **87**, 568, 1938. R. F. Sanford, *P.A.S.P.*, **51**, 238, 1939. W. S. Adams, *Ap. J.*, **97**, 105, 1943. P. M. Routley and L. W. Spitzer, *Ap. J.*, **115**, 227, 1952.

† P. W. Merrill, R. F. Sanford, O. C. Wilson and Cora G. Burwell, *Ap. J.*, **86**, 274, 1937.

illustrating differences between Victoria and Mount Wilson measures. These comparisons were based on relatively few stars and the data of this paper make possible a considerably more extensive comparison though the results are similar. In Figs. 6 and 7 Victoria values of intensity from Table I for calcium and sodium are plotted against those of the Mount Wilson catalogue, as well as a number of additional intensities derived by Spitzer and others from Mount Wilson plates. It will be seen that, on the average, the Victoria values are systematically greater by approximately 30 per cent. The similarity between the slopes of the straight lines for calcium and sodium is striking. The dispersions used at Mount Wilson and at Victoria for the measurement of a majority of the lines are comparable. For

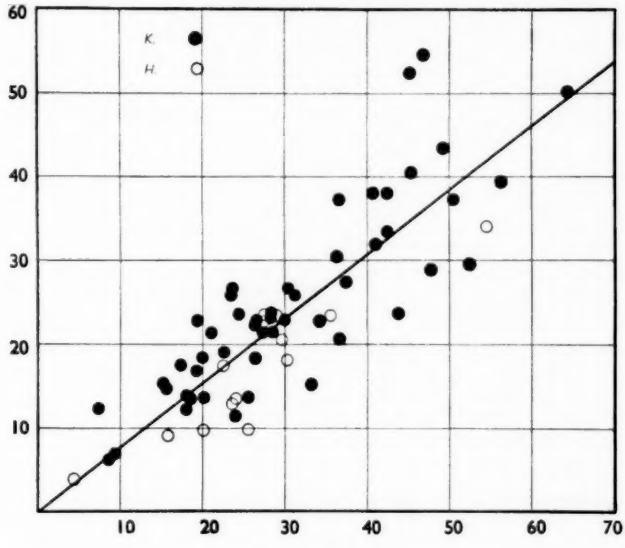

FIG. 6.

Ordinates: Calcium intensity—Mount Wilson.
Abscissae: Calcium intensity—Victoria.

calcium *K* the dispersion ordinarily used at Mount Wilson was 24 A per mm, though a few bright stars were observed with 17 A per mm or greater. At Victoria the usual dispersions were 20 A per mm and 35 A per mm, a few bright stars being observed with higher dispersions.

For the sodium *D* lines the Mount Wilson dispersions were 34 A per mm and 66 A per mm, while that normally used at Victoria was 31 A per mm. It is thus apparent that the average dispersion for the two sets of observations is about the same and it seems very unlikely that this is the cause of the systematic difference between them. A previous discussion of this matter has been presented by Beals and it is suggested that the relation between equivalent width and dispersion is definite only for rather large differences in dispersion. The systematic differences in intensities have been discussed with the Mount Wilson astronomers but no conclusion has been reached as to the cause of the discrepancies.

In comparisons of distance–intensity curves it is, of course, necessary to take account of systematic differences in observations such as those referred to above. This has been done for the curves published by Sanford, Merrill, Evans and van Rhijn and their values of intensity have been converted to the Victoria scale. In addition, since Evans's curve relied mainly on galactic rotation, his normal points have been re-computed using a galactic rotation constant of 17 km s^{-1} kps^{-1} instead of 16 which he used. A similar correction has been applied to van Rhijn's results. These revised curves are compared with our distance–intensity curves in Figs. 8 and 9.*

In comparing the various curves it should first be pointed out that those of Merrill and of Sanford, published 15 years ago, depend upon an absolute magnitude scale very different from that commonly regarded as valid today. For example,

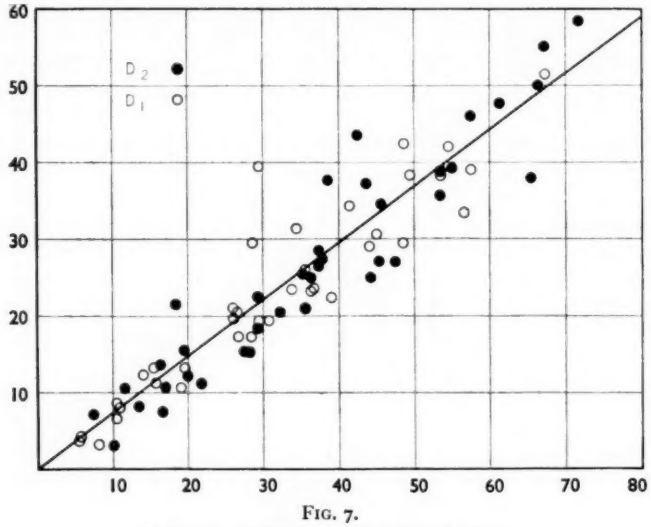

FIG. 7.

Ordinates: Sodium intensity—Mount Wilson.
Abscissae: Sodium intensity—Victoria.

their scale is correlated with spectral types almost exclusively and they utilize a value of $-3{\cdot}3$ for the mean absolute magnitude for O to Bo stars, whereas many of the absolute magnitudes of Morgan and Petrie for stars in these spectral classes are as much as three magnitudes brighter. It should further be noted that they utilize a value for general absorption of $0^{m}{\cdot}35$ per thousand parsecs, less than half of the value of $0^{m}{\cdot}8$ per kiloparsec which is now considered closer to the true value. A shift in their absolute magnitude scale in the direction of higher values would displace their curve in the sense that each value of intensity would be associated with a larger value of distance. The adoption of a larger value for the coefficient of general absorption would displace it in the opposite direction. It appears, however, that the first effect would be considerably greater and it is possible that this would account, at least in part, for the differences between our curves and those of the Mount Wilson observers.

* Another discussion of the relation between distance and interstellar line intensity has recently been published by L. Binnendijk, *Ap. J.*, **115**, 428, 1952.

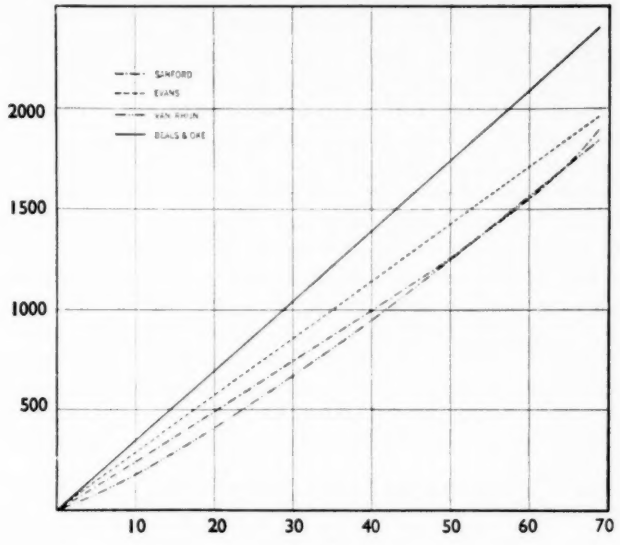

FIG. 8.

Ordinates: Distance, parsecs.
Abscissae: Calcium intensity, km/sec.

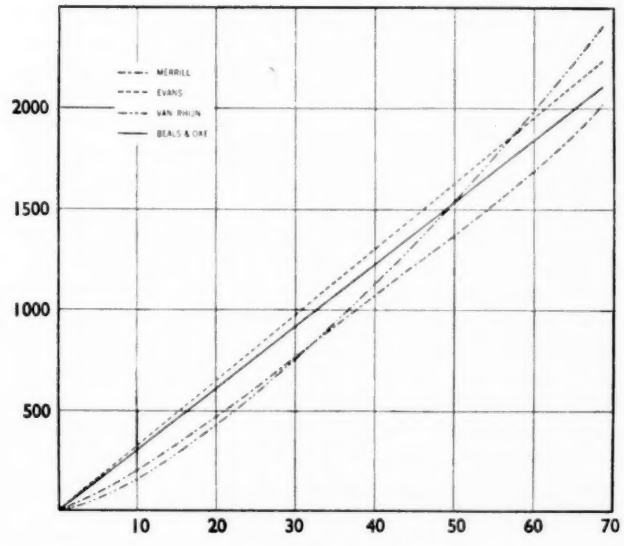

FIG. 9.

Ordinates: Distance, parsecs.
Abscissae: Sodium intensity, km/sec.

The curves of Evans and van Rhijn are both based on Mount Wilson data and both employ mainly galactic rotation as a criterion of distance. However, it will be seen that Evans's results correspond quite closely to ours (the curve for sodium is little different in slope) while van Rhijn's show a considerable deviation.

Without actually re-working the data it would be hazardous to speculate on the precise reasons for the differences between the various distance–intensity curves. It should be emphasized, however, that all modern evidence points to considerable irregularity in the distribution of interstellar material. Moreover, it is reasonable to suppose that there are regular variations from centre to circumference of the Galaxy and in the direction perpendicular to the galactic plane (e.g. van Rhijn attempts to correct the observed interstellar line intensities for distance from the plane). There is thus no reason to suppose that there is any single distance–intensity relationship which will hold unambiguously for all parts of the Galaxy, and no two graphs should be expected to coincide unless derived from identical data. In spite of these considerations it appears that there is enough evidence for statistical uniformity to make the intensities of interstellar calcium and sodium lines a very valuable indication of distance for individual stars or groups of stars.

In conclusion we wish to express our thanks to Dr R. M. Petrie for his generosity in supplying valuable absolute magnitude and radial velocity data, as well as for helpful discussions on various aspects of the work. Special thanks are also due to Dr W. W. Morgan for supplying absolute magnitude values in advance of publication. We are also indebted to Dr J. A. Rottenberg, Mrs Dorothy Edmonds and Mr R. W. Tanner for help with the calculations, and to Mr John O'Connor for measuring the velocities of many of the sodium lines.

Dominion Observatory,
Ottawa :
1953 *January* 22.

THE CONSTANTS OF THE VELOCITY ELLIPSOID FROM THE RADIAL VELOCITIES OF 820 STARS

D. G. Ewart

(Communicated by the Director, University Observatory, Glasgow)

(Received 1953 June 25)

Summary

The radial velocities of 820 stars (HD photographic magnitudes $8^{m}\cdot5$ to $8^{m}\cdot6$) measured at Lick Observatory have been examined for the effects of solar motion and preferential motion.

The results for the solar motion are :

$$U=20\cdot36 \text{ km/sec}; \quad A=275^{\circ}\,07'; \quad D=+40^{\circ}\,44'.$$

They are slightly lower (arithmetically) than those of Moore and Paddock.

A negligible K term is found.

The constants of the velocity ellipsoid found agree well for all stars with previous results, except that no deviation of the vertex is apparent.

Features suggesting the need of further examination are :

(i) possible variation of the declination of the solar apex with apparent magnitude, and

(ii) dependence of deviation of vertex on distances of the stars used in its determination.

---

1. A number of derivations of the constants of the velocity ellipsoid, such as those of H. Nordström (**1**) and W. M. Smart (**2**), have been made utilizing radial velocities. They have, however, been confined to the brighter stars. In this investigation, the radial velocities of a sample group of faint stars have been analysed, to ascertain whether the features of the velocity ellipsoid, as derived from radial velocities, are dependent to any extent on the magnitudes of the stars employed, as is suggested by the results of proper motion analyses.

The radial velocities used in this investigation were taken from a list compiled by the late J. H. Moore and G. F. Paddock (**3**) and prepared for publication by N. U. Mayall. The plates were taken and measured at Lick Observatory.

The stars are all of spectral types F–M and lie in the HD photographic magnitude range of $8^{m}\cdot5$ to $8^{m}\cdot6$. The list is not, of course, exhaustive, and the stars are all north of declination -21°. It must be noted that for stars of spectral types F to K5, only those in the even zones of declination were chosen.

Also listed are the visual magnitudes, the probable errors of the radial velocities, the Lick estimates of luminosity classes and spectral types and the HD spectral classification. The luminosity classification is that introduced by Morgan, Keenan and Kellman in their *Atlas of Stellar Spectra*, 1943.

2. The material was analysed for solar motion by the compilers of the Catalogue, and in regard to the giant stars—mainly of luminosity class III—for galactic rotation. For the solar motion, the material was divided into three groups: luminosity classes II to III–IV, IV and V. Five stars with velocities greater than 80 km/sec, 63 stars of variable or possibly variable velocity, 74 stars of luminosity class V in the spectral ranges F0–F4 and G5–K4, 3 stars of

luminosity class Ib and 9 stars of unclassified luminosity were excluded, leaving 666 stars for the final analysis.

The results for each group are in good agreement and within their probable errors, but the declination of the apex is much higher than other determinations from radial velocities. For later work the authors assume a mean apex of $A = 280°$, $D = +44°{\cdot}5$, with the solar velocity as derived for each group.

3. It was felt that, as there were so few stars in the list and as their distribution over the sky was only approximately uniform, it would not be profitable to attempt an analysis by spectral or other groups, as no significance could be attached to any resulting data. Accordingly, all 820 stars have been used in this analysis. Since the Lick paper gives only a rounded mean apex for all stars and obtains the results from stars limited in number, it was decided to examine the material anew, *in toto*, and obtain the appropriate solar motion.

4. The method used was that given by Smart (**4**), which permits the use of large areas of the sky, thereby simplifying the calculations involved. The sky was divided into 34 areas, according to galactic latitude. Antipodal areas were combined to give 17 regions over one hemisphere.

The resultant equations of condition, excluding the correction C_z, were then solved for the solar motion and the K term. The uncorrected results were:—

$$U = 19{\cdot}38 \text{ km/sec}; \; G = 36° \, 05'; \; g = 21° \, 31'; \; K = -0{\cdot}18 \text{ km/sec}.$$

Using the above values of the solar motion, the corrections C_z were calculated for each region and inserted in the normal equations. These were then solved for the solar motion. The final results were :—

$$U = 20{\cdot}36 \text{ km/sec}; \; A = 275° \, 07'; \; D = +40° \, 44'; \; G = 35° \, 53'; \; g = +21° \, 18'$$

with a K term of $-0{\cdot}22$ km/sec. For comparison, the mean results of Moore and Paddock were:—

$$U = 22{\cdot}44 \text{ km/sec}; \; A = 280°; \; D = +44° \, 30'.$$

It will thus be seen that the high value of the declination of the solar apex obtained by Moore and Paddock has been, to some extent, confirmed. Whether or not the difference from previous determinations is real it is impossible to say, as the method used assumes a uniform distribution of stars over the sky. It should, however, be mentioned that in the earlier work on radial velocities the stars used were usually those brighter than the sixth apparent magnitude, whereas those at present under discussion are of photographic apparent magnitude 8·5. There may thus be a magnitude variation in the solar motion.

5. For the determination of the constants of the velocity ellipsoid, the same division of the sky was used as above. The method used was that developed by Smart and Chandrasekhar (**5**) and later applied by the former (**2**) to the stars of Schlesinger's *Catalogue of Bright Stars* (1930).

The velocities were each corrected by an amount $C_z - K$. The values of the mean radial speeds $\overline{R}_0$ for each region were then obtained.

From the elements of the solar motion obtained above, the quantity $U \cos \lambda$, where U = solar velocity and λ = distance from centre of region to solar apex or antapex, whichever is less than 90°, was calculated for each region, and hence the values of $t \, (= \pi^{1/2} \overline{R}_0 / U \cos \lambda)$. From them the values of ξ, where $t = (1/\xi)(e^{-\xi^2} + 2\xi \int_0^{\xi} e^{-x^2} dx)$, were obtained. From these the values of the

quantities $C(=U^2\xi^{-2}\cos^2\lambda)$ were calculated. It is assumed that the major axis of the velocity ellipsoid lies in the galactic plane at longitude G_0. We thus obtain for each region, centre (G, g), an equation of condition:—

$$P+Q\cos 2G+R\sin 2G=C,$$

where

$$P=\frac{1}{H^2}+\frac{1}{2}\left(\frac{1}{K^2}-\frac{1}{H^2}\right)\cos^2 g,$$

$$Q=\frac{1}{2}\left(\frac{1}{K^2}-\frac{1}{H^2}\right)\cos^2 g\cos 2G_0,$$

and

$$R=\frac{1}{2}\left(\frac{1}{K^2}-\frac{1}{H^2}\right)\cos^2 g\sin 2G_0.$$

Thus from the equations of condition for each region we obtain, by the usual methods, the quantities P, Q and R, from which we can calculate $1/K$, $1/H$ and G_0, thus obtaining the main features of the velocity ellipsoid.

A number of solutions were made by galactic zones. The only result to which we can attach any significance is, however, the result for all stars. The results are exhibited in the table below. The results of Smart's analysis of the stars of Schlesinger's catalogue are given in brackets.

Zone	No. of stars	$\frac{1}{K}$	$\frac{1}{H}$	$\frac{K}{H}$	G_0
0°	167	38·89	32·56	0·837	292° 27′
	(619)	(33·70)	(20·90)	(0·619)	(340° 30′)
20°	277	41·45	26·11	0·630	324° 22′
	(981)	(30·10)	(26·40)	(0·879)	(332° 12′)
45°	296	53·52	17·94	0·336	343° 42′
	(1068)	(37·20)	(22·10)	(0·594)	(338° 48′)
All	820	37·24	25·80	0·693	321° 44′ ± 3° 31′
	(2668)	(33·70)	(23·10)	(0·697)	(339° 30′ ± 1° 24′)

6. The main features to be noted are as follows.

(*a*) *All stars.*—(i) Preferential motion, i.e. the ratio K/H, is seen to be well defined. The value obtained (0·693) agrees closely with Smart's value, and with proper motion results.

(ii) The deviation of the vertex is barely evident in the result for all stars, it being noticed that the direction of the centre of the Galaxy lies within the probable error of the result. It may thus be that this result confirms the results of Delhaye (**6**), who obtained similar results from analysing the proper motions of faint stars in the Boss *G.C.* and who suggests that the phenomenon of the deviation of the vertex is confined to the nearer stars and is not exhibited by the fainter and more distant stars. The mean distance of the giant stars amongst the above is found by Moore and Paddock to be 300 parsecs.

(*b*) *Galactic zones.*—(i) There would not appear to be any confirmation of the high value of K/H for the 20° belt obtained by Smart.

(ii) Preferential motion appears to be more clearly defined as the galactic latitude increases. This may be, however, a feature of observational selection.

7. In conclusion, I wish to thank Professor W. M. Smart for suggesting the investigation, and for his advice whilst it was being conducted. I also wish to tender my thanks to the Department of Scientific and Industrial Research for the award of a maintenance grant, during the tenure of which the investigation was performed.

University Observatory,
Glasgow, W.2 :
1953 *June* 24.

References

(1) H. Nordström, *Lund. Medd.*, Ser. II, No. 79, 1936.
(2) W. M. Smart, *M.N.*, **99,** 61, 1939.
(3) J. H. Moore and G. F. Paddock, *Ap. J.*, **112,** 48, 1950.
(4) W. M. Smart, *M.N.*, **96,** 461, 1936.
(5) W. M. Smart and S. Chandrasekhar, *M.N.*, **98,** 658, 1938.
(6) J. Delhaye, *Contribution à l'étude de la distribution des vitesses stellaires*, Paris, 1952.

THE IONIZED HELIUM SERIES ORIGINATING FROM THE FIFTH QUANTUM LEVEL

R. Wilson

(Communicated by the Astronomer Royal for Scotland)

(Received 1953 June 8)

Summary

A number of the higher components of the hitherto unobserved series of ionized helium originating from the fifth quantum level (He II 5 ^{2}G$-n$ ^{2}H^0, etc.) have been detected in the spectra of stars of Draper type Oe5. The lines are broad but very shallow, having central depressions of the order of one per cent of the continuum. They therefore require high photometric accuracy for their detection and this was achieved by the application of the Greaves–Baker method of reduction of spectrograms. One of the main features of this method consists, in essence, of the combination of the measures of a number of negatives *without* smoothing, thus preserving any real features. The total intensities of some of the series members were computed and compared with the results for other lines of ionized helium originating from the third and fourth quantum levels. The wave-lengths of the centres of gravity of the lines were calculated using an approximation for determining the relative strengths of the fine-structure components.

One member of this He II series is blended with He I λ 6678 and affects previous measures of the intensity of the latter. The blending contribution is of the order of 0·2 equivalent angstroms for the stars investigated.

1. *Introduction.*—The first lines of ionized helium (the Pickering series) were discovered in the spectrum of the star ζ Puppis by E. C. Pickering (**1**) in 1896. Since their wave-lengths could be represented by an expression of similar nature to that for the Balmer series of hydrogen, their origin was first ascribed to some form of cosmic hydrogen, which could only exist in the hotter stars. The subsequent fitting of the observed wave-lengths of the series to Bohr's formula for ionized helium constituted one of the first major successes of the Bohr atom (**2**).

Bohr's model for a single-electron atom gives the general expression for the wave-numbers N of the spectral lines to be

$$N = RZ^2(1/n_1^2 - 1/n_2^2),$$

where Z is the atomic number, n_1 and n_2 are integers and R is the Rydberg constant, given by

$$R = 2\pi^2 me^4/ch^3(1 + m/M),$$

where m and e are respectively the mass and charge of the electron, c the velocity of light, h Planck's constant and M the mass of the nucleus.

The above expression for N is not strictly accurate. The spectral lines are actually composite in nature, and the complete expression for N, as derived from Sommerfeld's extension of the Bohr atom and giving the fine-structure components, can be obtained from the general expression for the term values of the quantum levels given in Section 5.

For ionized helium ($Z=2$; $R=109722$ cm^{-1}), the Pickering series is given by $n_1=4$, $n_2=5, 6, 7 \ldots$. The series originating from the third level ($n_1=3$, $n_2=4, 5, 6 \ldots$) has been examined in the laboratory by Fowler (**3**). The first line of this series ($\lambda 4686$) is a conspicuous feature of the spectra of O-type stars and is very often in emission. The series originating from the first ($n_1=1$, $n_2=2, 3, 4 \ldots$) and second ($n_1=2$, $n_2=3, 4, 5 \ldots$) levels have been found in the extreme ultra-violet region of the helium spectrum by Lyman (**4**).

In the case of hydrogen ($Z=1$; $R=109678$ cm^{-1}), five series have been found experimentally, namely, those originating from the first five quantum levels ($n_1=1$ to 5 inclusive). These are named in their respective order, the Lyman, Balmer, Paschen, Brackett and Pfund series.

The present investigation levels the score between hydrogen and ionized helium. A number of the higher components of the ionized helium series originating from the fifth quantum level (designation He II $5\,^2G$–$n\,^2H^0$, etc.) have been detected in the red-orange-yellow region of the spectra of stars of Draper type Oe5. The lines are very weak, having central depressions of the order of one per cent of the continuum. They therefore require high photometric accuracy for their detection. How this was achieved will be explained in the following text.

2. ***The material.***—The material consists of thirty-nine spectrograms, embracing seven stars of Draper type Oe5, taken at Edinburgh during 1938–48 in the general observing programme of the early-type stars. The individual stars, together with the number of plates involved, are as follows: ξ Persei (7), λ Orionis (5), ι Orionis (5), 15 Monocerotis (6), 68 Cygni (5), 19 Cephei (6) and 10 Lacertae (5).

The stellar spectra were photographed on Ilford Astra VIII panchromatic emulsion, using the 36-inch Cassegrain reflector and its attached Hilger universal spectrograph. The latter instrument was used with its two-prism arrangement, giving dispersions 132, 45 and 28 A/mm at Hα, Hβ and Hγ respectively. Each plate was calibrated by means of two exposures in a multiple slit spectrograph, and brush developed in Ilford I.D.2 developer.

The measurement of the plates was carried out by means of a non-recording thermoelectric microphotometer. Wave-lengths were determined from the positions of those stellar lines which were free from disturbing blends; or, when the plates had a comparison spectrum and the radial velocity was known, wave-lengths were determined from the positions of the comparison lines, making allowance for the radial velocity, the Earth's orbital motion and the curvature of the slit image. In each case a determined Hartmann formula was used as an intermediary.

The measurements of the spectrograms were carried out directly in terms of Baker's function Δ, where

$$\Delta = \log_{10}\left(\frac{1-T}{T}\right),$$

T being the transparency of the negative (see Section 2 of reference **5**). The choice of this function Δ was made because of its approximate linearity with the logarithm of monochromatic light intensity.

The measurements of the spectra of the different stars were carried out with different widths of analysing slit. The reason for this is that different slit widths

were used with the spectrograph in photographing the spectra of stars of different magnitudes. In order to lose no resolving power due to the measurement of spectrograms, the principle was adopted to use an analysing slit whose width of geometric image on the plate was about one-third to one-half of that of the geometric image of the spectrograph slit on the plate. The variation of the former was 12 μ–20 μ, and of the latter 25 μ–50 μ.

For a complete and detailed account of the instruments and the technique of observation and measurement, the reader is referred to a paper by Baker (**5**). This paper also gives the results for the total intensities of a number of the stronger lines in the spectra of the same seven Oe5 stars, using the same plates and procedure as adopted in the present investigation. The reason why the series in question was not discovered then lies principally in the fact that the regions of wave-length then measured did not cover any components of the series which were both free from blends and strong enough for detection. The measures have since been extended by the writer to cover all the components of the series which lie within the sensitivity range of the emulsion. The result is a continuous series of measures covering the wave-length range $\lambda\lambda$ 5625–6825, and embracing the thirteenth (λ 6683) and all higher members of the series up to the series limit at λ 5695. From now on, descriptions of measurements and reductions will refer to this spectral range as a whole.

The measuring mesh was adopted to suit the main characteristics of the spectrum and also for convenience. By far the greatest part of the spectral range is covered by measures at intervals of five divisions of the microphotometer screw drum-head (25·4 μ). As far as we are concerned, this is the effective mesh, since all the components of He II 5 $^2G - n\,^2H^0$, etc. for which intensities were computed are covered by it.

The calibration spectra were measured at five wave-lengths only, and the measures at each wave-length were reduced to values of the contrast factor F, where

$$F = -\Delta/m$$

and

$$m = 2{\cdot}5 \log_{10} (i/I).$$

I is the monochromatic light intensity which produces a blackening Δ and i is the corresponding light intensity which produces a blackening $\Delta = 0$. Bearing in mind the method of zero reference, we can regard m as a kind of monochromatic magnitude.*

Since Δ is approximately proportional to m, then F varies little with Δ. It is also found that F does not vary rapidly with wave-length. Hence, although the calibration spectra were measured at only a limited number of wave-lengths, interpolation of plate characteristics could be carried out with sufficient accuracy for other wave-lengths. How this was done will be explained in the following section, and it will also be seen that there is a further reason for the use of contrast factors as defined above, since they are also instrumental in a considerable saving of the computational labour involved in the Greaves–Baker method of reduction of spectrograms.

3. *The reductions.*—The specialized method by which the measures of the spectra were reduced is in general use at this Observatory. The method was

* m is not a monochromatic magnitude in the strict sense, since the zero point used is the magnitude corresponding to $\Delta = 0$, and so varies from plate to plate, the variation depending on the conditions of exposure including the altitude of the star.

initiated by Greaves and developed and applied by Baker (**5**). Only the main features will be described here, in reference to the present investigation, since the technical details can be found in the above reference.

The method has two main features. The first can be described as the combination of the measures of several negatives *without* smoothing. This was achieved as follows. The measures of the individual spectrograms of each star were superimposed numerically, wave-length for wave-length, to give a value of $\Sigma\Delta$ at every measured wave-length. Similarly, the sum of the effective contrast factors ΣF was determined at each wave-length by interpolation between the values of ΣF applicable to the five wave-lengths at which the calibration spectra were measured (see Section 2), account being taken of any variations in ΣF through spectral lines. The values of ΣF were then applied to the corresponding values of $\Sigma\Delta$ to give values of m_s, where

$$m_s = -\Sigma\Delta/\Sigma F.$$

This value m_s is the weighted mean of the individual magnitudes m with weights F. It is chosen in preference to the straight mean of $m = n^{-1}(\Sigma\Delta/F)$ because of the considerable saving of computational labour. It should be pointed out that the operation is made possible only by the use of contrast factors F as here defined.

Looking ahead, however, it will be noticed that any method of determining the hypothetical continuum within a spectral line will give corresponding values of m_s which are the weighted means of the individual values of m in the "continuum", the weights being the contrast factors F' applicable to the "continuum". Hence, if there is any variation in F through a spectral line, then a point on the line profile has a system of weighting different from that of its corresponding point in the hypothetical continuum. In computing the magnitude in a line profile relative to its hypothetical continuum, this is taken account of by the application of a small correction (see Section 8 of reference **5**) which reduces the weighting to F' in each case. The correction depends on the dispersion of the quantity F'/F for the spectrograms involved. It is very often zero and usually only becomes appreciable for strong lines. For such faint lines as the components of the series investigated here, it is completely negligible, and no more reference need be made to it in this paper.

The second main feature of the Greaves–Baker method of reduction lies in the method of determining the hypothetical continuum within a spectral line. This represents one of the most troublesome problems of stellar spectrophotometry. Indeed, the large differences sometimes found between the results of different observers are probably due partly to this cause. The method used here is to reduce the measures to a function which gives an approximately linear plot against $1/\lambda$. This was achieved as follows.

Five of the stars quoted above were selected as having narrow lines (ξ Persei and 68 Cygni were omitted because of their relatively broad lines) and the values of m_s for these stars were meaned wave-length for wave-length. The result was a narrow-lined spectrum of high accuracy, involving twenty-seven negatives, through which a "continuum" could be drawn with considerable accuracy. The individual stellar spectra were then reduced with reference to this "mean Oe5 continuum" ($\bar{m}'$), giving values of $m_s - \bar{m}'$.

The result of the above operation was to reduce substantially the observed continuum curvature of the individual spectra, and it could be assumed*, within the limits of accuracy, that the plot of $m_s - \bar{m}'$ against $1/\lambda$ gave a linear "continuum" *throughout the restricted spectral range* embracing any one spectral line and those points, free from real disturbance, which lie close to it and which form the basis of reference for the determination of the hypothetical continuum within the line. How these continuum reference points were selected for the present investigation will be explained in the next section.

The method of measurement and reduction described above was designed by Greaves and Baker so as to minimize the considerable amount of labour involved. It seeks to attain as high a standard of spectrophotometry as is possible with the material available, and it is hoped that it has considerably reduced two of the worst types of errors which afflict stellar spectrophotometry, namely, systematic errors and errors of personal judgment.

The manner of combining the measures of individual negatives, outlined above, has the effect that random fluctuations due to photographic plate grain, etc. are reduced, whereas any real features are preserved. For the detection of faint lines, such as the higher members of the series He II $5\,^2G - n\,^2H^0$, etc., a method which means the unsmoothed measures of individual negatives is essential, since the disturbances caused by these lines are less than the fluctuations arising from "graininess", and cannot be detected on individual negatives. The work described in the following section of this paper, consisting in essence of the detection and measurement of the series He II $5\,^2G - n\,^2H^0$, etc., could not have been carried out using the "normal" spectrophotometric procedure whereby the microphotometer tracings of individual spectrograms are smoothed "free-hand", thus suppressing any real features which are masked by photographic grain.

4. *The results.*—It was seen in the two preceding sections how the measures of the individual spectrograms of each star were combined without smoothing and reduced with reference to the "mean Oe5 continuum" to give values of $m_s - \bar{m}'$ at each measured wave-length. The results for all seven stars investigated were then combined, again without smoothing, by meaning the values of $m_s - \bar{m}'$ at each measured wave-length. The result was a mean Oe5 spectrum of high accuracy, incorporating data from seven stars and thirty-nine spectrograms. A section of this mean spectrum, over the wave-length range $\lambda\,5955$–$\lambda\,6543$, is reproduced in Fig. 1 as a plot of the mean relative magnitude $\bar{m}_s - \bar{m}'$ against $1/\lambda$. Adjacent measures are joined by a straight line. Each individual point has a mean square error of $\pm 0{\cdot}004$ magnitudes.

The effect of the meaning technique now becomes apparent. The camouflage of photographic plate grain has been largely removed, thus bringing into relief the components of He II $5\,^2G - n\,^2H^0$, etc., the positions and upper quantum numbers of which are indicated in the figure. It will be noticed that the wave-lengths of the series lines correspond to depressions in the plot. A similar plot for stars of type B1, constructed as a check, gave no such correspondence.

Ten components of the series (given by $n = 14$ to $n = 23$ inclusive) are covered by the wave-length range plotted in Fig. 1. Their central depressions below the continuum have an average value of about one per cent, which is only two to three

* See Section 7 of reference **5**.

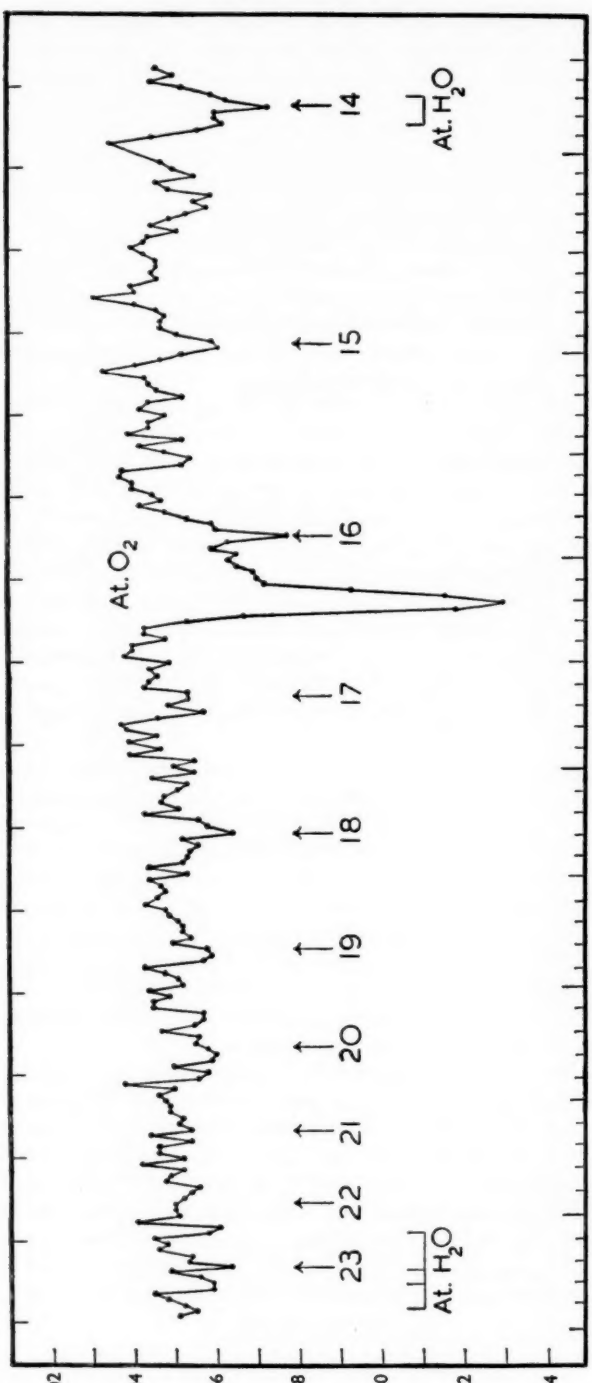

FIG. 1.—*Plot of mean relative magnitude of seven Oe5 stars (thirty-nine plates) against* $1/\lambda$, *showing presence of a number of the higher components of He II* $5\,{}^2G - n\,{}^2H^0$, *etc., the upper quantum numbers (n) of which are indicated.*

times the mean square error of a single point. An observation of a single series member, therefore, cannot be taken as conclusive proof of the existence of the series. However, the cumulative evidence, arising from the observations of a number of components, puts the matter beyond doubt.

Intensity measurements were carried out on those members of the series which are free from interference. It was seen in the preceding section how the spectra were reduced to an approximately linear continuum, and it only remains to select points free from real disturbance, on either side of each spectral line, in order to be able to interpolate linearly between their means and obtain the hypothetical continuum within the lines.

These continuum reference points were obtained from an examination of the seven-star mean Oe5 spectrum. An identification of the stellar, interstellar and atmospheric lines causing real disturbance was carried out and the measured points affected were eliminated. In those cases where it was doubtful whether disturbances in the spectrum were real or not, the points involved were also eliminated.

The greatest difficulty encountered in selecting continuum reference points lay in determining the ranges of wave-length affected by the lines of the series under consideration. These ranges were also required to be known for purposes of integration for total intensity.

With such faint lines, one individual line profile is not sufficiently accurate for this purpose. It was therefore decided to construct a mean profile for those members of the series which are free from blends for a considerable range of wave-length on either side of the line centre. There are six such lines, namely, those given by $n = 15, 17, 18, 19, 20, 21$. For simplicity, the superposition and meaning of these line profiles were carried out on the basis of microphotometer screw revolutions. Since the same measuring mesh was used in each case, this was done by meaning the corresponding measures of each profile taken with reference to the measured points whose wave-lengths were nearest to the true line centres. Over the range of wave-length affected, this is almost the same as using a $(1/\lambda)$ basis.

The mean profile of the six lines is depicted in Fig. 2. The mean relative magnitudes $\overline{(\bar{m}_s - \bar{m}')}$ are plotted against microphotometer screw revolutions Δx with reference to the line centre. The means of the conversions of intervals of 0·1 in Δx to intervals of $\Delta\lambda$ and $\Delta(1/\lambda)$ are 5·5 A and 14·4 cm^{-1} respectively. Since the individual line profiles are obtained from thirty-nine spectrograms, each point on the mean profile is obtained from two hundred and thirty-four measures, and has a mean square error of $\pm 0{\cdot}002$ magnitudes.

From this mean profile, the range of microphotometer screw revolutions affected by the lines was adopted to be 0·5, and the eleven measured points within this range were eliminated in selecting continuum reference points for each line. The "continuum" given in Fig. 2 is a linear interpolation between the means of the remaining four points on either side of the line. For purposes of total intensity measurements, the range of integration was adopted to be 0·6 microphotometer screw revolutions.

The above method of determining the range of disturbance of the components is not perfect, since the range may vary with different series members. In fact, Fig. 1 suggests that the line intensity decreases with increasing n, and it would seem possible that intensity determinations of the components would be

underestimated for the smaller values of n as a result of the adopted continuum being affected by the line absorption and the range of integration being too short. But an examination of the measured profile of that line whose upper quantum number ($n=15$) is the lowest examined for total intensity does not suggest that the line covers a wave-length range in excess of 37 A (corresponding to 0·6 screw revolutions) and it seems that the error, if it exists at all, is trivial. It is considered that the method used, which is free from the personal judgment involved in assigning, *ad hoc*, a separate wave-length range to each line, represents the best that can be done.

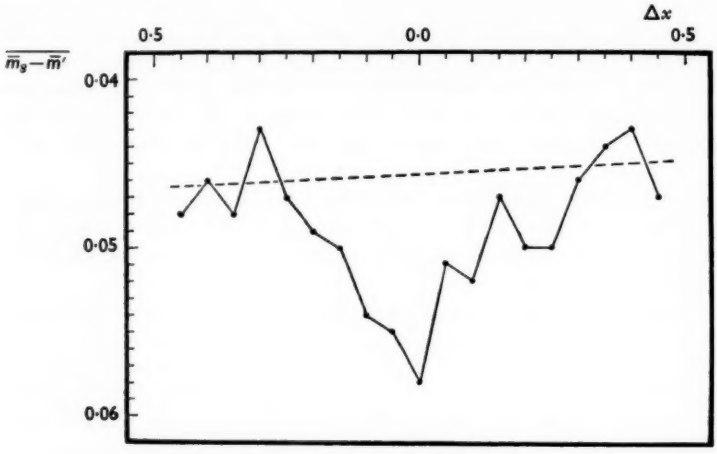

FIG. 2.—*Mean profile of six members of He II* 5 $^2G-n\,^2H^0$, *etc. (red right).*
$(\overline{m_s-m'})$—*mean relative magnitude.*
Δx—*microphotometer screw revolutions with respect to line centre.*
Mean conversions: 0·1 *in* $\Delta x=5{\cdot}5$ *A and* 14·4 cm^{-1}.

Measurements were made of the observed intensity depression (I_c) at the line centre in terms of percentage of continuum, and the total intensity W in equivalent angstroms. The measurement of I_c was made at the exact wave-length of the line centre using spectrum plots which have consecutive points linked by a straight line. Thus the magnitude of the profile at the line centre was determined by the weighted mean of the adjacent measured points, obtained by a linear interpolation between them.

The results for the mean of the seven stars are given in Table I. The first column gives the upper quantum number n of the components of the series. The second column gives the wave-length λ, the computation of which is explained in the next section. The third column gives the observed intensity depression I_c at the line centre in percentage of continuum. The fourth and fifth columns give respectively the range of integration a in angstroms and the total intensity W in equivalent angstroms. The final column, headed "Remarks", is self-explanatory.

The mean square errors given for I_c and W are average values for the results given in the table. Briefly, they were obtained as follows. The mean square error of a single point in the seven-star mean spectrum was computed from the

deviations of the continuum reference points from the determined continuum. The value obtained was $\pm 0{\cdot}004$ magnitudes, and from this the mean square errors of I_e and W were calculated.

The values of I_e do not give the true values of the central intensity depressions in the lines, due to the instrumental distortion of the profiles. They do, however, give estimates of the relative strengths of the components, and the results given in Table I clearly indicate the decrease in intensity of the components with increasing n.

TABLE I

Results for He II $5\ {}^2G - n\ {}^2H^0$, *etc.*

I_e—observed intensity depression at line centre in percentage of continuum
W—total intensity in equivalent angstroms integrated over wave-length range a in angstroms
Values given are for mean of seven Oe5 stars

n	λ (*I.A.*)	I_e	a	W	Remarks
13	6683·23				Blended with He I λ 6678
14	6527·13	2·2			Wings affected by At. H_2O
15	6406·41	1·6	37	0·17	
16	6310·89				Blended with At. O_2
17	6233·85	0·9	34	0·12	
18	6170·72	1·3	33	0·14	
19	6118·29	0·8	32	0·15	
20	6074·23	0·9	31	0·23	
21	6036·81	0·5	31	0·05	
22	6004·75	0·3			Violet wing affected by At. H_2O
23	5977·06				Blended with At. H_2O
24	5952·96				Blended with At. H_2O
25	5931·86				Blended with At. H_2O
26	5913·27				Blended with At. H_2O
27	5896·81				Blended with Na I (D_1)
28	5882·15				Blended with He I (D_3)
29	5869·05				Blended with He I (D_3)
30	5857·29	0·7			
31	5846·68	0·1			
32	5837·09	0·5			
33	5828·39	−0·1			
34	5820·46	0·0			
M.S. Error		±0·3		±0·05	

The lowest member ($n = 13$) of the series which is inside the sensitivity range of the emulsion is blended with the He I line at λ6678. This will affect any determinations of the strength of He I λ6678 in early-type stars. As can be seen from Table I, the strength of the thirteenth member in Oe5 stars is possibly greater than 0·2 A and will therefore seriously affect any previous determinations of the strength of He I λ6678 in such stars.

The highest members of the series ($n = 30$ to 34 inclusive) for which intensity measures were made lie in a "window" of the spectrum between He I (D_3) and a pair of C IV lines. No measures of W are given for these lines since, if the mean profile of the lower series members, given in Fig. 2, is any indication, the profiles of these higher members will overlap. Only measures of I_e were made, therefore,

and these clearly indicate the weakening of intensity in the higher members of the series. However, the criterion (stated above) for determining continuum reference points could not be observed for these components, and the values of I_c may be slightly underestimated since, if the profiles do overlap, the reference points from which the "continuum" within the lines was determined will be affected by the line absorption.

As was mentioned in Section 2, measures were made to cover the series limit at $\lambda 5695$. Hopes of detecting any small discontinuity were destroyed, however, by the presence of C III $\lambda 5696$, which appears in emission.

The results, given above in Table I, are for the mean of the seven Oe5 stars investigated. The reason for this, as was explained above, is the relatively large mean square error of the determination of the intensities of such faint lines in the individual stellar spectra. In order to determine the strength of the series in the different stars, therefore, the individual total intensities were meaned in each star for those components which are free from interference. Since there are six such components (given by $n = 15$, and 17–21 inclusive) the mean square error of their average total intensity in one stellar spectrum is reduced to a reasonable value, namely, $\pm 0{\cdot}06$ A.

The mean total intensity of these six components is given in Table II for the individual stars. Also given are the results for some other He II lines obtained by Baker (**5**). These were obtained using the same material and method as for the present investigation. The results given in the table, therefore, are strictly homogeneous. The values given are the actual total intensities integrated over the ranges of wave-length given at the foot of the intensity columns. The results, therefore, include the intensity effects of any other lines which may be present within the range of integration. Estimates of the intensities of these blended lines are given in the table. Only two lines are affected, namely, $\lambda 4542$ and $\lambda 4200$. The blend estimates for these were obtained by Baker (**5**) from an examination of the mean profiles for five of the stars (all except ξ Persei and 68 Cygni). This must be remembered in applying them to individual star results. The blends for $\lambda 4542$ are due mostly to N III and the blends for $\lambda 4200$ are due entirely to N III.

The name, HD number and Victoria spectral classification of the stars are given in the first three columns. The next five columns give the total intensities, in equivalent angstroms, of the various He II lines. The last column gives the number of plates used for each star. The values in brackets refer to $\lambda 5412$, for which a number of plates had to be rejected because of low photographic density, this line lying in a rather insensitive region of the emulsion. The mean square errors, given at the foot of the intensity columns, are averages for the seven stars.

Only one comment will be made about the results given in Table II. The total intensities given for the line which originates from the third quantum level ($\lambda 4686$) are much smaller than would be expected from normal considerations. This indicates the presence of incipient emission, and this must be borne in mind before using the results for any theoretical investigations.

5. *Wave-lengths.*—Approximate values of the wave-lengths of the series He II $5\,{}^2G - n\,{}^2H^0$, etc. can be easily computed from Bohr's simple formula given in Section 1. This formula was obtained on the assumption of circular electron orbits and does not, therefore, include the Sommerfeld fine-structure modification (**6**). Since the spectral lines of the series in question exhibit wide fine-structure, any accurate calculation of their wave-lengths must take account of this.

The Sommerfeld fine-structure expression for the term value T_n of the nth quantum state of a single-electron atom has been determined by Gordon (**7**) using the wave-mechanical theory of the hydrogen atom as developed by Dirac (**8**). This expression has been slightly modified in recent years by Lamb and Retherford (**9**), who have shown that the s-levels are subjected to a shift.

TABLE II

Total intensities of He II lines in equivalent angstroms for individual stars

A: *He II* $3\ ^2D-4\ ^2F^0$, *etc.* $\lambda 4686$
B: *He II* $4\ ^2F^0-7\ ^2G$, *etc.* $\lambda 5412$
C: *He II* $4\ ^2F^0-9\ ^2G$, *etc.* $\lambda 4542$
D: *He II* $4\ ^2F^0-11\ ^2G$, *etc.* $\lambda 4200$
E: *He II* $5\ ^2G-n\ ^2H^0$, *etc.* (*mean of six components—see text*)

Star	HD No.	Vict. Type	Total Intensity W					No. of Plates
			A	*B*	*C*	*D*	*E*	
ξ Per	24912	O7nk	0·36	1·10	0·78	0·51	0·20	7(5)
λ Ori	36861	O8sk	0·82	0·80	0·71	0·48	0·11	5(5)
ι Ori	37043	O8sk	0·43	0·70	0·42	0·37	0·11	5(4)
15 Mon	47839	O7sk	0·83	0·68	0·61	0·37	0·18	6(4)
68 Cyg	203064	O8nnk	0·53	1·05	0·59	0·39	0·14	5(4)
19 Cep	209975	O9k	0·42	0·74	0·46	0·36	0·14	6(4)
10 Lac	214680	O9sk	0·98	0·88	0·79	0·42	0·13	5(3)
Integration Range			12	21	18	12	(33)	
Blend Intensity			...	...	0·10	0·06	...	
M.S. Error			±0·06	±0·09	±0·07	±0·05	±0·06	

The exact formula for T_n may be expressed by

$$T_n = \frac{RZ^2}{n^2} - \frac{R\alpha^2 Z^4}{n^3}\left(-\frac{1}{J+\frac{1}{2}} + \frac{3}{4n} + \Lambda\right) + \ldots,$$

where R is the Rydberg constant, Z is the atomic number, J is the inner quantum number, Λ is the s-shift parameter and α is the Sommerfeld fine-structure constant, given by

$$\alpha = 2\pi e^2/hc,$$

where e is the charge of the electron, h is Planck's constant and c is the velocity of light.

The expression is an infinite series for which only the first two terms have been given, the higher terms being negligible. The first term is the same as derived by Bohr for circular orbits, and is by far the greatest. It will be noticed that fine-structure levels with the same J-values are coincident (except for the s-terms).

For ^{4}He II ($Z=2$), the values of the constants are :

$$R = 109\,722{\cdot}264\ \text{cm}^{-1},$$
$$\alpha^2 = 5{\cdot}325\,6 \times 10^{-5},$$
$$\Lambda = 0{\cdot}040 \text{ for an } s\text{-level},$$
$$= 0 \text{ for other levels.}$$

These constants are the best available and were taken from a publication of the U.S. National Bureau of Standards (**9**) in which a number of the term values of the He II levels were calculated by Mack.

The fifth level embraces the L-values 0–4 (S–G) and the J-values 1/2–9/2. For the series $5\,^2G - n\,^2H^0$, etc., the effective higher levels are therefore embraced by the L-values 0–5 (S–H) and the J-values 1/2–11/2. The application of selection rules gives the total number of fine-structure components in each spectral line of the series to be twenty-five. It is necessary to know the relative strengths of these fine-structure components, as well as their wave-lengths, in order to compute the wave-lengths of their centres of gravity. The method of approach was to determine the effective centres of gravity of the fine-structure term values for the various levels and to convert to wave-lengths for the different transitions.

Since we are only concerned with the wave-lengths of the higher components ($n = 13$ to 34 inclusive) of the series, the fine-structure separation is due almost entirely to the fifth level. This is shown by the separations of the extreme effective terms ($^2P^0_{1/2}$ and $^2H^0_{11/2}$), which are 0·036 cm^{-1} and 0·002 cm^{-1} for the levels $n = 13$ and $n = 34$ respectively. These values correspond to a fine-structure separation in the 13th and 34th members of the series of 0·016 A and 0·001 A respectively. The effective centres of gravity of the higher levels, therefore, can be determined by some simple approximation which would give an accuracy, expressed in terms of the wave-lengths of the series, of something better than 0·01 A. The approximation adopted was to use the term value T_n corresponding to a central J-value (5/2), and the computations were carried out for $n = 13$ to 34 inclusive.

Such a simple approximation is not possible for the fifth level, the separation of the extreme terms ($^2P^0_{1/2}$ and $^2G_{9/2}$) being 0·599 cm^{-1}, which corresponds to a fine-structure separation in the 13th and 34th members of the series of 0·269 A and 0·203 A respectively. It is therefore necessary to determine the relative intensities of the fine-structure components in the spectral lines, thereby obtaining weights applicable to the individual term values of the fifth level in order to give its centre of gravity.

Each individual member of the series is composed of nine multiplets giving a total of twenty-five individual components. Since the components have approximately the same wave-lengths, then the relative intensities within each multiplet are easily determined from the summation rule, which gives the same result as the equations derived with the quantum mechanics by Dirac (**10**).

It is now required to obtain the relative intensities of the individual multiplets, i.e. to assign a common unit to the relative intensities derived from the summation rule. The analytical solution of this problem has been obtained by Schrödinger (**11**) using wave-mechanics. However, the labour involved in computing the values for the present case is quite prohibitive, relative multiplet intensities having only been computed in the comparatively simple cases of Hα and He II λ4686 by Sommerfeld and Unsöld (**12**).

An approximation was given, in part, by the work of Heitler (**13**). Using the Bose–Einstein statistics, Heitler obtained for the intensity θ of a multiplet, formed by a transition $1 \rightarrow 2$ or $2 \rightarrow 1$, the expression

$$\theta = f(E_1 E_2) g_1 g_2,$$

where E_1 and E_2 are the energies and g_1 and g_2 the statistical weights of the respective levels 1 and 2. As E_1 and E_2 vary little for the different multiplets within a spectral line of the series under consideration, then we have the intensity θ of the various multiplets to be given by

$$\theta \propto g_1 g_2 = \Sigma(2J_1+1)\,\Sigma(2J_2+1).$$

A comparison of the results obtained from this formula for the multiplets of He II $3\,^2D-4\,^2F^0$, etc. (λ4686) with the wave-mechanical results of Sommerfeld and Unsöld (**12**) shows reasonable agreement for those multiplets formed by transitions which have $\Delta L=+1$, but large differences for those which have $\Delta L=-1$. The above formula heavily overestimates the latter type of multiplet. It gives the same intensities to two multiplets such as ($^2P^0-{}^2D$) and ($^2D-{}^2P^0$), whereas it is a well-known fact of observational spectroscopy that the latter type of multiplet ($\Delta L=-1$) is relatively very weak.

It was therefore decided to neglect the multiplets for which $\Delta L=-1$ and apply Heitler's formula to those multiplets for which $\Delta L=+1$.

The approximation was first carried out in the case of He II λ4686. The fine-structure pattern thus obtained compared reasonably with that obtained from the wave-mechanical calculations of Sommerfeld and Unsöld. What we are most concerned with, however, is the wave-length difference between the centres of gravity of the fine-structure components as computed from the two types of intensity determination. This was found to be 0·005 A.

This value cannot be taken to give a strict guide to the accuracy with which the intensity approximation can be applied to the series in question. However, since the fine-structure components are closer for the members of He II $5\,^2G-n\,^2H^0$, etc. than for He II λ 4686 (the ratio of the separations of the extreme fine-structure components in the respective cases is about 1 : 2), it is reasonable to assume that the approximation would give an accuracy, in terms of wave-length, of something better than 0·01 A.

Carrying out the summation rule, and applying Heitler's formula for the relative intensities of multiplets with the proviso that those multiplets involving transitions $L\rightarrow L-1$ are negligible, the relative intensities of the fine-structure components in a spectral line of the series He II $5\,^2G-n\,^2H^0$, etc. are found to be:

$^2S-{}^2P^0$	$^2P^0-{}^2D$	$^2D-{}^2F^0$	$^2F^0-{}^2G$	$^2G-{}^2H^0$
1, 2	1, 9, 5	1, 20, 14	1, 35, 27	1, 54, 44

The order of the tabulated intensities in each multiplet is given by the transitions $J\rightarrow J$, $J\rightarrow J+1$, $J-1\rightarrow J$.

These intensities were applied as weights w to the fine-structure terms of the fifth quantum level. These terms have been calculated by Mack (**9**) using the same expression and constants as given above and adopted for this investigation. The term values of the fine-structure levels are given in Table III together with their intensity weights w.

From these, the effective centre of gravity $\overline{T}_5$ of the terms in the fifth quantum level is calculated to be 17 555·682 cm^{-1}.

The method of determining the centres of gravity $\overline{T}_n$ of the fine-structure terms of the upper levels of He II $5\,^2G-n\,^2H^0$, etc. has already been described above. Arguments were given for supposing the accuracy of the determinations of both $\overline{T}_5$ and $\overline{T}_n$ to be something better than 0·01 A in terms of wave-length.

The resulting calculations of the wave-lengths of the series were therefore rounded off to 0·01 A. These wave-lengths are given in Table I (Section 4). In converting from wave-numbers (vacuum) to international angstroms, Kayser's Tables (**14**) were used.

TABLE III

Fine-structure terms T of fifth quantum level of He II giving intensity weights w (see text)

Designation		T (cm^{-1})	w		Σw
	$^2P^0_{1/2}$	17556·198		5	5
$^2S_{1/2}$		17556·168	1+ 2		3
$^2D_{3/2}$	$^2P^0_{3/2}$	17555·824	14;	1+ 9	24
$^2D_{5/2}$	$^2F^0_{5/2}$	17555·699	1+20;	27	48
$^2G_{7/2}$	$^2F^0_{7/2}$	17555·637	44;	1+35	80
$^2G_{9/2}$		17555·599	1+54		55

Acknowledgments.—The substance of this paper formed part of a thesis presented to the University of Edinburgh for the degree of Doctor of Philosophy. The research was carried out under the supervision of Professor W. M. H. Greaves, to whom I am greatly indebted. My thanks are also due to Dr E. A. Baker, from whose work this investigation developed, for his constant interest and advice.

Royal Observatory,
Edinburgh:
1953 *June* 4.

References

(1) E. C. Pickering, *Harvard Circulars*, Nos. 12 and 16, 1896–97.
(2) N. Bohr, *Phil. Mag.*, **26,** 1 and 476, 1913.
(3) A. Fowler, *M.N.*, **73,** 62, 1912.
(4) T. Lyman, *Ap. J.*, **60,** 1, 1924.
(5) E. A. Baker, *Pub. Royal Obs. Edinburgh*, **1,** 15, 1949.
(6) A. Sommerfeld, *Ann. d. Phys.*, **51,** 1, 1916.
(7) W. Gordon, *Zeits. f. Phys.*, **48,** 11, 1928.
(8) P. A. M. Dirac, *Proc. Roy. Soc.* A, **117,** 610, 1928; A, **118,** 351, 1928.
(9) *U.S. Dept. of Comm., Nat. Bureau of Standards*, Circular 467, 1949.
(10) P. A. M. Dirac, *Proc. Roy. Soc.* A, **111,** 281, 1926.
(11) E. Schrödinger, *Ann. d. Phys.*, **80,** 437, 1926.
(12) A. Sommerfeld and A. Unsöld, *Zeits. f. Phys.*, **38,** 237, 1926.
(13) W. Heitler, *Zeits. f. Phys.*, **36,** 101, 1926.
(14) H. Kayser, *Tabelle der Schwingungszahlen*, 1925.

SPECTRA OF THE LATE N-TYPE STARS IN THE ULTRA-VIOLET, VIOLET AND BLUE-GREEN REGIONS

P. Swings, A. McKellar and K. Narahari Rao†*

(Received 1953 June 12)

Summary

Spectrograms of several late N-type stars have been obtained covering the far violet spectral region from λ 4100 to λ 3900. One plate of Y CVn extends the observations into the ultra-violet, radiation being detectable below λ 3500. A list of the wave-lengths of the absorption features and the emission-like spaces between them is given for the interval λ 3400 to λ 4100.

The ultra-violet spectrum of Y CVn is dominated by a series of newly discovered broad absorption bands centred about $\lambda\lambda$ 3790, 3700, 3595 and 3480, for which no identification is found.

The λ 4100–λ 3900 region of the several late N-type stars exhibits the series of absorption bands previously found for Y CVn, these bands being separated by comparatively sharp regions of background radiation. The λ 4050 group of bands as found in the laboratory and in cometary spectra, currently provisionally ascribed to C_3, is discussed. Comparison of the stellar absorptions with the laboratory and cometary bands is made. While the stellar bands cannot be identified with the others for certain, the previous tentative identification is believed strengthened.

The unidentified blue-green bands characteristic of late N-type spectra, as photographed with moderately high resolution, are found to reveal no rotational structure. Hence the suggestion that they might arise from a diatomic hydride must be abandoned. It is noted that the spectrum of the irregular variable, U Hya, sometimes shows the blue-green bands and, when it does, the λ 4050 group and high opacity in the far violet, associated with late N-type spectra, are also present. When the blue-green bands are absent, the violet bands are also absent and the spectrum is of early N-type. Various considerations are believed to favour a polyatomic molecular origin for the blue-green bands; as for the high opacity in the far violet, it is related to the formation of the molecules responsible for the λ 4050 absorption.

Introduction

The violet and ultra-violet regions of the spectra of the cool carbon stars are notoriously difficult to photograph. This is so particularly for the late N-type stars with which the present paper deals. The spectra of R-type and early N-type stars can be photographed down to λ 3500 by exposures several times as long as for M-type stars of comparable class. However, the later N-type spectra (which are *quite* distinct from the early N-type) fall so rapidly in intensity from λ 4400 and even more extremely from λ 4100 to shorter wave-lengths that the spectra of the brightest stars had not been recorded below λ 3900.

The earlier investigators, for example Shane (**1**), were well aware that the extreme decrease in intensity toward the violet was much more than expected

* On leave of absence from Institut d'Astrophysique, Liège, Belgium.
† Present address: National Physical Laboratory of India, New Delhi.

from a source at the temperature indicated for late N-type stars, but the agent giving rise to the opacity was not apparent. In 1947 Shajn and Struve (**2**) photographed the spectrum of UU Aur (N3) to about λ 3900 and by comparing it with an M-type spectrum advanced reasons for supposing the source of extra opacity in the violet and ultra-violet to be at least partly molecular absorptions. In 1948 McKellar (**3**) described a survey of the spectra of several N-type stars in the λ 4000 region and noted that a well-marked group of absorption bands occurred in the spectrum of Y CVn. The strongest band was at λ 4053, and the group was tentatively identified with the λ 4050 group, long known in emission in cometary spectra and first produced in the laboratory by Herzberg in 1942. The likelihood of occurrence of polyatomic molecules in the atmospheres of N-type stars and their possible role in causing the far-violet opacity in the stellar atmospheres were discussed briefly by Swings and McKellar (**4**).

In view of the continuing lack of knowledge of the agent or agents responsible for the high violet and ultra-violet opacity of the late N-type atmospheres, and the provisional nature of the identification of the stellar λ 4053 bands with the laboratory λ 4050 group, it was considered important to secure further spectrographic observations of the late N-type stars. Also, it is possible that observations on stellar spectra may prove of value to the laboratory spectroscopists who are studying the interesting problem of the nature of the emitter of the λ 4050 bands.

Spectrographic observations were therefore undertaken to explore the spectra of the late N-type stars as far into the ultra-violet as possible, and to photograph the already recorded λ 3900–λ 4100 region with the highest practicable resolution. Also, as noted below, certain observations of the unidentified blue-green bands have been obtained and are discussed, since they appear to have some relevance to the general subject under investigation.

Observations and Measurements

The observations were made mainly at the McDonald Observatory in 1949 April and May by P. Swings and K. N. Rao, and at the Dominion Astrophysical Observatory by A. McKellar from 1947 to 1950. The stars observed were the brightest available of type N, the earlier N stars being for comparison with the later types. Spectrograms of several M-type stars were also obtained for comparison purposes. The stars observed included RY Dra (N4p), Y CVn (N3), X Cnc (N3), U Hya (N2), VY UMa (Na), 19 Psc (No), RS Cyg (Nope), Z Psc (No) and UX Dra (No). The dividing line between early N-type and late N-type, judged by marked changes in the far-violet spectrum, and by the occurrence of the blue-green bands, is at N2. As will be discussed later, U Hya (N2) sometimes shows an early and sometimes a late N-type spectrum. The M-type comparison stars, of which spectra in the violet and ultra-violet regions were secured at the McDonald Observatory, included 56 Leo (gM5), BD 15° 2620 (dM3), and BD 9° 1633 (M6).

The spectrograms in the far violet were, of necessity, obtained with low dispersion. One such plate of the star Y CVn (vis. mag. 4·8–6·0) obtained by Swings on 1949 April 22 in an exposure of 6 hours 22 minutes, with a quartz spectrograph and $f/1$ camera at the McDonald Observatory, records the spectrum farther into the ultra-violet than yet reported for a late N-type star.

Upon this plate radiation is detectable as far as about λ 3400 (see Plate 5). In addition, several McDonald spectrograms obtained with somewhat higher dispersion show the λ 3900–λ 4100 region in the spectra of Y CVn and RY Dra with superior resolution (see Plate 6).

Certain spectrograms of the region λ 4800–λ 5200, showing the blue-green unidentified bands, were secured with the three-prism spectrograph at Victoria.

Three of the best plates of Y CVn, two plates of RY Dra and one each of U Hya and X Cnc were measured by P. Swings and K. N. Rao. The results of these measurements, extending from about λ 3400 to λ 4100, are given in Table I. This table is necessarily a rather involved one since, in order to describe the spectrograms, wave-lengths must be recorded not only for the absorption bands or lines, but also for the " apparent emissions " which are actually the spaces between absorption features.

The Ultra-violet Region and the New Wide Bands

The appearance of the ultra-violet spectrum of Y CVn as revealed by spectrogram Q *f*/1, 11931 of the McDonald Observatory, already referred to, is shown in the top strip of Plate 5. From about λ 3880 towards shorter wave-lengths, the intensity is sufficiently depressed to suggest general absorption arising from the λ 3883 sequence of violet CN bands, and, indeed, the CN bands may make a contribution. The structure in the λ 3830–λ 3880 region is, however, certainly not the vibrational structure of the CN system; it is much more irregular and similar in general nature to that in the λ 4100–λ 3900 region of the spectrum of Y CVn. Thus we must conclude that the major contributor to absorption in the λ 3830–λ 3880 region is not CN. The region farther into the ultra-violet seems characterized by a series of wide absorption bands (centred about $\lambda\lambda$ 3790, 3700, 3595, 3480) separated by groups of radiations having almost the appearance of emission lines. The wave-lengths of some of these features are shown on Plate 5, while all that were measurable are recorded in Table I. Spectrograms of the stars RY Dra and U Hya extending weakly as far as λ 3750 show also the existence of the wide absorption centred about λ 3790 and the brighter region near λ 3750.

Several questions arise regarding the new ultra-violet bands. (1) Are the wide absorption bands, or the " apparent emission " regions between them, detectable as such in the spectra of earlier N-type stars or late M-type stars ? (2) Are the " apparent emission " features real emissions or simply regions between absorption bands ? (3) Is there any obvious identification for the wide absorption bands ? Our conclusions on these questions follow.

(1) Along with the spectrum of Y CVn on Plate 5, reproductions are shown from plates of an M-type star and an early N-type star, all obtained with the same spectrograph. These two comparison spectra exhibit no similarity, either in gross or detailed structure, to the spectrum of Y CVn. Additional careful comparisons in the ultra-violet, involving McDonald and Victoria plates of M-, R- and early N-type spectra, as well as reproductions given in Sanford's atlas of spectra of the cool carbon stars (**5**), have indicated no similarities with the spectrum of Y CVn, with the exception of the few coincidences to be expected on the basis of chance. Therefore we conclude that essentially all the prominent features of the ultra-violet spectrum of Y CVn do not occur in

TABLE I

Wave-length measurements on the spectra of late N-type stars in the λ 3380–λ 4150 region

IA. *Region λ 3380–λ 3900 in the spectrum of Y CVn*

Spectral feature	Absorption maxima	Bright maxima	Notes
Maximum in wide bright background		3380 (1⁻nn)	
Centre of wide absorption	3418 (2nn)		
Maximum in wide bright background		3455 (1⁻nn)	
Maximum of wide absorption	3480 (3nn)		
Bright region extending from λ 3535 to λ 3572 with intensity maxima estimated at		3541 (1⁺) 3550 (1) 3558 (1) 3568 (1⁻)	
and with absorption maxima estimated at	3546 (2n) 3554 (2n) 3563 (2n)		
Deep and wide absorption (extension 60 A), with maximum at	3595 (4nn)		
Bright region extending from λ 3634 to λ 3673 with intensity maxima at		3635·6 (3) 3642·6 (2) 3654·5 (3n) 3671·2 (2)	1
and with absorption maxima at	3639 (3) 3649 (3n) 3663 (3nn)		
Deep wide absorption centred near	3700 (4nn)		
with bright region at		3689·4 (1⁺)	
and secondary absorption centres at	3681 (4n)		
and near	3710 (4nn)		
Bright region extending from λ 3728 to λ 3756 with intensity maxima at		3730·5 (1⁺) 3741·7 (2) 3753·6 (4)	2
and with absorption maxima at	3736 (4) 3748 (4)		
Deep wide absorption centred near	3790 (5nn)		
extending from λ 3760 to λ 3815, with bright structure near		3810 (1)	3
and maximum absorption at	3806·7 (6)		
Complex region	3825 (4n) 3840 (4n) 3848 (4n) 3858 (4n) 3870 (4n) 3876 (3n) 3886·8 (4s) 3895·7 (2)	3835·7 (3) 3843·8 (3⁻) 3851·6 (3) 3865·1 (3) 3874·3 (3⁺) 3877·9 (2) 3890·7 (3)	

IB. *Region λ3900–λ4150 in the spectra of Y CVn, RY Dra, U Hya and X Cnc*

Wave-length				Adopted wave-length		
Y CVn	RY Dra	U Hya	X Cnc	Absorption maxima	Bright maxima	Notes
3900·1 (3⁺Sn)	01·0 (0S)				3900·1 (3⁺n)	
07 (2A)				3907 (2)		
08·7 (1S ?)					3908·7 (0)	
14·3 (3⁺S)	14·8 (1S)	16·3 (1S)			3914·6 (3⁺)	
19 (3A)	19 (1A)	19 (1A)		3919 (3)		
23·3 (4S)	26·0 (1S)	24·8 (0S)			3923·9 (4)	4
33·4 (3An)		35·4 (1A)		3934 (3n)		5
40·5 (1S)	39·6 (1S)				3940 (1)	
48·1 (5S)	48·4 (3S)	46·3 (0S)			3948·1 (5)	
54 (2A)	53 (2A)	52 (2A)		3953 (2)		
57·9 (6S)	58·0 (4S)	58·0 (0S)			3957·9 (6)	
65 (2As)	65·4 (1A)	65 (2A)	64·4 (2A)	3965 (2)		
69 (0S)	70·3 (0S)		69·4 (0S)		3969·6 (0)	
76 (3An)	76·8 (2A)		76·3 (2A)	3976 (3n)		
82·4 (8S)	82·5 (6S)	81·3 (1S)	83·8 (1S)		3982·4 (7)	
85 (1A)		84·3 (1A)		3985 (1)		
87 (1S)		87·9 (1S)			3987·5 (1)	
94·1 (5An)	94·7 (1A)	92 (1A)	92 (1A)	3994 (5n)		
3999·6 (1S)					3999·6 (1)	
4002 (1A)				4002 (1)		
04 (1S)		03·7 (0S)			4003·9 (1⁻)	
06 (1A)		06·6 (1A)		4006 (1)		
10·1 (7Sn)	09·7 (5S)	09·1 (3S)	09·0 (2S)		4009·6 (6n)	
18 (1S)	16 (0S)	17·2 (0S)			4017·1 (1⁻)	
19·8 (5An)	20 (1An)			4019·8 (5n)		6
	25·3 (0S)	24·3 (1S)			4024·7 (1)	
		28·0 (0S)			4028·0 (0)	
		30·8 (0S)			4030·8 (0)	
37·8 (4S)		36·1 (3S)	36·6 (2S)		4036·4 (3)	
40 (2A)				4040 (2)		
	42·4 (0S)		41·8 (1S)		4042·1 (1⁻)	
		47·5 (1S)	45·3 (1S)		4046·8 (1)	
53·2 (7A)	52·2 (6A)	52·5 (2A)	53·8 (2A)	4052·8 (6)		
62·1 (0S)	65·4 (1S)		65·9 (1S)		4064·5 (1)	
4075·1 (3A)	75·4 (1A)		75·1 (3A)	4075·2 (3)		7
	89·7 (0A)		87·4 (0A)	4088·6 (0)		
4102·2 (2A)	04·0 (1A)	02·3 (2A)	01·8 (1A)	4103·1 (2)		
		12·2 (0A)		4112 (0)		
		24·7 (0A)		4125 (0)		
		29·4 (0A)		4129 (0)		
	32·4 (0A)	34·9 (0A)		4134 (0)		
	44·8 (0A)			4145 (0)		

NOTES

n, wide. nn, very wide. A, absorption. S, bright region (space between absorptions).

1 : probably double.

2 : possibly with longward emission wing.

3 : accompanied by a sharper absorption feature at 3806·7.

4 : perhaps double.

5 : probably Ca II absorption line.

6 : In the spectrum of X Cnc a double absorption line was measured at λ 4016 (2A) and λ 4027 (2A) with a bright maximum at λ 4021.

7 : In the spectrum of U Hya the absorption line is double at λ 4073·4 (1A) 4076·8 (2A) with a bright maximum at λ 4074·8. For Y CVn a weak absorption appears at 4079·0 (0A).

R-type, early N-type or M-type spectra, but are characteristic of late N-type spectra.

(2) As will be described in more detail in discussing the λ 4050 region, the apparent emissions are undoubtedly only regions of the stellar spectrum showing through between absorption bands and, despite their appearance, are not emission lines.

(3) The wide absorption bands, which on the one available plate seem possibly to be slightly shaded toward shorter wave-length, do not correspond, in so far as we can determine, to any set of bands yet produced in the laboratory.

The λ 4050 Wave-length Region

The region of wave-lengths λ 3900 to λ 4100 in the spectra of the late N-type stars will be called the λ 4050 region both for brevity and also because of the possible connection of the absorption bands appearing in this region with the well-known λ 4050 group of cometary bands. Considerable work on the λ 4050 bands has been done in recent years by laboratory spectroscopists. We shall describe briefly the cometary and laboratory bands, then the stellar bands, and examine the question of whether they are the same group or system.

The λ 4050 group of cometary bands.—The λ 4050 group of emission bands in cometary spectra has been known since the beginning of the century. The strongest band is centred at λ 4051 and the other more prominent bands occur at about λλ 3992, 4014, 4020, 4039, 4043, 4069, 4074 and 4100. With the low dispersion required for photographing cometary spectra, the bands show neither well-defined heads nor uniform shading either to red or violet, but rather appear as a group of semi-headless bands, the intensities of the individual bands decreasing with distance from the main band at λ 4051. The extent of the band in space from the cometary nucleus is greater than that of CH, but not as great as CN or C_2. The intensity of the λ 4050 group relative to the CN and C_2 bands is greater at larger heliocentric distances (>1 astronomical unit) than at smaller heliocentric distances. This, on currently accepted ideas of the increase of photo-dissociation and photo-ionization of cometary gases with decreasing heliocentric distance, is suggestive of a polyatomic rather than diatomic origin for the bands. The several attempts by various investigators prior to 1940 to account for the group as CH Raffety bands, CN tail bands, etc. gave unacceptable results.

The λ 4050 group of bands in the laboratory.—In 1942, Herzberg (**6**) produced in the laboratory a set of bands undoubtedly identical with the cometary λ 4050 group. These bands were excited by an interrupted discharge in a rapidly moving stream of methane, and what appeared to be good reasons were advanced for attributing the bands to the molecule CH_2. In the years immediately following 1942, while Herzberg did secure spectrograms of the λ 4051 band with a 21-ft. grating and was able to distinguish Q- and R-like branches, attempts to obtain the system in absorption and to analyse it in detail met with little success. From 1946 onward, more intense sources of the λ 4050 bands were developed by Mme Herman (**7**), by Goldfinger, LeGoff and Letort (**8**), by Monfils and Rosen (**9**) and by Etienne (**10**). These sources allowed the bands to be photographed more easily with higher dispersion, but did not enable a vibrational analysis or a complete rotational analysis to be made. The results

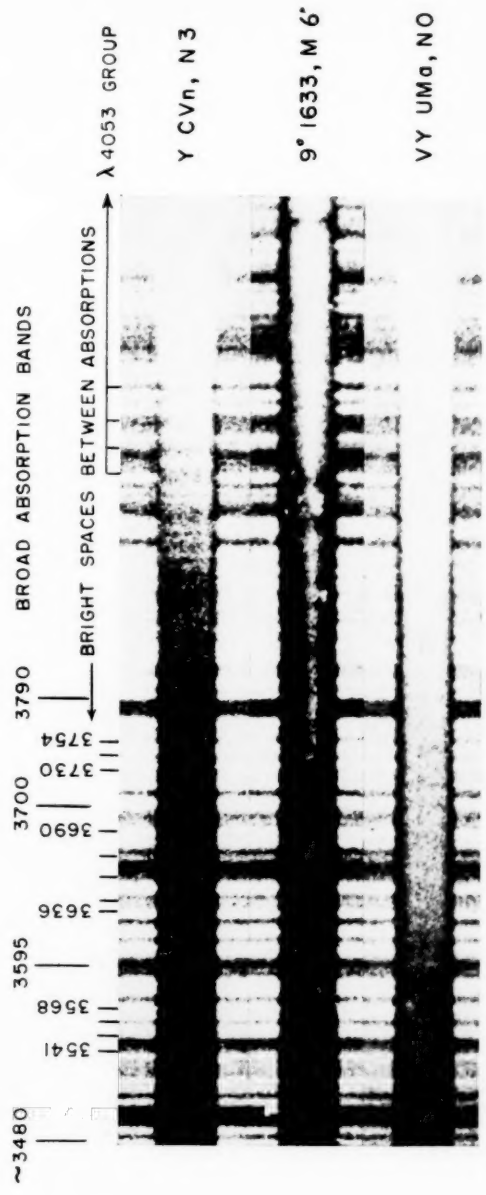

P. Swings, A. McKellar and K. Narahari Rao, Spectra of the late N-type stars in the ultra-violet, violet and blue-green regions

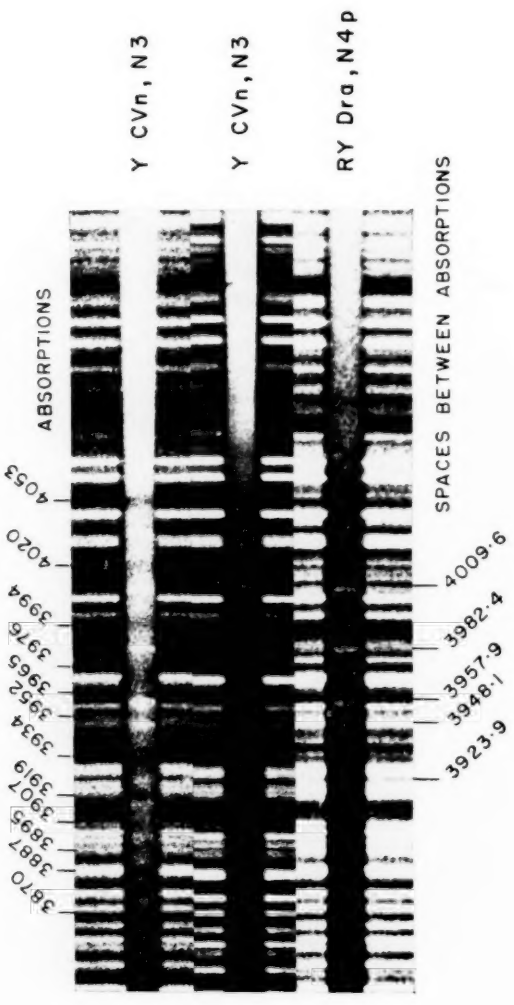

P. Swings, A. McKellar and K. Narahari Rao, *Spectra of the late N-type stars in the ultra-violet, violet and blue-green regions*

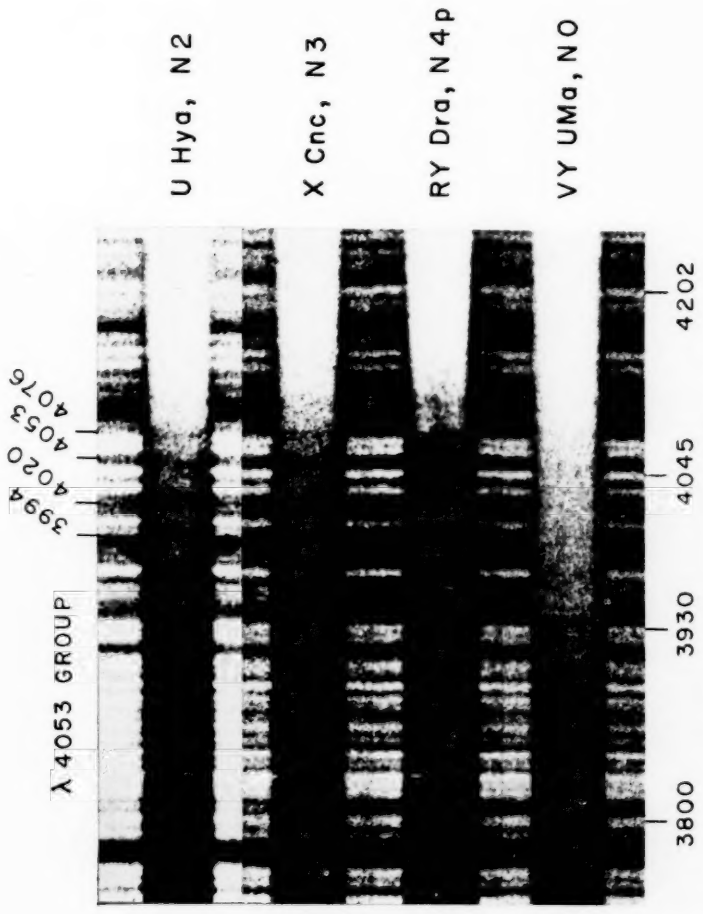

P Swings, A. McKellar and K. Narahari Rao, Spectra of the late N-type stars in the ultra-violet, violet and blue-green regions

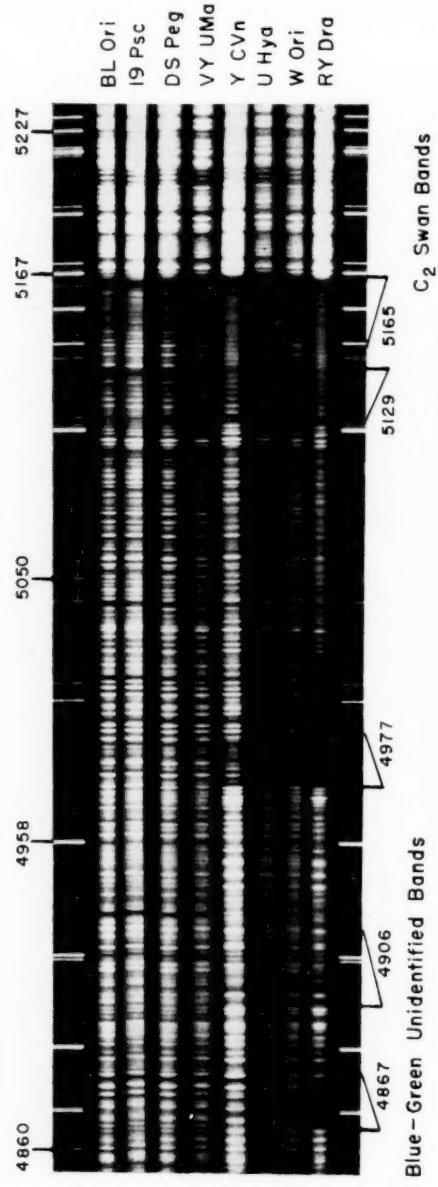

THREE-PRISM SPECTROGRAMS OF EIGHT N-TYPE STARS

P. Swings, A. McKellar and K. Narahari Rao, Spectra of the late N-type stars in the ultra-violet, violet and blue-green regions

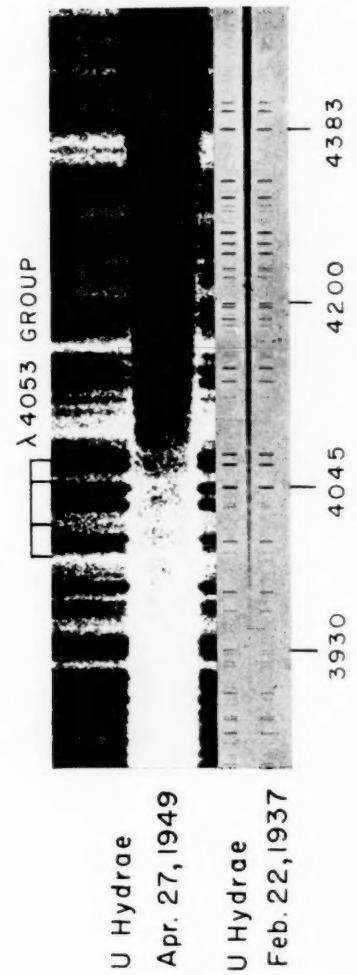

P. Swings, A. McKellar and K. Narahari Rao, Spectra of the late N-type stars in the ultra-violet, violet and blue-green regions

of Monfils and Rosen were of particular importance. They found that when deuterium was substituted for hydrogen in their hollow-cathode source, the structure of the λ 4050 band remained unaltered. This showed that the emitting molecule could not contain hydrogen, therefore could not be CH_2. Douglas (**11**), using the type of source developed by Mme Herman, repeated the experiment of Monfils and Rosen and verified their conclusion. He went further by using in the source a mixture of the carbon isotopes ^{12}C and ^{13}C. This caused the structure of the λ 4051 band to become very complicated, the single main head now becoming one of six heads; the emitting molecule thus was shown to contain probably more than one atom of carbon. Douglas was able to suggest a rotational analysis of the λ 4051 band. At this stage, the possibility that the λ 4050 group might arise from the triatomic molecule C_3 was considered by various investigators interested in these bands*; this suggestion was stated in several lectures by Swings (**12**) in 1951 and was recorded also by Douglas (**11**). Probably the most convincing evidence of this identification to date is the occurrence of the six band heads when a mixture of ^{12}C and ^{13}C is used; the bands would correspond to the six possible isotopic species of C_3. Douglas hopes to secure enough pure ^{13}C to test more rigorously whether the emitter is a linear C_3 molecule. The latest development is the production of the $\lambda\lambda$ 4051 and 4074 bands of the group in absorption by Norrish, Porter and Thrush (**13**), who found the bands in the absorption spectrum of the gaseous mixture resulting from an oxygen-acetylene explosion induced by ultra-violet light. The experiment has been repeated at Ottawa by D. A. Ramsay, who has photographed the λ 4051 absorption band using a 21-ft. grating, and has shown (**14**) the band to be the same, line for line, as its emission counterpart. The production of the λ 4050 group in absorption is important astrophysically since it verifies that the group arises from the normal state of its emitting molecule; this is in keeping with the presence of the bands in cometary spectra (resonance-fluorescence) and gives some support to their suggested presence in the spectra of the late N-type stars.

The present status of the λ 4050 group of bands may be summarized as follows: it has been produced and photographed with high dispersion in the laboratory, both in emission and absorption; there is as yet no vibrational and only an incomplete rotational analysis; the most likely assignment is to an electronic transition from the ground state of a linear or nearly linear C_3 molecule; there is no doubt that the laboratory and the cometary bands are the same.

After describing the absorption bands in the λ 4100–λ 3900 region of the spectra of the late N-type stars, we shall try to decide whether they are actually the λ 4050 group described above.

The λ 4050 group of bands in late N-type stellar spectra.—The appearance of the λ 4100–λ 3900 region in the spectra of the late N-type stars is shown in Plates 6 and 7. Plate 7 illustrates in particular how the three late N-types differ from the early N-type spectrum of VY UMa. Here, as well as in the ultra-violet, the regions between some of the absorptions are so narrow, and so

* One of the authors (A. McK.) was in a particularly favourable position to know the history of the proposed assignment of the λ 4050 bands to C_3. He visited Drs G. Herzberg and A. E. Douglas in Ottawa in 1950 June, at which time the possibility of the C_3 identification was discussed. He also, during 1950, was in correspondence with Dr P. Swings who, with his group in Liège, had independently, on both astronomical and laboratory grounds, considered the same identification, and who suggested, in analogy to oxygen, the descriptive name "carbozone" for C_3.

resemble emission lines, that it seems necessary to establish whether they are, in fact, emission lines or merely narrow zones of radiation escaping between absorption features. The whole spectrum from λ 4100 to the ultra-violet was carefully examined. It was verified that the bright regions did not correspond to known permitted or forbidden atomic or molecular transitions. To examine whether they might arise as some molecular fluorescence pattern, a search was made among their frequencies for coincidences in wave-number interval; only three coincidences were found and were more directly explained as spaces between absorptions of similar band groups. Furthermore, comparison of the late N-spectra with M-, R- and early N-types showed that those bright regions did not, to any significant extent, correspond to wave-lengths between absorption lines or bands characteristic of these types. Therefore all the evidence pointed toward the bright lines being primarily narrow regions of radiation escaping between absorption features characteristic of the late N-type spectra.

The absorption bands in the λ 4050 region in the spectra of Y CVn, RY Dra and U Hya were compared with the λ 4050 bands as measured in cometary spectra. The positions of the emissions of the λ 4050 group in cometary spectra were plotted on enlarged prints of the stellar spectra, and it was found that all such emissions fell in the regions of N-type absorption. Furthermore, there was an overall similarity in the appearance of the bands for the two sources, which might not even be anticipated in view of the different means of excitation in the two cases. From the wave-length measurements there is an apparent tendency for the cometary bands to fall at slightly shorter wave-lengths than the stellar bands; this might be expected since the excitation in the comet corresponds probably to a few hundred degrees while that in the stellar atmosphere to 1 000°–1 500 °K. The present data seem, therefore, to strengthen the case for the identity of stellar and cometary λ 4050 groups.

The absorption in the λ 4050 region of the late N-type stars was next compared with the laboratory bands. The average wave-length of the main band in the stellar spectra, λ 4052·8, falls between one and two angstroms to the violet of the maximum of intensity in the Q-branch of the laboratory band, which extends from the P-branch head at λ 4049·77 to about λ 4065. (See reproduction by Douglas (**11**).) This measured stellar wave-length, when suitable cognizance is taken of the probably lower excitation temperature of the stellar compared to laboratory bands, and of the ^{13}C isotopic shift to shorter wave-lengths, demonstrated by Douglas, together with the presence of bands involving ^{13}C in the spectra of the N stars, seems to be about where the maximum of the band should occur. Similarly for comparison with cometary spectra, the wave-lengths of the other laboratory bands were plotted on enlargements of the stellar spectra. Again the general agreement was good, the only apparent inconsistency being that a group of laboratory lines near λ 4036·2 falls near a bright region in the stellar spectrum at λ 4036. Perhaps this one apparent difficulty may arise because of the different excitation conditions; this cannot be checked until an analysis of the λ 4050 group is available.

Taken altogether, the evidence in favour of the identity of the stellar and laboratory λ 4050 group is fairly strong. Therefore, while our conclusion cannot yet be taken as certain, we are of the opinion that the stellar bands are the same as the laboratory λ 4050 group. If so, and if the currently favoured identification of the bands is correct, the C_3 molecule occurs in the atmospheres of the late N-type stars, as well as in the comets and in laboratory sources.

The Unidentified Blue-Green Bands

The blue-green unidentified bands present in the spectra of certain of the coolest carbon stars were brought into the present investigation because of their possible relation to the violet and ultra-violet bands.

It has long been known that the presence of the blue-green bands distinguished late N-type stars from the earlier subtypes. At the time of the discovery of the λ 4977 band by Merrill (**15**) in 1926, a study of the bands in the λ 4800–λ 5000 region was made by Sanford (**16**). Two years later a similar and related group of bands was found by Shane (**1**) in the λ 4540 to λ 4640 region. The most recent investigation of the bands, in which further members were found in the λ 4260–λ 4350 region, was carried out by McKellar (**17**) in 1947. The molecule responsible for the bands is still not known. A provisional vibrational analysis given indicated that the bands could be assigned to two systems, one strong and the other weaker. The vibrational constants found were in some respects suggestive of a hydride origin, which would mean that the bands should have an open rotational structure. To investigate this point, three-prism spectrograms of several stars, of early and later N-type, were secured at Victoria with dispersion 20 A/mm at λ 5000. Examples of these spectrograms are shown in Plate 8, where the reproductions are arranged in order of increasing strength of the unidentified bands. On the lower spectrograms the heads of the bands at λλ 4977 and 4867 are clearly seen.

Careful comparison of the spectra showing the unidentified bands with the earlier N-types, where the bands do not occur, failed to show any differences that could be ascribed to rotational structure of the bands. Yet, as may be seen on Plate 8, the Swan band of C_2 at λ 5165 shows resolved structure at some distance from its head. The conclusion is that the unidentified bands do not have as open a structure as the C_2 bands. Thus they almost certainly do not arise from a diatomic hydride molecule. If their source is a diatomic molecule, it must be a heavy one. There are arguments against a diatomic molecule as the source, one being that the longer wave-length bands of the pairs are the more intense, which is difficult to understand. In view of the polyatomic origin of the λ 4050 group of bands, we favour a polyatomic molecule as the source of the unidentified blue-green bands.

Probable Relation between New Ultra-violet, λ 4050 and Blue-Green Bands

In considering possible identifications for the new ultra-violet, the λ 4053 and the blue-green bands, an interesting set of wave-number coincidences was found. When the λ 4053 band was taken as a central fixed point, and the wave-numbers of the blue-green and of the ultra-violet bands considered with respect to it, five fairly equal intervals were found, varying between that from the λ 4053 to the λ 4352 and λ 3790 bands ($\sim$1700 cm^{-1}) and that from the λ 4053 to the λ 4977 and λ 3418 bands ($\sim$4580 cm^{-1}). At first we were inclined to think that these coincidences might have some significance, such as being suggestive of a common origin for all three groups of bands. Various difficulties in this interpretation, both theoretical and observational (such as the non-occurrence of the other groups along with the λ 4050 bands in the laboratory) led us to abandon it for the present. If, however, the wave-number coincidences are significant, this fact will probably eventually be shown by laboratory results.

resemble emission lines, that it seems necessary to establish whether they are, in fact, emission lines or merely narrow zones of radiation escaping between absorption features. The whole spectrum from λ 4100 to the ultra-violet was carefully examined. It was verified that the bright regions did not correspond to known permitted or forbidden atomic or molecular transitions. To examine whether they might arise as some molecular fluorescence pattern, a search was made among their frequencies for coincidences in wave-number interval; only three coincidences were found and were more directly explained as spaces between absorptions of similar band groups. Furthermore, comparison of the late N-spectra with M-, R- and early N-types showed that those bright regions did not, to any significant extent, correspond to wave-lengths between absorption lines or bands characteristic of these types. Therefore all the evidence pointed toward the bright lines being primarily narrow regions of radiation escaping between absorption features characteristic of the late N-type spectra.

The absorption bands in the λ 4050 region in the spectra of Y CVn, RY Dra and U Hya were compared with the λ 4050 bands as measured in cometary spectra. The positions of the emissions of the λ 4050 group in cometary spectra were plotted on enlarged prints of the stellar spectra, and it was found that all such emissions fell in the regions of N-type absorption. Furthermore, there was an overall similarity in the appearance of the bands for the two sources, which might not even be anticipated in view of the different means of excitation in the two cases. From the wave-length measurements there is an apparent tendency for the cometary bands to fall at slightly shorter wave-lengths than the stellar bands; this might be expected since the excitation in the comet corresponds probably to a few hundred degrees while that in the stellar atmosphere to 1 000°–1 500 °K. The present data seem, therefore, to strengthen the case for the identity of stellar and cometary λ 4050 groups.

The absorption in the λ 4050 region of the late N-type stars was next compared with the laboratory bands. The average wave-length of the main band in the stellar spectra, λ 4052·8, falls between one and two angstroms to the violet of the maximum of intensity in the Q-branch of the laboratory band, which extends from the P-branch head at λ 4049·77 to about λ 4065. (See reproduction by Douglas (**11**).) This measured stellar wave-length, when suitable cognizance is taken of the probably lower excitation temperature of the stellar compared to laboratory bands, and of the ^{13}C isotopic shift to shorter wave-lengths, demonstrated by Douglas, together with the presence of bands involving ^{13}C in the spectra of the N stars, seems to be about where the maximum of the band should occur. Similarly for comparison with cometary spectra, the wave-lengths of the other laboratory bands were plotted on enlargements of the stellar spectra. Again the general agreement was good, the only apparent inconsistency being that a group of laboratory lines near λ 4036·2 falls near a bright region in the stellar spectrum at λ 4036. Perhaps this one apparent difficulty may arise because of the different excitation conditions; this cannot be checked until an analysis of the λ 4050 group is available.

Taken altogether, the evidence in favour of the identity of the stellar and laboratory λ 4050 group is fairly strong. Therefore, while our conclusion cannot yet be taken as certain, we are of the opinion that the stellar bands are the same as the laboratory λ 4050 group. If so, and if the currently favoured identification of the bands is correct, the C_3 molecule occurs in the atmospheres of the late N-type stars, as well as in the comets and in laboratory sources.

The Unidentified Blue-Green Bands

The blue-green unidentified bands present in the spectra of certain of the coolest carbon stars were brought into the present investigation because of their possible relation to the violet and ultra-violet bands.

It has long been known that the presence of the blue-green bands distinguished late N-type stars from the earlier subtypes. At the time of the discovery of the λ 4977 band by Merrill (**15**) in 1926, a study of the bands in the λ 4800–λ 5000 region was made by Sanford (**16**). Two years later a similar and related group of bands was found by Shane (**1**) in the λ 4540 to λ 4640 region. The most recent investigation of the bands, in which further members were found in the λ 4260–λ 4350 region, was carried out by McKellar (**17**) in 1947. The molecule responsible for the bands is still not known. A provisional vibrational analysis given indicated that the bands could be assigned to two systems, one strong and the other weaker. The vibrational constants found were in some respects suggestive of a hydride origin, which would mean that the bands should have an open rotational structure. To investigate this point, three-prism spectrograms of several stars, of early and later N-type, were secured at Victoria with dispersion 20 A/mm at λ 5000. Examples of these spectrograms are shown in Plate 8, where the reproductions are arranged in order of increasing strength of the unidentified bands. On the lower spectrograms the heads of the bands at $\lambda\lambda$ 4977 and 4867 are clearly seen.

Careful comparison of the spectra showing the unidentified bands with the earlier N-types, where the bands do not occur, failed to show any differences that could be ascribed to rotational structure of the bands. Yet, as may be seen on Plate 8, the Swan band of C_2 at λ 5165 shows resolved structure at some distance from its head. The conclusion is that the unidentified bands do not have as open a structure as the C_2 bands. Thus they almost certainly do not arise from a diatomic hydride molecule. If their source is a diatomic molecule, it must be a heavy one. There are arguments against a diatomic molecule as the source, one being that the longer wave-length bands of the pairs are the more intense, which is difficult to understand. In view of the polyatomic origin of the λ 4050 group of bands, we favour a polyatomic molecule as the source of the unidentified blue-green bands.

Probable Relation between New Ultra-violet, λ 4050 and Blue-Green Bands

In considering possible identifications for the new ultra-violet, the λ 4053 and the blue-green bands, an interesting set of wave-number coincidences was found. When the λ 4053 band was taken as a central fixed point, and the wave-numbers of the blue-green and of the ultra-violet bands considered with respect to it, five fairly equal intervals were found, varying between that from the λ4053 to the λ4352 and λ3790 bands ($\sim$1700 cm^{-1}) and that from the λ4053 to the λ4977 and λ3418 bands ($\sim$4580 cm^{-1}). At first we were inclined to think that these coincidences might have some significance, such as being suggestive of a common origin for all three groups of bands. Various difficulties in this interpretation, both theoretical and observational (such as the non-occurrence of the other groups along with the λ 4050 bands in the laboratory) led us to abandon it for the present. If, however, the wave-number coincidences are significant, this fact will probably eventually be shown by laboratory results.

An interesting observational fact came to light, however, for the star U Hya (N2). While Sanford's atlas of spectrograms of R- and N-type spectra (**5**) showed the blue-green unidentified bands not present, the Victoria three-prism plate showed them present with considerable strength (see Plate 8). Therefore a search was made through the available spectrographic material at the McDonald, Mount Wilson and Victoria Observatories, to compare the behaviour in the blue-green and the λ 4050 regions. We are grateful to Dr T. L. Page of the McDonald Observatory, and Dr A. Deutsch of the Mount Wilson and Palomar Observatories for their kind cooperation in obtaining spectrograms of U Hya.

The results of this investigation are summarized in Table II. From this table it can be seen, so far as can be concluded from the rather scattered data, that when the blue-green bands are present in the spectrum, so also are the λ 4050 bands, and the light decreases rapidly toward the violet. The spectrum then is of late N-type. When, however, the blue-green bands are absent, so also are the λ 4050 bands, and the spectrum resembles that of an early N-type star. Spectrograms of U Hya are shown in Plate 9, where the upper reproduction, from a McDonald plate, shows a late N-type spectrum, and the lower, from a Mount Wilson plate, is of early N-type.

TABLE II

Occurrence of the blue-green bands and the λ 4053 group in the spectrum of U Hydrae

Date	Photographic magnitude*	Intensity of blue-green bands	Intensity of λ 4053 group	Observatory
1914 Apr.	8·65	strong		Mt. Wilson
1923 Feb.	8·50	present		Mt. Wilson
1937 Feb.–Apr.	8·90	absent	absent	Mt. Wilson
1939 May	8·25	absent		Mt. Wilson
1941 Mar.–May	8·10–8·50 (7)	absent		Victoria
1943 Apr.	8·65–9·25 (3)	absent		Mt. Wilson
1944 Feb.	8·20	absent		Victoria
1949 Jan.–May	8·30–9·35 (10)	strong	strong	McDonald and Victoria
1950 Apr.	8·45–8·85 (4)	strong		Victoria
1951 Feb.–Mar.	8·30–8·65 (3)	strong	strong	Mt. Wilson and Victoria

* Magnitudes from Dr S. Gaposchkin's estimates. Where there were determinations on several days in the interval, the range is given, and the number of estimates is shown in brackets.

An attempt was made to relate the occurrence of the bands to the varying brightness of U Hya. A series of estimates of the brightness of the star at and near the times of spectrographic observations was provided by Dr S. Gaposchkin of the Harvard College Observatory, to whom we wish to record our thanks. Gaposchkin's estimates show that U Hya is an irregular variable, with a range in photographic magnitude from 8·1 to 9·4. Changes in brightness of several tenths of a magnitude can take place in a day or two. There is no apparent correlation between the brightness of the star and the occurrence of the bands, on the basis of our present data.

We are able to conclude that the occurrence of the blue-green bands and of the λ 4053 group, and the sharp increase in far-violet opacity can be linked together. This does not solve the problem of the identifications of the molecules

responsible for any of the bands. It does, however, show that the change occurring in the atmosphere of the star, causing the alteration from early to late N-type spectrum, gives rise to absorption both in the blue-green and λ 4053 bands, and strongly suggests that the increased opacity in the far violet and ultra-violet is closely related to the formation of the molecules responsible for the λ 4050 absorption.

Conclusions

The results of our investigation may be summarized as follows.

(1) A series of wide deep absorption bands was found in the ultra-violet region (λ 3800–λ 3400) of the one spectrogram of Y CVn extending into this region.

(2) The λ 4053 group of bands and the associated drop in intensity shortward of λ 4100 occur together for all of the several late N-type stellar spectra studied.

(3) The likelihood of the identity of the λ 4053 group of bands with the λ 4050 laboratory and cometary bands is strengthened by the new data, but cannot yet be regarded as certain.

(4) It was not possible to identify the molecule responsible for the ultra-violet bands, but it is felt that the two unidentified sets of bands (ultra-violet and blue-green) may arise from polyatomic molecules.

(5) The behaviour in the spectrum of U Hya of the blue-green bands and the λ 4053 group, and the rapid decrease in intensity in the far-violet region, tend to support the idea that the great opacity of the atmospheres of the late N-type stars in the far-violet region is related to the presence of polyatomic molecules.

Note added in proof (1954 *January*).—In a private communication Dr G. Herzberg has informed us that K. Clusius and A. E. Douglas in Ottawa, by obtaining spectrograms of the λ 4050 bands using almost pure ^{13}C, have conclusively proved their emitter to be the C_3 molecule. (See paper by K. Clusius and A. E. Douglas to be published in *Canadian Journal of Physics*, 1954.)

McDonald Observatory,
Fort Davis,
Texas:
1953 *June* 10.

Dominion Astrophysical Observatory,
Victoria,
British Columbia.

References

(1) C. D. Shane, *L.O.B.*, **13,** 123, 1928.
(2) G. A. Shajn and O. Struve, *Ap. J.*, **106,** 86, 1947.
(3) A. McKellar, *Ap. J.*, **108,** 453, 1948; *Contr. Dom. Ap. O.*, No. 15, 1948.
(4) P. Swings and A. McKellar, *Ap. J.*, **108,** 458, 1948; *Contr. Dom. Ap. O.*, No 16, 1948.
(5) R. F. Sanford, *Ap. J.*, **111,** 262, 1950.
(6) G. Herzberg, *Ap. J.*, **96,** 314, 1942.
(7) R. Herman, *C. R. Acad. Sci.*, Paris, **223,** 280, 1946.
(8) P. Goldfinger, P. LeGoff and M. Letort, *C. R. Acad. Sci.*, Paris, **227,** 632, 1948.
(9) A. Monfils and B. Rosen, *Nature, Lond.*, **164,** 713, 1949.
(10) R. Etienne, Thesis, Liège, 1950 (unpublished).
(11) A. E. Douglas, *Ap. J.*, **114,** 466, 1951.
(12) P. Swings, *La Physico-Chimie des Comètes*, Université de Paris, Les Conférences du Palais de la Découverte, 1951.
(13) R. G. W. Norrish, G. Porter and B. A. Thrush, *Nature, Lond.*, **169,** 582, 1952.
(14) Private communication from G. Herzberg.
(15) P. W. Merrill, *P.A.S.P.*, **38,** 175, 1926.
(16) R. F. Sanford, *P.A.S.P.*, **38,** 177, 1926.
(17) A. McKellar, *J.R.A.S. Can.*, **41,** 141, 1947; *Contr. Dom. Ap. O.*, No. 7, 1947.

THERMAL RADIO EMISSION FROM THE SUN AND THE SOURCE OF CORONAL HEATING

J. H. Piddington and R. D. Davies

(Received 1953 February 10)

Summary

Measurements of *thermal* solar radio noise confirm the existence of a hot corona and indicate the presence of even hotter regions above sunspots. These regions are proposed as a source of coronal energy and their properties investigated. Radio data extending over a period of several years are statistically analysed to separate the total radiation into two components, one associated with sunspots and the other showing no such connection.

The following conclusions are reached :

(*a*) The sunspot radiation and the very hot regions responsible for it diminish less rapidly than the spot area and exist for a month or more after the spot has vanished.

(*b*) For this and other reasons, the non-spot or " basic component " at some frequencies is much lower than previously believed. Its actual value is uncertain but it is thought that if spots were absent for many months, most of the radiation would cease.

(*c*) This is interpreted as showing that the corona, at least during the period 1947–1951, was mainly due to an agency appearing with sunspots and providing fresh hot gases above the spots. These gases remained after the spots vanished, spreading out to replenish the corona. They appear capable of completely replacing the corona every four days or so.

---

1. *Introduction.*—Thermal radio-frequency radiation from the Sun originates throughout the hot coronal and chromospheric gases. If the electron temperature and density are known, then the radio emission spectrum may be deduced (Martyn (**1**) and others). Alternatively, if the spectrum is known, then some of the gas properties may be deduced (Piddington (**2**) and others). In the frequency range with which we are concerned (above 600 Mc/s) most of the radiation is thermal. The intensity is steady, varying from a minimum in the absence of sunspots to two or three times this value at some frequencies when the Sun is very spotted. This excess radiation appearing with sunspots is also thermal (**3**), originating in relatively confined regions above spots or the sites of dead spots. The gas temperatures in these bright emitting regions attain 10^7 deg. K or more and the pressures are generally higher than elsewhere, perhaps 100 times or so above normal.

One of the major mysteries of solar physics is the origin of the high coronal temperatures. The very hot regions above sunspots may provide a source of at least part of this energy. It is reasonable to assume that they would heat some of the surrounding corona. Thus, although the origin of the hot regions themselves is not known, one step would have been made in explaining the origin of the corona. In the present paper an investigation of this possibility is described.

The data used in the investigation were measurements of solar radiation at frequencies between 600 Mc/s and 9400 Mc/s made on many days over a period of several years. A statistical analysis was made of these data to separate the total radiation into two components, a "sunspot component" S associated with sunspots and a "basic component" B showing no such connection. The results of the analysis were then interpreted, according to thermal emission theory, in terms of volumes of hot gases capable of providing the radiation.

Before commencing the analysis, previous attempts to isolate basic and sunspot components are discussed.

2. *Previous analyses.*—Separation of basic and sunspot components has been attempted by the simple statistical method (**4**) of plotting the day-to-day values of the total observed intensity against corresponding values of visible sunspot area as in Fig. 1. A line of best fit is then drawn through the scatter of points, intersecting the axis at a level which defines the basic component. The slope of the line indicates the average effectiveness of sunspots in providing additional radiation. Although this method was useful as a first approximation it is found unsatisfactory when scatter diagrams for various periods are compared. For example, Figs. 1 (*a*) and 1 (*b*) for 1200 Mc/s for periods during 1947 and 1950 respectively* show quite different line slopes. Figs. 1 (*c*) and 1 (*d*) for 600 Mc/s for the same periods show even less agreement; in fact, it is difficult to determine any base level or slope in the latter as the scatter is too random. Other indications of an anomaly are found in conflicting reports by Covington (to the U.R.S.I. conference in 1950) and Christiansen and Hindman (**5**). The former finds a drop in the minimum level of radiation at 2800 Mc/s between 1947 and 1950. The latter find no such fall at 600 Mc/s, 1200 Mc/s or 3000 Mc/s during this period but do find a large drop in a few months during 1950.

There are sound physical reasons why the above method of analysis is unsatisfactory and provides a fluctuating basic component, always larger than the true one. The main reason is that the radiation from dying spots diminishes more slowly than the spot area and continues after the spot has vanished. Evidence of this effect in a few cases was found during eclipse observations (**6, 7**). It is shown below to apply generally. This and other factors are discussed more fully.

3. *Radiation from dead and dying spots.*—Since radiation from some recently dead spots has been observed, it is possible that this is the general rule. If so, then the law of decrease of F must differ from that of sunspot area. The effect would be important in determining the components and must be investigated.

A rough test of the effect was first tried by plotting values of F against various functions of A_0, A_{-27}, A_{-54}, etc., where A_{-n} is the value of sunspot area† n days before the date in question. Some decrease in the scatter of points as compared with Fig. 1 was found, but the improvement was limited. An examination of the scatter diagrams, marking each point with the appropriate date, showed that while decreases in F tended to be steady, relatively large and sudden increases occurred without corresponding increases in A_0, A_{-27}, etc. This suggested that the relation between the radiation and area of different spots

* Figs. 1 (*a*)–(*d*) are reproduced from papers by Pawsey and Yabsley (**4**) and Christiansen and Hindman (**5**).

† The values of A used throughout the paper (except in Fig. 1, where Mount Stromlo data are used) are the corrected values published in the United States Naval Observatory Circulars. They are in units of 10^{-6} of the solar disk.

might differ in a rather random manner and that average values of F over periods of some days or longer might be necessary to smooth the data.

Three-day means were first tried, with little success, and then rotational means. A period of one solar rotation (27·3 days) is preferable to one month

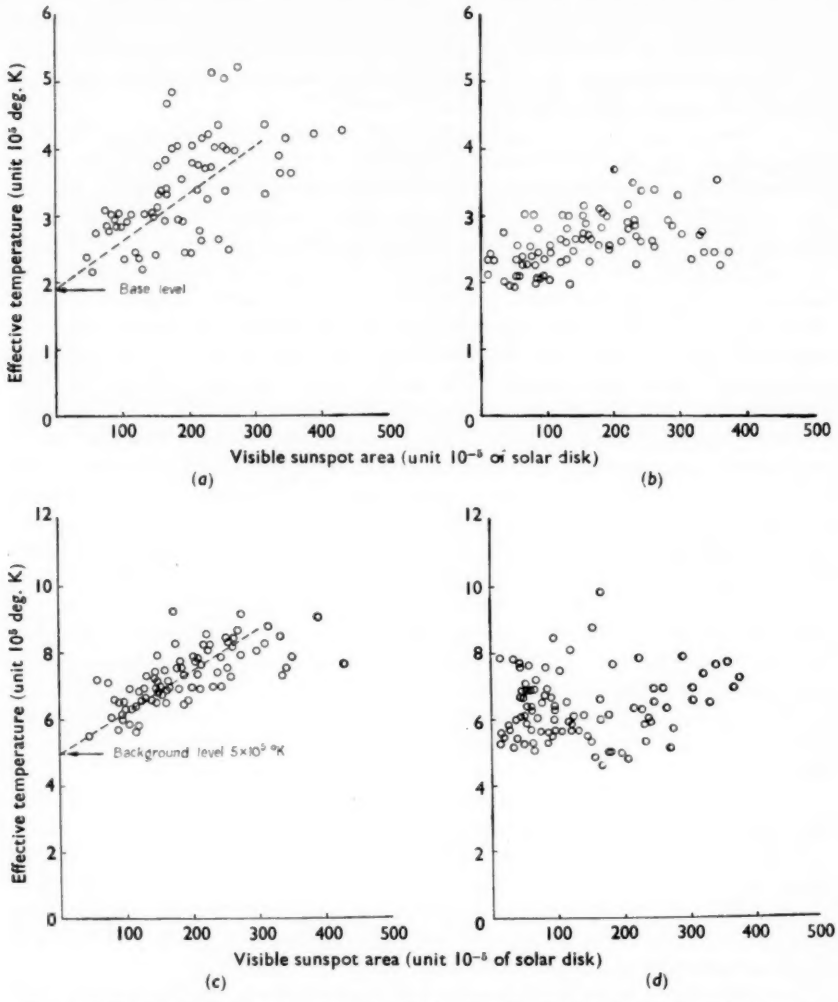

FIG. 1.—*The flux density of solar thermal radiation* ($F=B+S$) *plotted against sunspot area* A.

(*a*) 1200 *Mc/s, period* 1947 *August–November.*
(*b*) 1200 *Mc/s, period* 1950 *January–June.*
(*c*) 600 *Mc/s, period* 1947 *August–November.*
(*d*) 600 *Mc/s, period* 1950 *January–July.*

(which would have involved less work), as it completely eliminates the rotational effect. It is also preferable to periods of two or more rotations, as it utilizes the data more efficiently.

In Fig. 2(*a*) rotational mean values of 600 Mc/s solar flux density (called $\bar{F}$) are plotted against rotational mean areas (called $\bar{A}_0$). The plot of points indicated by full dots refers to all of 1950 and may be compared with Christiansen and Hindman's (**5**) Fig. 2 for 1950 January–October or the present Fig. 1(*d*) for 1950 January–July. There is a considerable reduction in scatter and further

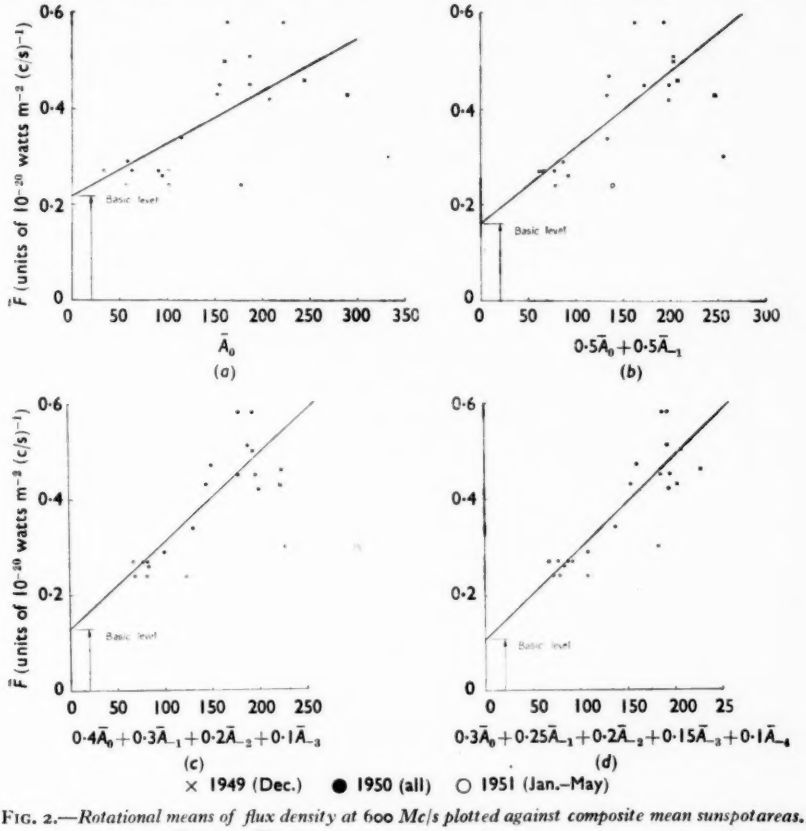

FIG. 2.—*Rotational means of flux density at 600 Mc/s plotted against composite mean sunspot areas.*

(*a*) $\bar{F}$ *against* $\bar{A}_0$.
(*b*) $\bar{F}$ *against* $0{\cdot}5\bar{A}_0+0{\cdot}5\bar{A}_{-1}$.
(*c*) $\bar{F}$ *against* $0{\cdot}4\bar{A}_0+0{\cdot}3\bar{A}_{-1}+0{\cdot}2\bar{A}_{-2}+0{\cdot}1\bar{A}_{-3}$.
(*d*) $\bar{F}$ *against* $0{\cdot}3\bar{A}_0+0{\cdot}25\bar{A}_{-1}+0{\cdot}20\bar{A}_{-2}+0{\cdot}15\bar{A}_{-3}+0{\cdot}10\bar{A}_{-4}$.

improvement is effected when past sunspots are taken into account (as described below) in Figs. 2(*b*), 2(*c*) and 2(*d*). In Fig. 2, which is only used for illustrative purposes, 600 Mc/s data are used because this shows up the effects of averaging and allowing for dead spots better than the higher frequencies. In the following statistical treatment arithmetical rather than graphical methods are used and data at four frequencies 600 Mc/s, 1200 Mc/s, 2800 Mc/s and 9400 Mc/s are analysed, using rotational mean values. Data at all frequencies have been treated similarly, but since there is much more information available at 2800 Mc/s it carries greater statistical weight and receives some separate mention.

In testing the effect on $\bar{F}$ of sunspots which occurred during previous rotations, correlation coefficients are calculated between $\bar{F}$ and $\bar{A}_{-n}$ where $\bar{A}_{-n}$ is the mean sunspot area n rotations earlier. However, it is known that some sunspot groups last for several rotations and also that sunspot groups sometimes tend to reappear in a given area for many months. Hence, even if the emission of excess radio noise did *not* outlast the sunspots, high values of the correlation coefficient $r(\bar{F}, \bar{A}_{-n})$ might be expected for values of n of 2, 3 or more rotations. This effect is allowed for by calculating values of r for positive as well as negative values of n. The test for the reality of the effect being investigated is that values of $r(\bar{F}, \bar{A}_{-n})$ should be consistently larger than corresponding values of $r(\bar{F}, \bar{A}_{+n})$.

The results for 2800 Mc/s* calculated for a period of 54 solar rotations from 1947 January to 1951 April are plotted in Fig. 3. To allow a more direct visual comparison of the positive and negative r values the former are plotted as dashed

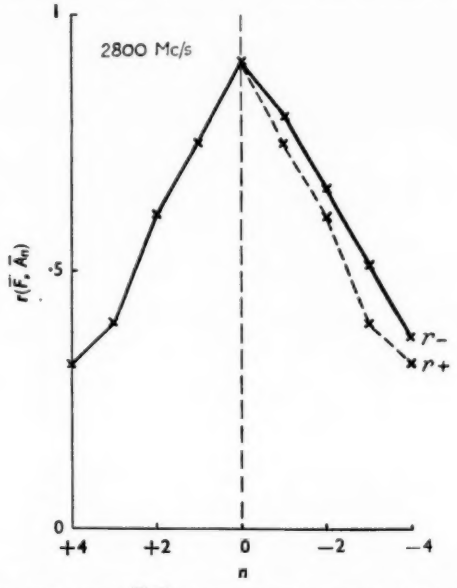

FIG. 3.—*Correlation coefficients $r(\bar{F}, \bar{A}_n)$ for rotational mean values of flux density and sunspot area n rotations later for 2800 Mc/s over 54 rotations.*

curves on the right-hand side of the diagram. The significance of the difference between the pairs of r values, $r(\bar{F}, \bar{A}_{-n})$ and $r(\bar{F}, \bar{A}_{+n})$, may be determined from a calculation of their respective z values.† The difference between each pair of z values is compared with the corresponding standard deviation; a significant difference exists at the 5 per cent probability level if the z difference is greater

* The 2800 Mc/s results are by A. E. Covington of the National Research Council of Canada and the remainder by observers at the Radiophysics Laboratory, Sydney. Most data have been published in the *Quarterly Bulletin of Solar Activity*.

† As it is more convenient to compare two normally distributed deviates than two skewly distributed **r values,** the following transformation is used. The normal deviate is $z = \ln\left(\frac{1+r}{1-r}\right)^{1/2}$ with a **standard deviation** $\frac{1}{N-3}$, where N is the number of values used in calculating r.

than twice the combined standard deviation $2(N-3)$. Such is the case for $n=1$, 2 and 3 but not for $n=4$. Plots for the four frequencies 600 Mc/s, 1200 Mc/s, 2800 Mc/s and 9400 Mc/s, each for a period of about 20 solar rotations during 1949–51, are shown in Figs. 4(*a*), (*b*), (*c*) and (*d*). The 9400 Mc/s plot does not carry as much weight as the others because there were fewer

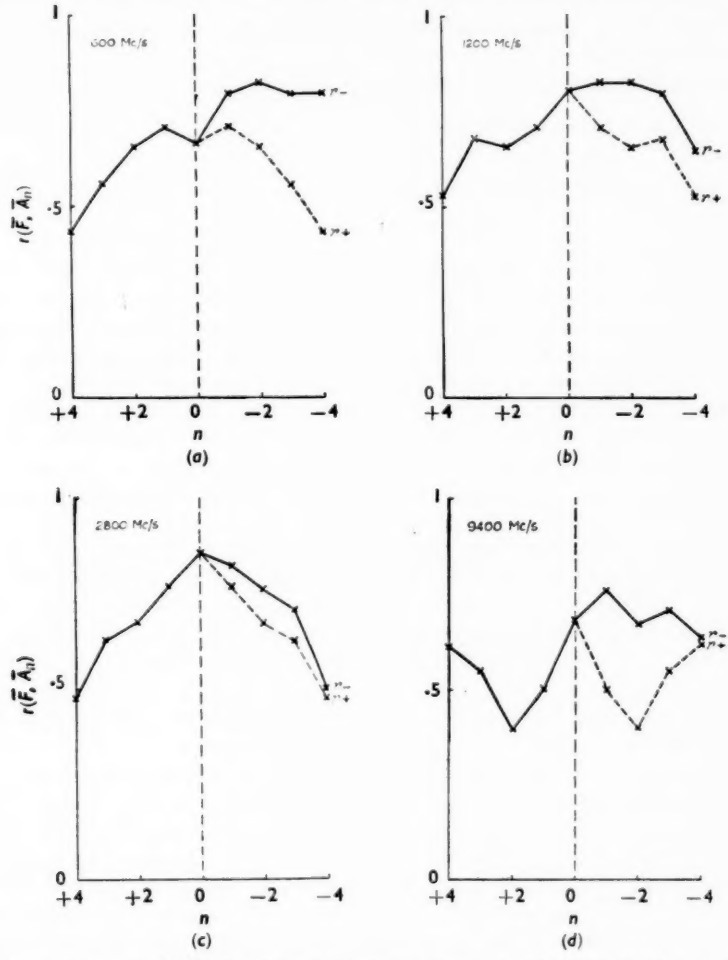

FIG. 4.—*Values of* $r(\overline{F}, \overline{A}_n)$ *for about* 20 *rotations at frequencies* (*a*) 600 *Mc/s*, (*b*) 1200 *Mc/s*, (*c*) 2800 *Mc/s*, (*d*) 9400 *Mc/s*.

(only 16) rotations considered in the analysis. Nevertheless, at all four frequencies every $r(\overline{F}, \overline{A}_{-n})$ value lies above the corresponding $r(\overline{F}, \overline{A}_{+n})$ value. The larger divergence of the positive and negative values at 2800 Mc/s does not conflict with the results shown in Fig. 3. This is because Fig. 4 uses less than half as many rotations as Fig. 3 and consequently the standard error is twice as large and the significance of a given difference between the pairs of r values

is smaller. Although, in Fig. 4, no single pair of r values shows a significant difference the displacement between positive and negative curves is significant at each frequency.

It is concluded that radio emission accompanying sunspots shows a time lag behind the spot and may outlive the spot. Contributions from spots observed one, two and three rotations earlier appear significant. In the following analysis an attempt is made to determine the relative importance of new and old spots on the radio emission.

The following composite sunspot areas were calculated:

$$A_{-\alpha}=0{\cdot}5\ \bar{A}_0+0{\cdot}5\ \bar{A}_{-1}.$$
$$A_{-\beta}=0{\cdot}5\ \bar{A}_0+0{\cdot}3\ \bar{A}_{-1}+0{\cdot}2\ \bar{A}_{-2}.$$
$$A_{-\gamma}=0{\cdot}4\ \bar{A}_0+0{\cdot}3\ \bar{A}_{-1}+0{\cdot}2\ \bar{A}_{-2}+0{\cdot}1\ \bar{A}_{-3}.$$
$$A_{-\delta}=0{\cdot}3\ \bar{A}_0+0{\cdot}25\ \bar{A}_{-1}+0{\cdot}2\ \bar{A}_{-2}+0{\cdot}15\ \bar{A}_{-3}+0{\cdot}1\ \bar{A}_{-4}.$$

Values of $A_{+\alpha}$, $A_{+\beta}$, etc. are similarly derived from $\bar{A}_{+1}$, $\bar{A}_{+2}$, etc. If $\bar{F}$ is now plotted against $A_{-\alpha}$, $A_{-\beta}$, etc. the effect of taking past spots into account in varying proportions may be seen. In Fig. 2, $\bar{F}$ at 600 Mc/s is plotted successively against $A_{-\alpha}$, $A_{-\gamma}$ and $A_{-\delta}$. There appears to be a steady improvement as more past spots are taken into account. As the various combinations of $\bar{A}_0$, $\bar{A}_{-1}$, etc. were chosen arbitrarily, further improvement might be possible by trial and error, but the very limited data hardly warrant this effort. Furthermore, part of the improvement observed is due to the averaging effect of the statistical procedure involved. Any set of data subjected to this arithmetical process of adding together fractions of successive values may show an improved scatter in summing more values, and this effect must be isolated from that due to longevity of sunspot radiation. The method used is to compare the effect of sunspots which appeared some rotations *before* that for which $\bar{F}$ is taken with the effect of those which occurred some months *after*.

In Fig. 5(*a*) successive values of the correlation coefficients between $\bar{F}$ (at 600 Mc/s) and A_0, $A_{+\alpha}$, $A_{+\beta}$ and so on are plotted and a curve drawn. The corresponding curve for $r(\bar{F}, A_{-\alpha})$ and so on is also drawn. The procedure is repeated in Figs. 5(*b*)–(*d*) for the other three frequencies. In order to allow a more direct comparison between the results at different frequencies the 2800 Mc/s data used were limited to the same period as that for the other frequencies. In each case the curve corresponding to the negative (past) values of $\bar{A}$ lies above that for the positive (future) values of $\bar{A}$. The statistical significance of the results was found by first transforming each r value to its normal deviate z (as above) and then comparing the difference between each pair of z values (for A_+ and A_-) with twice the standard deviation. The ratios for the $A_{\pm\alpha}$ values are 2·0, 3·0, 0·7 and 0·6 for frequencies of 600, 1200, 2800 and 9400 Mc/s respectively. The ratio for the A_β values for 600 and 1200 Mc/s is also greater than unity. Moreover, for each frequency the points taken as a whole show the A_- curve significantly higher than the A_+ curve. One further check was made to show that the effect was real and not due, say, to the asymmetrical curves of growth and decay of spot areas. The correlation coefficients between $\bar{A}_0$ and $A_{\pm\alpha}$ were calculated and compared. Their values were identical at 0·81, so that although $r(\bar{F}, A_{-\alpha})$ is greater than $r(\bar{F}, A_{+\alpha})$, the two coefficients are the same when $\bar{F}$ is replaced by A_0.

It is concluded that at the frequencies of 600 Mc/s and 1200 Mc/s a sunspot area measured at a given time contributes on an average to radio noise at least one and perhaps two or more rotations later, with decreasing effectiveness. In the cases of 2800 Mc/s and 9400 Mc/s the inferences from the curves are less definite. Some effect due to old spot areas is indicated but it is less than at the lower frequencies, and the time delay has not been assessed. It is also concluded that for the purpose of determining the base level (as in Fig. 2 or by a corresponding arithmetical process), values of $A_{-\alpha}$ should be used at all frequencies rather than values of A_0. It is likely that values of $A_{-\beta}$ or even $A_{-\gamma}$ might be even more suitable.

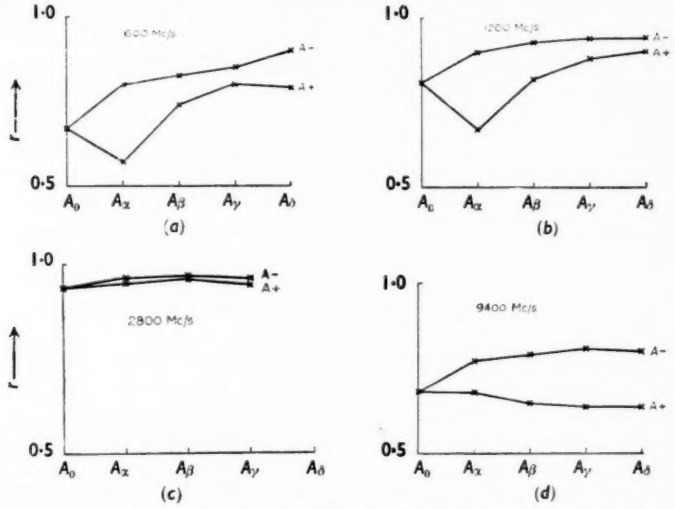

FIG. 5.—*Correlation coefficients for rotational mean values of flux density and composite sunspot areas taking successively more months into account.* (*a*) 600 *Mc/s*, (*b*) 1200 *Mc/s*, (*c*) 2800 *Mc/s*, (*d*) 9400 *Mc/s*.

A curious feature of Fig. 5 is the high values of correlation coefficients at 2800 Mc/s for both positive and negative curves. This may be due, at least in part, to a tendency for sunspots to reappear again and again in a given region. In any case it precluded the use of the more extensive 2800 Mc/s data in Fig. 2 as no noticeable improvement would be detected by a visual comparison of the different plots.

4. *The basic component.*—If we continue to define the basic component as the level of radiation from the spot-free Sun, then it undoubtedly *has* fallen during the years since sunspot maximum. The greatest fall has occurred during 1950, when there was a large drop in the three-monthly average values of total sunspot area, as shown in Fig. 6.

In view of the long life of the sunspot radiation, the above definition of B is hardly satisfactory. It means, in effect, that some sunspot radiation is reclassified as part of the basic component as soon as the area of the parent spot starts to decrease. An alternative definition which will be adopted here is radiation from the Sun which has been spot-free for some months. At present its value must be inferred from measurements made with spots present or recently vanished. If the new definition is adopted, then there was no marked fall in base level

during 1950, the observed effect being due to the prolonged absence of appreciable sunspot activity. The new basic component may, perhaps, hold throughout the sunspot cycle.

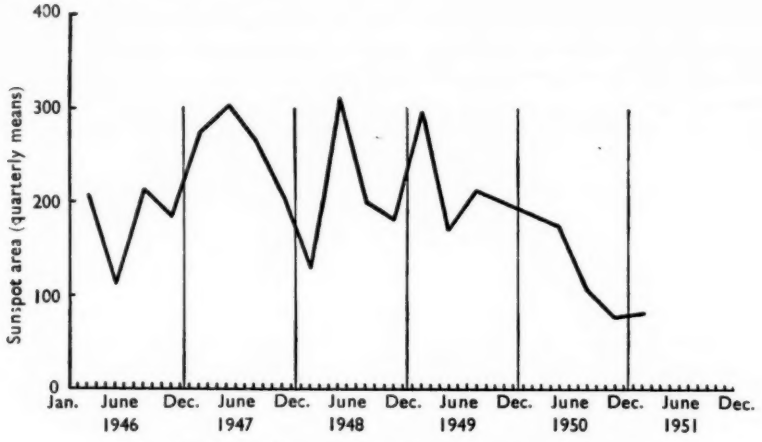

FIG. 6.—*Quarterly mean values of sunspot areas* 1946–1951.

To eliminate all the spot radiation from the observed values of solar radiation it is necessary to find the relative importance of live sunspots and those dead one, two, three, etc. rotations. For the arbitrarily chosen functions, $A_{-\alpha}$, $A_{-\beta}$, etc., it was shown above that $A_{-\alpha}$ should be used in preference to A_0 and that $A_{-\beta}$ or $A_{-\gamma}$ might be even more suitable. The values of B found by using $A_{-\alpha}$ and $A_{-\gamma}$ are given in Table I. Values determined by the old method* are listed for comparison.

TABLE I

Values of the basic thermal component of solar radiation

Frequency (Mc/s)	The basic components in units of 10^4 deg. K apparent disk temperature		
	Values based on spot-free Sun (*circa* 1948)	Value based on $A_{-\alpha}$	Value based on $A_{-\gamma}$
600	50	21	17
1200	28	8·0	5·9
2800	6·0	3·5	3·2
9400	1·7	1·6	1·6
24000	1·0	...	...

The surprisingly large reduction in the basic component, particularly at 1200 Mc/s, suggests a possible error in the statistical analysis. Before critically examining the factors involved it is desirable to consider our objectives. The

* Summarized by Piddington (**2**). All the 1200 Mc/s data are revised upward by a factor of 1·4 to conform with a recent revision of the gain of the aerial used made by Piddington and Minnett (**8**). The 2800 Mc/s data are also slightly modified in accordance with a recent re-examination of Covington's data.

first is to consider the possibility that the regions above sunspots are the sources of *some* coronal energy and material. This is attained whatever the value of B. The second is to estimate the *importance* of this source of energy. If the old value of B were correct, then this source would only account for a fraction (perhaps a fifth or less over the period concerned) of the coronal energy. If the real value of B is substantially lower at 1200 Mc/s*, say 14 or less instead of 28 units, then this source of coronal heating is found to be the *major* one. Accurate values of B are not, therefore, required. The value at 1200 Mc/s could lie anywhere between zero and about 14, well outside the limits indicated in Table I.

In estimating the accuracy with which the new value of B is determined, both mathematical and physical considerations are important. The former are as follows: it is well known that by combining data by an averaging process as used above (rotational means from daily values of $F\alpha$, $F\beta$, etc. from rotational means), the regression line is moved and lower values of B may be obtained. This is true whether the actual facts warrant the averaging process or not and may appear to cast doubt on the accuracy of the new value of B. However, the reverse is equally true, that if the facts *do* warrant a certain averaging process (such as the use of $\bar{F}$ or $F\alpha$, $F\beta$, etc.) and this is not adopted, then *again* an incorrect value of B is obtained. Our procedure has been first to establish as far as possible the correct degree of averaging and then use it to find B. The improved correlation found when combinations of two or more rotational means are used shows that the averaging process should be taken past that of rotational averages; how far past, however, is not clear. Fortunately, for the present purposes, the exact degree of averaging is not important because the difference in the values of B found by using $F_{-\alpha}$ (2-month averages) and $F_{-\gamma}$ (4-month averages) is relatively unimportant. In fact, most of the reduction in B is obtained simply by using rotational mean values instead of daily values and taking no account of spots seen on previous rotations. Thus at 1200 Mc/s B falls from 28×10^4 deg. K to 12×10^4 deg. K when $\bar{A}_0$ is used (a factor of 2·3) and then only to $6{\cdot}8 \times 10^4$ when $A_{-\beta}$ is used (a further factor of 1·8). The required degree of averaging (which is poorly determined) is therefore not important.

It is evident that the statistical results would be strengthened if physical reasons were available. There appear to be two principal reasons why a reduction in base level is effected by using rotational means instead of daily values of F and A.

The first reason is the persistence of radiation during and after the disappearance of the spot. It is considered that this effect has been definitely established in the analysis. Spots grow rapidly and die away slowly (**9**) so that most spots seen at a given time are dying. When B is found by plotting daily values of A and F, excess radiation from dying (and also some dead) spots raises the whole scatter of points and leads to too high a value of B; the factor involved could be 2 or more. The new method corrects this effect.

The second reason results from the fact that spots lie somewhat below the photosphere and the emitting regions much above it. An examination of the sunspot records used shows that only spots within about $\pm 75^\circ$ of the centre of the disk are listed; that is, spots on less than 42 per cent of the solar surface. On the other hand, the hot emitting regions above sunspots probably project far into the corona (**3**). Thus, when they are on or beyond the limb, parts of them

* The reason why the effect is so marked at this particular frequency will be seen later.

projecting beyond the surrounding cooler coronal gases provide radiation at the Earth. It is not possible to evaluate the effect quantitatively but it may be important. When B is found by daily plots the obscuration of spots on the visible disk moves the scatter of points towards lower values of A. The visibility of hot regions beyond the limb moves the scatter towards higher values of F. Both effects result in too high a value of B but are corrected when rotational mean values are used.

It is concluded that the basic component as determined by the old method is certainly too high. The true value is somewhat uncertain but it is considered that the value found by using rotational mean values of A and F (that is $\bar{A}_0$ and $\bar{F}_0$) are almost certainly too large. The true value probably lies within or at least close to the limits given in Table I.

Our analysis throws light on an effect noticed by Christiansen and Hindman (**5**) in the 1950 and 1951 records at 600, 1200 and 3000 Mc/s. The " base level " (as previously defined) fell continuously for several rotations. It is now seen that the effect was mainly due to the decreasing contributions from dead spots as the three-monthly average sunspot area decreased (Fig. 6). If suitable composite spot areas are used the effect vanishes as shown in Fig. 2. The fall in base level at 2800 Mc/s between 1947 and 1950 reported by Covington was also tested by plotting rotational mean values of F and A but making no allowance for dead spots. A marked drop was found which might be interpreted as a fall in base level or an effect due to the integrated small effects of many dead spots during a period when the yearly average sunspot area was decreasing.

An interesting deduction from the above results is that the Sun is a variable star, the variation being most marked near 1200 Mc/s. This has already been pointed out by van de Hulst (**10**) who suggested a variation by a factor of 2. Our results indicated a larger factor, perhaps 4. The most interesting deduction, however, is that the major source of coronal heating, indeed of the corona itself, is in the vicinity of sunspots. This is discussed below.

5. *The sunspot component.*—It has been shown that the sunspot component of solar thermal radiation lags behind the spot area itself, so that an area measured at a given time is effective at least one and perhaps two or more rotations later in producing radio emission. This effect might be due either to emission of radio noise mainly during the latter part of the life of a spot or, alternatively, to the emission of some radio noise after the spot has disappeared. However, the half-life of even a large spot is not usually more than about a month, so that a delay of one month would necessitate all the radio noise being emitted during the last week or so of the spot life. This is contrary to the observational evidence, so that the radio emission must occur after the spot has vanished.

Eclipse results show that the origin of at least part of the sunspot component is in the vicinity of the spots themselves either during or after their visible lifetime. Other solar phenomena which correlate closely with sunspot area appear to have their origins near the spots themselves and it is reasonable that all the radio noise components should do likewise. However, it is possible that some of it might originate elsewhere; an examination of the available data was made to settle this point but without success. Several reasons contributed to this failure: it is not known from how far around the limb radiation from a hot region may be received; the maximum sizes of more than half of all sunspots are not known; finally the day-to-day relationship between F and A is not known.

6. *The density and extent of the corona.*—The above results are concerned only with the radio noise emitted from the corona and chromosphere. It is possible, however, to make a further advance by deducing from the radio results other properties of the solar atmosphere of more general interest. A knowledge of the emission spectrum of radio noise permits estimates to be made of the density and extent of the atmosphere (**2**). If the spectrum differs on two occasions then corresponding differences in the atmosphere may be determined.

The best available model of the "average" solar corona is probably given by the Allen–van de Hulst electron density distribution and a uniform temperature of about 10^6 deg. K. It is not clear to what conditions this model corresponds, as the data on which it depends were the average for several occasions. We will assume that it corresponds to fairly quiet conditions, say with 100 units of sunspot area, averaged in the period 1947–50. The corresponding spectrum of radio noise is given in column 2 of Table II. This spectrum is very similar to that of the old basic component; the inclusion of the small amount of sunspot area is not important. The spectrum shows satisfactory agreement with that derived theoretically from the model.

TABLE II

Solar radiation from an "average" solar atmosphere and one spot-free for some months

Frequency f (Mc/s)	Apparent disk temperatures (units of 10^4 deg. K)		Frequency f'	f'/f	τ/τ'
	For a sunspot area of 100 units	For complete absence of spots for some months			
600	63	19	1850	3·1	9·6
1200	38	6·9	2900	2·4	5·8
2800	7·4	3·3	4900	1·7	2·9
9400	1·8	1·6	10800	1·15	1·3

Another spectrum of solar radio noise, corresponding to prolonged absence of spots, has now been found. This is listed in column 3 of Table II.* It must correspond to a different solar atmosphere and it is required to determine this difference.

The apparent temperature of a section of the (radio) disk of the Sun is

$$T = \int_0^\infty T_e \, e^{-\tau} \, d\tau,$$

where T_e is the electron temperature at a level of optical depth τ. Since τ is inversely proportional to the square of the frequency f, radiation at higher frequencies comes generally from lower levels. The steadily decreasing values of temperature in columns 2 and 3 show that both corresponding atmospheres have a negative inward temperature gradient. Also, since values in column 3 are all lower than those in column 2, the corresponding atmosphere must have a lower optical depth to a region of given electron temperature.

* The values used are the means of the pairs of values listed in Table I.

To determine the fall in τ between the two atmospheres let us assume tentatively that the decrease in optical depth is in the same (unknown) ratio everywhere throughout the regions concerned. Then, since τ is inversely proportional to the square of the frequency, the change in τ is exactly equivalent to a certain change in frequency.* For example, the reduction in apparent disk temperature at the frequency $f = 1200$ Mc/s from $3{\cdot}8 \times 10^5$ deg. K to $6{\cdot}9 \times 10^4$ deg. K is effected if, instead of reducing τ, the frequency is suitably increased to f'. The value of f' is found by plotting the data of column 2, Table II (the disk temperature before τ is reduced) against frequency. The frequency which corresponds to the new disk temperature is then found to be 2900 Mc/s. Other values of f' are listed in column 4 and the ratio f'/f in column 5 of Table II. The corresponding ratio by which τ is decreased is listed in column 6.

Evidently our assumption that the change in optical depth was everywhere equal was not justified; the ratio at low levels where the gas temperature is about 10^4 deg. K is small and increases steadily with increasing height and gas temperature. If a second approximation to the various ratios τ/τ' were made the spread would be even larger. Accurate determinations are not required here, however, and the important conclusion is that at levels where the gas temperature is a few $\times 10^5$ deg. K or more (that is, throughout the corona and upper chromosphere) the optical depth would fall by a factor of roughly 10 or more. This fall could be caused by a decrease in the density or extent of the region or an increase in the temperature. The required temperature increase, if uniform, is by a factor of about 4 and should provide a corresponding increase of radiation at lower frequencies. As no increase has been observed during periods of falling sunspot area this possibility may reasonably be precluded. It is concluded that in the continued absence of spots the electron density of the corona would decrease by a factor of about $3{\cdot}2$ or its extent by a factor of 10 or both decrease by smaller factors. In other words the corona, as it has been recognized during the few years preceding 1950, would largely disappear, leaving a residue of some 10–30 per cent or even less. It may further be inferred that unless some new factor becomes important during the period of sunspot minimum the extent or density (or both) of the corona will vary by a large factor between sunspot maximum and minimum. This conclusion is consistent with that of van de Hulst (**10**) who suggested a decrease in electron density by a factor of $1{\cdot}8$. The factor suggested by our results is considerably higher but it is possible that some form of coronal replenishment operates during sunspot minimum which we have not considered. The marked change in shape of the corona between maximum and minimum suggests such a possibility.

7. *The source of the corona.*—Evidence has been given that the corona would largely disappear during the prolonged absence of sunspots. Let us consider the reverse process in which spots appear after the corona has been depleted. The radio evidence shows that excess thermal radio emission then occurs, largely from regions above the spots themselves. This is interpreted as indicating that fresh hot gas has appeared in these regions. After sufficient spots have appeared the resulting emission (both before and after their visible life) constitutes most of the solar thermal radiation. It seems safe to conclude that the hot gases formed with the spots then constitute most of the corona. In other words the

* This is only true for frequencies of about 600 Mc/s and above, where the value of the refractive index does not differ appreciably from unity.

thermal energy of the corona, and presumably also its material, appear to originate largely in regions above sunspots.

It may be desirable to examine some of the processes involved in terms of the theory of thermal radiation from these regions (called *S*-regions) of Piddington and Minnett (**3**). They showed that the spectrum, polarization and other properties of the observed sunspot component of solar radiation could all be explained in terms of thermal emission from volumes of gas of extent of the order 10^5 km, temperature 10^7 deg. K or more, and pressure considerably higher than that in the average (Allen–van de Hulst) corona. During the spot life these clouds of gas would be retained by the spot magnetic field but later would expand and diffuse through the surrounding atmosphere, some of the gas leaving the Sun altogether, the remainder heating and replenishing the corona. On this picture the Sun should present a mottled appearance when viewed at a frequency of about 1000 Mc/s. There should be small bright patches over sunspots and more diffuse less bright patches covering regions where spots had recently existed. Most of the solar radiation would be made up of these continually expanding and overlapping patches. Magnetic fields of long duration, if they existed, would have a marked effect on the pattern observed, as movement across the field would be largely inhibited.

The source of *S*-region energy is not known but evidence regarding the level where heating occurs is found in 24 000 Mc/s observations of Piddington and Minnett (**11**). Even during a period of intense activity (radiation at 2800 Mc/s fluctuated over a 2 to 1 range) no *S*-radiation could be detected, the apparent disk temperature remaining at 10 000 deg. K $\pm$ 5 per cent. It is concluded that little or no heating occurs in the region from which most of the 24 000 Mc/s radiation emerges; this region has an average temperature of 10^4 deg. K. At lower frequencies increased radiation does occur, so that the 10^4 deg. K level in the chromosphere may be taken as the approximate lower limit of the heated region; the upper limit is not defined.

If *S*-regions are the source of coronal energy they must be capable of replenishing this energy as fast as it is dissipated. Two model *S*-regions, one for a large (130 units) and one for a small (5 units) spot have been proposed by Piddington and Minnett (**3**). These provide radiation which corresponds to that observed from the vicinity of such sunspots and may be taken to represent roughly the amount of hot gas necessary to provide the observed thermal radiation. The total kinetic energy of the gases in the two models is found to be about 200 per cent and 3 per cent respectively of that of an average corona at 10^6 deg. K. Thus each unit of sunspot area is accompanied by hot gas with kinetic energy between 1·5 and 0·6 per cent of the coronal energy. During the years for which the radio data apply, the average sunspot area over the whole Sun (back and front) has been about 400 units, and if the average life of a unit of spot area is one month then new areas are appearing at the rate of about 13 units per day. It is evident, therefore, that new *S*-region energy, equal to that of the whole corona, appears every 8 days or so.* The required rate of replenishment is not known but replacement every few days appears reasonable.

It is of interest to consider previous theories of coronal heating in the light of the new evidence. The theory of Bondi, Hoyle and Lyttleton (**12**) of heating

* The *S*-region radiation given by the simple models above is only about half that observed. A corresponding alteration in the models would reduce the time from 8 days to about 4.

by the accretion of interstellar gas appears to conflict with the radio evidence. It might be possible to explain how regions over sunspots become hottest at the expense of the surrounding regions. This effect would not, however, explain the large change in average level from years of spot maximum to minimum. It also seems to have difficulty in explaining the marked fluctuations in sunspot thermal radio emission as the Sun rotates. Theories depending on the upward transference of energy by sound or shock waves (**13, 14**) would need modification to explain why heating occurred mainly above sunspots. Theories which predict most of the heating occurring above sunspots are favoured by the new evidence. Alfvén's (**15**) magneto-hydrodynamic wave theory falls into this category if transmission by spot magnetic fields rather than the general magnetic field is postulated.

Division of Radiophysics,
C.S.I.R.O.,
Sydney, Australia:
1953 *January* 19.

References

(1) D. F. Martyn, *Proc. Roy. Soc.* A, **193,** 44, 1948.
(2) J. H. Piddington, *Proc. Roy. Soc.* A, **203,** 417, 1950.
(3) J. H. Piddington and H. C. Minnett, *Aust. J. Sci. Res.* A, **4,** 131, 1951.
(4) J. L. Pawsey and D. E. Yabsley, *Aust. J. Sci. Res.* A, **2,** 198, 1949.
(5) W. N. Christiansen and J. V. Hindman, *Nature*, **167,** 635, 1951.
(6) W. N. Christiansen, D. E. Yabsley and B. Y. Mills, *Aust. J. Sci. Res.* A, **2,** 506, 1949.
(7) J. H. Piddington and J. V. Hindman, *Aust. J. Sci. Res.* A, **2,** 524, 1949.
(8) J. H. Piddington and H. C. Minnett, *Aust. J. Sci. Res.* A, **4,** 459, 1951.
(9) T. G. Cowling, *M.N.*, **106,** 218, 1946.
(10) H. C. van de Hulst, *Nature*, **163,** 24, 1949.
(11) J. H. Piddington and H. C. Minnett, *Aust. J. Sci. Res.* A, **2,** 539, 1949.
(12) H. Bondi, F. Hoyle and R. A. Lyttleton, *M.N.*, **107,** 184, 1947.
(13) L. Bierman, *Naturwiss.*, **33,** 118, 1946.
(14) M. Schwarzschild, *Astrophys. J.*, **107,** 1, 1948.
(15) H. Alfvén, *M.N.*, **107,** 211, 1947.

THE DISTRIBUTION OF RADIATION ACROSS THE SOLAR DISK AT METRE WAVE-LENGTHS

P. A. O'Brien

(Communicated by M. Ryle)

(Received 1953 March 27)

Summary

Measurements of the distribution of radio " brightness " across the solar disk have been made at wave-lengths of 1·4, 3·7 and 7·9 metres, using interferometers of variable aperture. The size of the emitting disk was observed to increase with increasing wave-length, the averaged equivalent temperature being reduced to 10 per cent of its central value at radii of 1·6 R_0, 2·2 R_0 and 2·8 R_0 for the wave-lengths 1·4, 3·7 and 7·9 metres respectively.

At 1·4 metres, using interferometers with axes inclined at various angles to the solar axis of rotation, it was shown that the shape of the Sun was approximately elliptical; the radial distance at which the brightness temperature was reduced to half was about 25 per cent greater at the equator than in the polar direction.

---

1. *Introduction.*—The earliest attempts to determine the distribution of radio "brightness" across the solar disk were based on eclipse observations at centimetre wave-lengths (**1, 2**), and such observations have now been made over the range 8·7 mm to 1·95 metres (**3, 4, 5, 6, 7, 8**). The results obtained in most of these experiments were not very conclusive, particularly at the longer wave-lengths where the large effective diameter of the Sun makes the observed eclipse curves insensitive to changes in the radial distribution of the emission.

The determination of the distribution by Fourier synthesis, using an interferometer aerial of variable aperture, was suggested by McCready, Pawsey and Payne-Scott (**9**), and this method was first used by Stanier (**10**) at a wave-length of 60 cm, and later by Machin (**11**) at 3·7 metres. In the interpretation of these results it was assumed that the emission was distributed over the solar disk with circular symmetry. The distributions obtained did not agree with those derived theoretically (**12**): at 60 cm the predicted limb-brightening did not occur and at 3·7 metres the amount of radiation from the outer corona was considerably greater than the theoretical values.

The present paper describes further experiments, using interferometers of variable aperture, during the period 1951 July to 1952 July. The method has been extended to wave-lengths of 1·4 and 7·9 metres, and further measurements have also been made at 3·7 metres. At 1·4 metres it has been possible to determine the distribution by a method which does not assume that the source has circular symmetry.

2. *Principles of the interferometer with variable spacing.*—Let the distribution of radio emission across the solar disk be represented by the function $F(r, \theta)$, where r is the radial distance from the centre of the disk, measured in terms of the radius R_0 of the photosphere as unit, and θ is the angle measured from the projection of the solar axis of rotation on to the plane of the visible disk. Consider an axis AB passing through the centre of the disk making an angle α with the axis of rotation (Fig. 1), and suppose that the function $F(r, \theta)$ is integrated in narrow strips along a direction parallel to this axis. The resulting function, $P_\alpha(r)$, represents, along the axis CD, a projected distribution of the emission which will in general be different for different values of α.

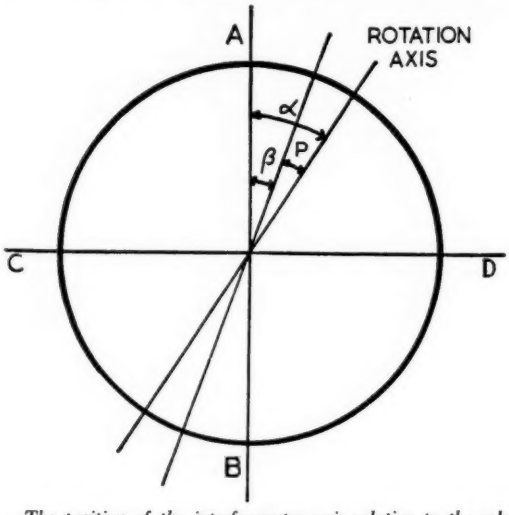

FIG. 1.—*The position of the interferometer axis relative to the solar disk*

Suppose now that two aerials spaced at a distance n wave-lengths apart are arranged so that the plane of symmetry of the interferometer (the plane normal to and bisecting the axis joining the two aerials) is parallel to the axis AB. The projection of the axis of the interferometer on the disk would then be parallel to CD, the radial direction of the projected distribution $P_\alpha(r)$, and we will now show that this projected distribution, for a particular value of α, may be deduced from measurements made using a variable aperture of the interferometer. The angle α may be described as the "interferometer position angle".

The two aerials are considered to be directed towards the centre of the disk and the power receptivity of each aerial may accordingly be represented by the function $A(r, \theta)$. When the centre of the Sun is at an angle H from the plane of symmetry of the interferometer the recorded deflection D of a phase-switching type of receiver (**13**) is given by

$$D = \cos(2\pi n \sin H) \int_{-\infty}^{+\infty} A(r, \theta) P_\alpha(r) \cos(2\pi n r)\, dr + \sin(2\pi n \sin H) \int_{-\infty}^{+\infty} A(r, \theta) P_\alpha(r) \sin(2\pi n r)\, dr, \qquad (1)$$

where the radial distance r is taken to be small.

It can be seen from equation (1) that as the Earth rotates the recorded deflection D becomes sinusoidal, except for small values of the aerial spacing. The type of record obtained (Fig. 2 *a*) shows that the amplitude of the sinusoidal trace depends on the distance between the two aerials of the interferometer. It will be convenient to call the peak-to-peak amplitude of the sinusoidal trace "the recorded excursion" R. Fig. 2 *b* shows how the recorded excursion was found to depend on the distance between the aerials for an interferometer inclined at an angle $\alpha = -19°$; it includes the results given in Fig. 2 *a*.

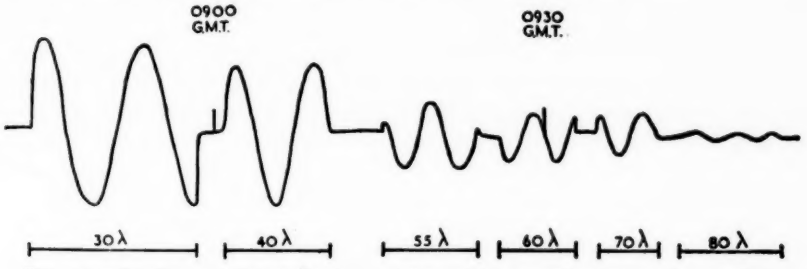

FIG. 2 *a*.—*Interference pattern for various aerial separations, 1952 January 31, $\lambda = 1{\cdot}4$ metres.*

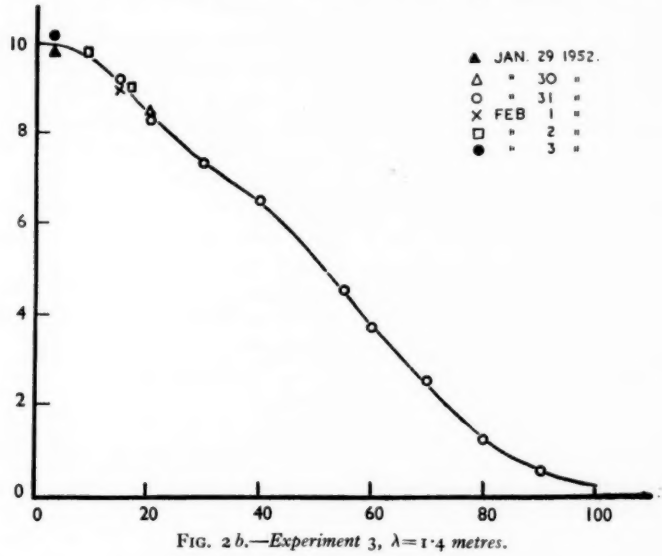

FIG. 2 *b*.—*Experiment* 3, $\lambda = 1{\cdot}4$ *metres.*
Ordinates: Relative recorded excursion.
Abscissae: Aerial separation in wave-lengths.

If the projected radial distribution $P_x(r)$ were symmetrical with respect to the axis AB all the sinusoidal traces would be symmetrical about the time at which the centre of the disk would cross the axial plane. If, however, the projected distribution is not symmetrical, some of the recorded traces will not be symmetrical about this time, and it is convenient to describe their time-displacement in terms of a recorded phase shift. The single curve shown in Fig. 2 *b* would then be replaced by two different curves corresponding to the

symmetrical and anti-symmetrical components of the projected distribution of emission. In this way, using the Fourier inversion of equation (1), the function $P_\alpha(r)$ could be determined for a particular value of α, the interferometer position angle.

The general distribution of the emission, $F(r, \theta)$, could be determined if a set of observations were carried out with the angle α taking values ranging over 180°. In the experiments described in this paper, however, it was not convenient to make observations over this range in α. It is therefore important now to consider two special cases of symmetry in the general distribution of emission.

(*a*) *The distribution of the emission is circularly symmetrical.*—If it is assumed that the radiation from the undisturbed Sun can be represented by a circularly symmetrical function, the projected distribution will be independent of the value of α. The distributions obtained by Stanier (**10**) and by Machin (**11**) were based on this assumption, and Machin has shown that the radial distribution $F(r)$ is given by the Fourier–Bessel transform of the equation

$$R(n) = 2\pi \int_0^\infty F(r) \,.\, r \,.\, J_0(2\pi n r \cos H)\, dr,$$

where $R(n)$ denotes the recorded excursion measured as a function of the separation of n wave-lengths between the aerials.

(*b*) *The distribution of the emission has rotational symmetry.*—On the assumption that there are no active areas on the Sun it would be reasonable to regard the distribution function $F(r, \theta)$ as being symmetrical about the solar axis of rotation. In this case the distribution may be derived from observations with an interferometer of variable spacing if α covers a range of 90° from pole to equator. The method of deriving the distribution is given in Section 5.

3. *The application of the interferometer with variable spacing.*—It was shown in the previous section that if observations are made over a range of at least 90° in α the results could be analysed to show whether there was any departure from circular symmetry in the function $F(r, \theta)$. The methods of varying α will now be considered. Since it is necessary to use aerial separations of about 100–200 wave-lengths for wave-lengths of several metres, we shall consider the movement of the aerials only in a horizontal plane.

3.1. *The method of varying the interferometer position angle* α.—It is clear from Fig. 1 that in order to vary α it is necessary to vary β, the inclination of the interferometer axial plane to the hour circle passing through the centre of the disk. The value of α also depends on the position angle P of the solar axis of rotation, which shows an annual variation from $-26°$ to $+26°$.

Consider an interferometer with variable azimuth. If the axis of the interferometer makes an angle a with the East–West direction, the magnitude of β will depend on the angle H between the axial plane of the interferometer and the direction of the centre of the solar disk, as given by

$$\sin \beta = \frac{\sin a \cos \phi}{\cos H \cos \delta} \pm \tan H \tan \delta,$$

where ϕ is the latitude of the observing site and δ the declination of the centre of the disk.

If the azimuth angle a remains constant, the value of β is seen to vary rapidly when H is near 90°, and it is possible, for all latitudes and by suitable

choice of a, to obtain $\beta = 90°$. This occurs when the periodicity of the sinusoidal trace is very large. It is not always possible with this type of measurement to obtain small values of β, and a coverage of 0°–90° is attainable in general only during the summer.

Alternatively, if observations are restricted to times when H is near zero, the value of β is given by $\sin \beta = \sin a \cos \phi / \cos \delta$. The maximum value of β, which occurs when $a = 90°$, is limited by the latitude, and for $\phi > \delta$ the value of β will always be less than 90°. The maximum value at Cambridge (latitude 52°) is $\beta = 42°$; this is attainable in practice for a short period during the summer when the declination of the Sun is great enough to allow measurements to be made.

The maximum aerial spacings attainable for different azimuths were determined by the nature of the observing site. Adequate resolving power was available for East–West axes at all three wave-lengths used in the experiments, but the North–South distance was adequate only for the experiments at 1·4 metres.

3.2. *The use of the phase-switching system.*—In Stanier's measurements, made at 60 cm, the power received from the background radiation was less than that received from the quiet Sun. It did not therefore overload the receiver and it was possible to use an arrangement in which the total received power was recorded. As the wave-length is increased, the ratio of power received from the Galaxy to power received from the Sun increases rapidly, even when aerials with considerable directivity are used. In Table I the ratios of these powers are listed for the aerials used in the experiments described in this paper.

TABLE I

Wave-length (metres)	Effective area of one aerial (metres^2)	Power from Galaxy / Power from Sun
1·4	4·7	4
3·7	23	50
7·9	400	100

When the power from the Galaxy exceeds that from the Sun to the extent indicated in Table I, Ryle (**13**) has shown that there is considerable advantage in using a phase-switching system. A system of this kind is particularly convenient when there are large distances between the aerials, because it allows preamplifiers to be used. Phase-switching receiver systems were used throughout the present experiments.

3.3. *The calibration of the equipment.*—The determination of the aerial temperatures was carried out by the usual method of substituting a standard noise signal generator for the aerials. The phase-switching system, however, was arranged in such a way that the gain of the receiver was controlled by the total power available at the input. The gain therefore altered as different parts of the Galaxy were observed, and also when the noise signal generator was substituted for the aerials. The magnitude of this effect was appreciable at 3·7 and 7·9 metres, and it was measured and corrected for in the way indicated by Ryle (**13**).

In the experiments at a wave-length of 7·9 metres, seven separate and slightly different fixed aerials were used. It was found convenient to calibrate the relative gains of these aerials by recording the traces produced by two radio stars, 05·01 and 12·01 (**14**), which lay near the Sun and which were taken as

standard and constant references. In the calibration it was assumed that the angular sizes of these sources were considerably smaller than the angular resolving power of the largest interferometers used. Recent measurements of the diameter of these stars have confirmed that this assumption is substantially correct.

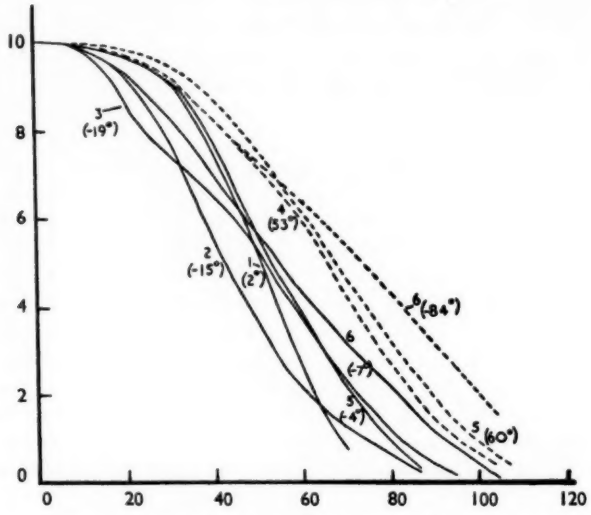

FIG. 3.—*Smoothed results of experiments* 1–6, $\lambda = 1{\cdot}4$ *metres.*
Ordinates: Relative recorded excursion.
Abscissae: Aerial separation in wave-lengths.

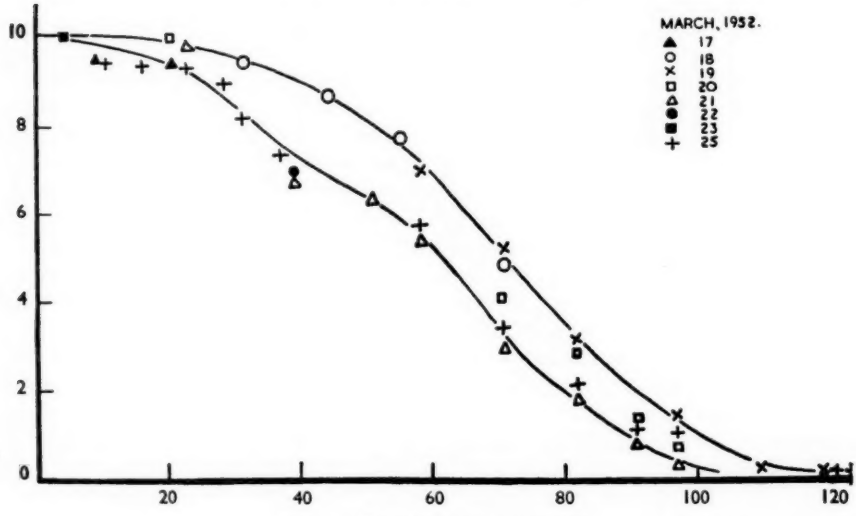

FIG. 4.—*Experiment* 4, $\lambda = 1{\cdot}4$ *metres.*
Ordinates: Relative recorded excursion.
Abscissae: Aerial separation in wave-lengths.

4. *The observations and results at wave-lengths of* 1·4, 3·7 *and* 7·9 *metres.*—Table II contains details of a number of measurements made between 1951 July and 1952 July. The experiments were carried out as far as possible at times of low sunspot activity. The level of any sunspot radiation present could usually be estimated approximately from a separate record obtained with a high-gain interferometer of large resolving power, and was generally not greater than about 5 per cent of the total radiation.

TABLE II

Wave-length (metres)	Date	Expt. no.	a	β	P	α	Duration of expt. (days)	Average number of daily spacings	Maximum aerial spacing (wave-lengths)	Mean Zürich sunspot number	Width of projected distribution to half power (R_0 as unit)
1·4	1951 Oct. 10–24	1	50°	28°	26°	2°	15	1	65	53	1·25
	1951 Dec. 2–8	2	0	−8 to 8	15	−23 to −7	7	3	100	32	1·22
	1952 Jan. 29–Feb. 3	3	−50	−30	−11	−19	3	2·5	90	15	1·07
	1952 March 17–25	4	50	28	−25	53	9	5	120	11	0·92 (mean)
			−55	−30		−4					1·1
	1952 April 1	5	−22	−13		13					
			26	16	−26	42	0·4	43	100	28	
			50	28		54					
			66	34		60					0·9
	1952 May 30	6	−50	−23 to −100	−16	−7 to −84	0·4	39	100	36	0·96
											0·77
3·7	1952 March 11–27	7	50	28	−25	53	17	1	58	17	1·18
	1952 April 28–30	8	7	0 to 15	−25	25 to 40	3	5·7	130	33	1·25
	1950 August 22–26	Machin's Expt.	7	4	18	−14	5	1·6	105	96	1·25
7·9	1951 July 17–26	9	7	7	7	0	10	1·2	54	47	1·4
	1952 July 18–26	10	7	7	7	0	9	1·4	84	19	1·56

4.1. *Results at a wave-length of* 1·4 *metres.*—Fig. 3 shows a series of smooth curves drawn through the experimental points determined in experiments 1 to 6. The curves are labelled with the numbers of the experiments and the values of α, the interferometer position angle, in brackets; for each of the experiments 5 and 6 two curves are shown corresponding to the limits of the values of α used.

The curves are divided into two groups corresponding to values of the magnitude of α of 2°–19° (full lines) and 53°–84° (dotted lines). The differences between the two sets of curves will be discussed in Section 6.

The detailed results for experiment 3, shown in Figs. 2*a* and 2*b*, are typical of experiments 1–3. During the course of experiment 4 the results altered from day to day, as shown in detail in Fig. 4; a mean curve is drawn in Fig. 3. When it was found that the results could vary in this way an attempt was made to complete a single set of observations as quickly as possible, and experiments 5 and 6 were carried out with this object in view.

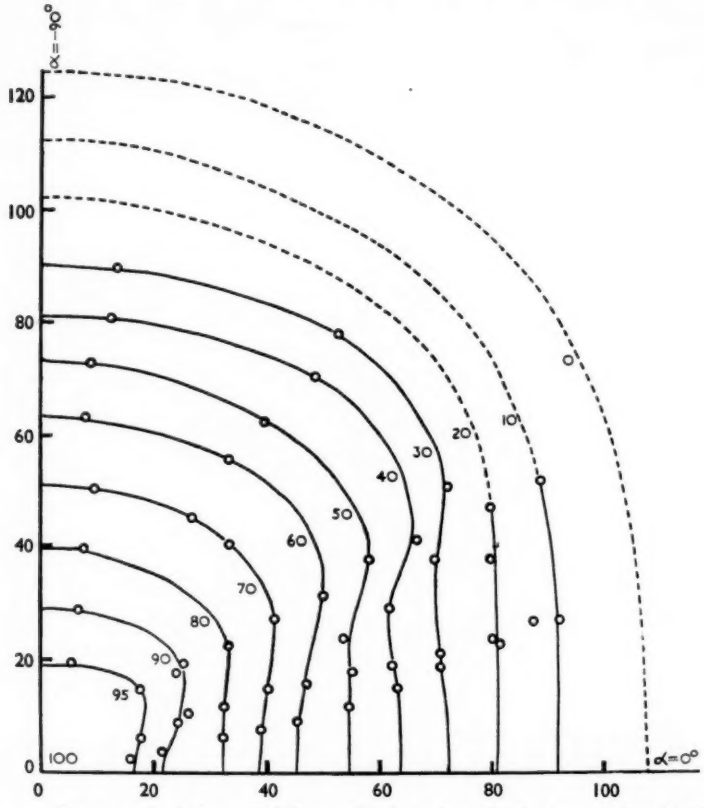

FIG. 5.—*Contours of relative recorded excursion for values of* α *between* $-7°$ *and* $-84°$, *experiment 6,* $\lambda = 1{\cdot}4$ *metres.*

Ordinates } *Aerial separation in wave-lengths.*
Abscissae }

In experiment 5 the value of α was altered from $-4°$ to 60° by using five different values of the azimuth angle of the interferometer, and for experiment 6 a variation in α from $-7°$ to $-84°$ was obtained using a fixed azimuth (see Section 3.1).

In these two experiments the recorded phase shift (see Section 2) was measured. In experiment 6 it was approximately zero, corresponding to a

symmetrical distribution of emission. In experiment 5 the phase shift was approximately zero for small values of the aerial spacing and increased to about 50° for spacings of 100 wave-lengths; these results could be explained on the assumption that about 10 per cent of the total radiation originated in a "bright" area situated on the western hemisphere of the disk near the equator.

The detailed results of experiment 6 are exhibited in Fig. 5, which shows the contours of constant recorded excursion corresponding to the variation in α from $-7°$ to $-84°$. The deductions from these observations are shown in Fig. 6 in the form of contours of the function $F(r, \theta)$. Fig. 6 was derived graphically in the way described in Section 5. The symmetrical component of the distribution determined from the observations of experiment 5 was very similar to that found for experiment 6.

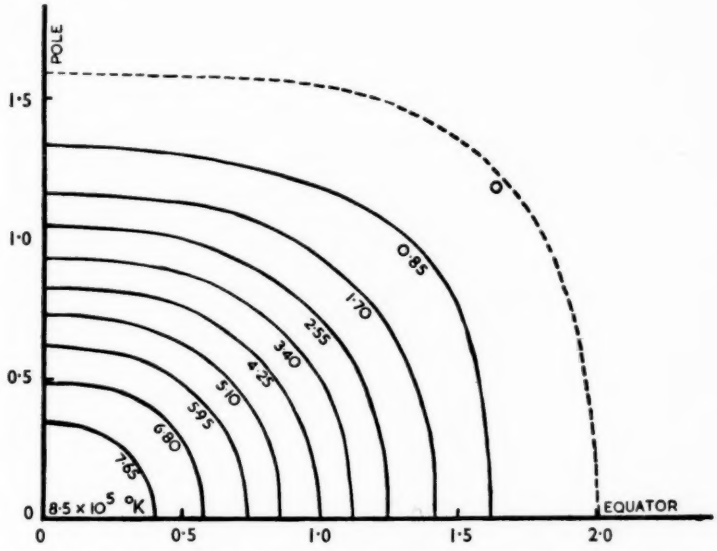

FIG. 6.—*The distribution of "brightness" temperature, experiment 6, $\lambda = 1{\cdot}4$ metres.*
Ordinates, Abscissae } *Distance from centre of disk, with radius of photosphere R_0 as unit.*

4.2. ***Results at a wave-length of 3·7 metres.***—The experimental results and the distributions of emission at a wave-length of 3·7 metres, derived by assuming circular symmetry, are compared in Figs. 7*a* and 7*b* with those obtained by Machin* at the same wave-length, and are seen to be appreciably different.

Experiment 7 was carried out at the same time as experiment 4 (at 1·4 metres), during which an appreciable change occurred in the distribution. It was not possible to determine any corresponding changes in the experiment at 3·7 metres because only one aerial spacing was obtained each day, but the individual points did show some scatter (Fig. 7*a*).

4.3. ***Results at a wave-length of 7·9 metres.***—At the longer wave-length of 7·9 metres space was not available for interferometers with axes inclined

* Machin has reported (private communication) that the original equivalent temperature at the centre of the disk should be 6×10^5 deg. K.

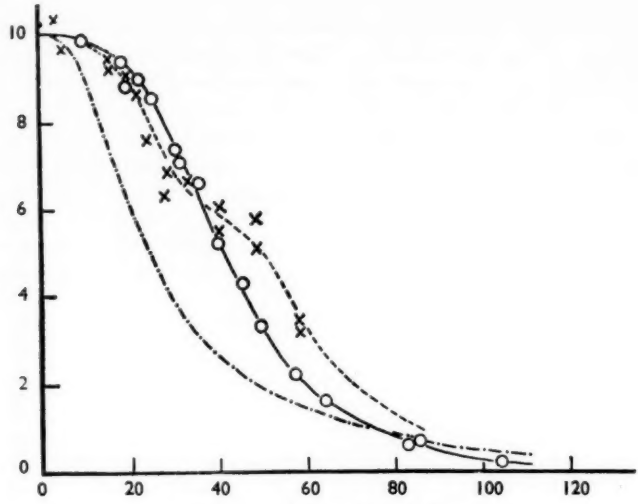

FIG. 7 *a.*—*Experiments for* $\lambda = 3{\cdot}7$ *metres.*

– – × – – *experiment* 7.
— o — *experiment* 8.
— · — *Machin's experiment.*

Ordinates: Relative recorded excursion.
Abscissae: Aerial separation in wave-lengths.

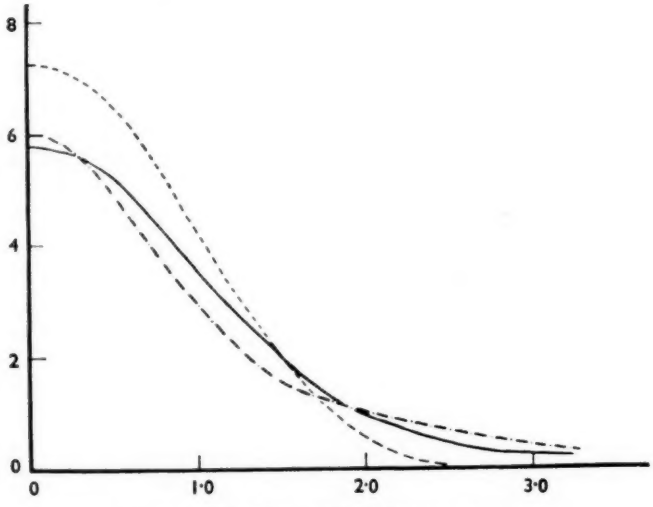

FIG. 7 *b.*—*Distribution of "brightness" at* 3·7 *metres.*

— — — *experiment* 7.
——— *experiment* 8.
· — · — *Machin's experiment.*

Ordinates: Equivalent temperature (unit $= 10^6$ *deg. K).*
Abscissae: Distance from the centre of the disk, with radius of the photosphere R_0 *as unit.*

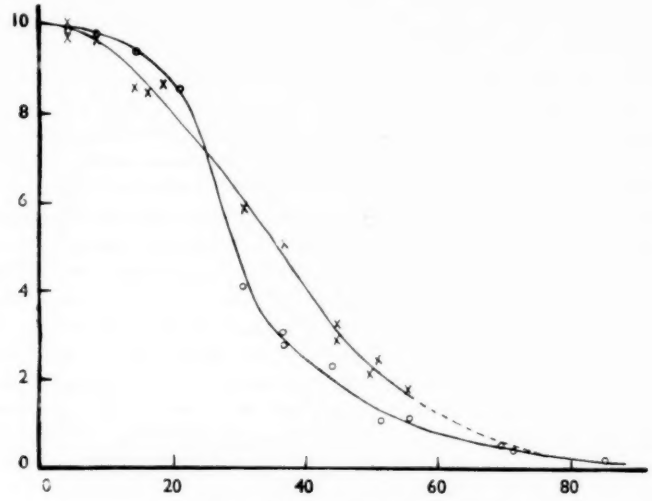

FIG. 8 *a.—Experiments at 7·9 metres.*
—×— *experiment 9.*
—o— *experiment 10.*
Ordinates: Relative recorded excursion.
Abscissae: Aerial separation in wave-lengths.

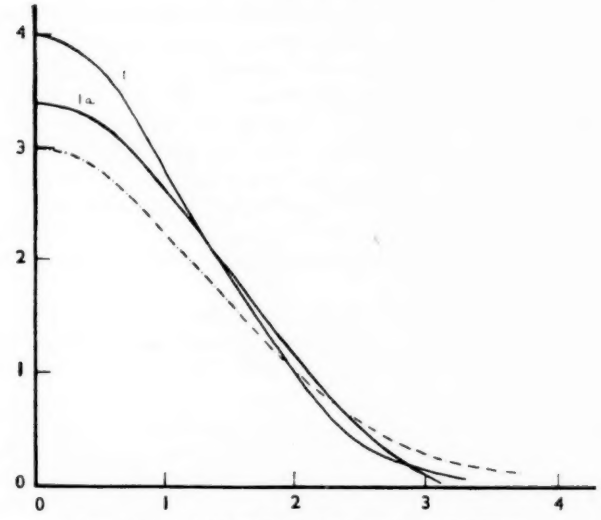

FIG. 8 *b.—Distribution of "brightness" at 7·9 metres.*
——— *(curve 1) experiment 9 with the recorded excursion extrapolated to zero amplitude.*
——— *(curve 1 a) experiment 9, using values of the recorded excursion up to a spacing of 54 wave-lengths only.*
— · — *experiment 10.*
Ordinates: Equivalent temperature (unit = 10^5 deg. K).
Abscissae: Distance from the centre of the disk, with radius of the photosphere R_θ as unit.

appreciably to the East–West direction. The results of the two experiments are shown in Fig. 8 *a* and the distributions, derived on the assumption of circular symmetry, in Fig. 8 *b*. Two distributions are shown for the first of these experiments (experiment 9, Table II), and the difference between them is explained in Section 5.

5. *The method of analysis of the experimental results.*—The distribution of the emission for those experiments where α was constant or extended over a few degrees was derived in terms of a function having circular symmetry. The Fourier–Bessel transform of an experimental curve was simply derived, using a process similar to the Lipson–Beever strips devised for crystallographic analysis.

For experiments 5 and 6, at a wave-length of 1·4 metres, the distributions with rotational symmetry were derived graphically in the following way. The experimental results, obtained in a form similar to that shown in Fig. 2 *b*, were replotted as the two-dimensional Fourier transform of the distribution (Fig. 5), and contours of constant recorded excursion were drawn through the points. This transform was then reduced to a series of one-dimensional transforms by projecting it on to axes through the origin corresponding to various values of α from 0° to 90°. The cosine Fourier transform of these projections represented the actual distribution of the emission along radii coincident with the axes used for the projections. These radial distributions then allowed contours of constant equivalent temperature of the emission to be drawn (Fig. 6).

In some of the experiments the recorded excursion for the maximum aerial spacing used was still appreciable, and extrapolations to zero were made when computing the Fourier transform. It can be shown, however, that this uncertainty in the value of the recorded excursion beyond a certain spacing does not produce a very large uncertainty in the Fourier transform. This is illustrated by the results at 7·9 metres, where, for experiment 9, the Fourier–Bessel transform of the curve ending abruptly at a spacing of 54 wave-lengths (Fig. 8 *b*, curve 1 *a*) is not very much different from the transform of the extrapolated curve (Fig. 8 *b*, curve 1). Small errors in the distribution curve are important, however, since they may introduce comparatively large errors in the scale of the central temperatures deduced from the total intensity. The absolute temperature scales of the distributions are therefore less reliable than the actual shapes of the distribution curves.

6. *Discussion of the results.*—The main conclusions drawn from the experiments are represented in Fig. 9, which shows averaged radial distributions of equivalent temperature over the solar disk at a series of different wave-lengths. The results for 60 cm are taken from Stanier's paper (**10**). It is seen that the size of the emitting disk increases with increasing wave-length, and it is satisfactory to note that present theories can explain this fact, at least qualitatively. An attempt by O'Brien and Bell (in preparation) to provide a detailed explanation of the experimental results may be important in giving evidence for the variation of the electron temperature and density with height in the corona.

6.1. *The variation with α of the radial distribution of emission.*—The departure from circular symmetry has been shown most conclusively for an observing wave-length of 1·4 metres. Experiments 5 and 6 showed that the radiating shape of the Sun was approximately elliptical and that the radial distance at which the emitted power was reduced to half was about 25 per cent greater at the

equator than in the polar direction. This difference between the equatorial and the polar widths of the distribution was shown very clearly by the combined results of experiments 1 to 6, as displayed in Fig. 3. All the "equatorial" curves (full lines) fall more rapidly towards zero than the "polar" curves (dotted lines), corresponding to a greater equatorial width of the distribution.

At 3·7 metres the distributions for $\alpha = 33°$ and $-14°$ were broader than for $\alpha = 53°$, indicating the same trend shown by the 1·4 metre results.

6.2. *Temporal variations in the distribution.*—It was found that for those experiments which lasted several days small changes usually occurred in the experimental curves. In experiment 4 the distribution was observed to change appreciably during the course of a few days. It is interesting to note that the

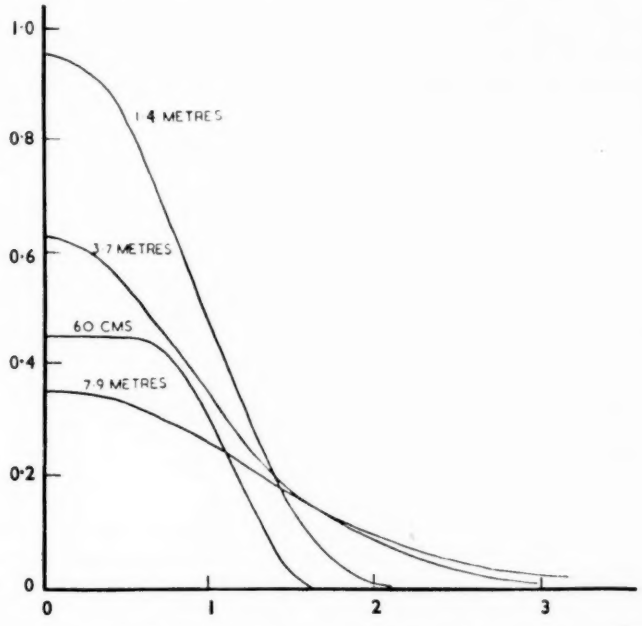

FIG. 9.—*Mean distributions of "brightness" at 60 cm, and 1·4, 3·7 and 7·9 metres.*
Ordinates: Equivalent temperature (unit = 10^6 deg. K).
Abscissae: Distance from the centre of the disk, with radius of the photosphere R_0 as unit.

intensity of the green coronal line λ 5303 A during the period of this experiment also showed appreciable variability (**15**). A comparison with the distributions derived from experiments 1 to 6 showed that the green line intensity measured at the limbs, when averaged over a region within $\pm 45°$ of the axis CD, was directly proportional to the radius at which the emitted power was reduced by half. This suggests that the radial extent of the corona increases with increasing line intensity measured very near the edge of the visible disk, in agreement with recent optical eclipse observations (**16**).

The "bright" area appearing in the distribution on 1952 April 1 (experiment 5) coincided with a region of pronounced coronal green line

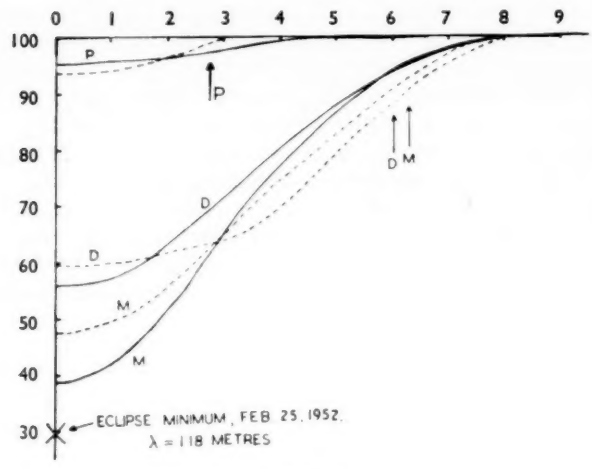

FIG. 10 *a*.

— — — *eclipse measurements at 1·78 metres (Denisse).*
——— *eclipse curve deduced from the distribution of " brightness " at 1·4 metres (1952 May 30, experiment 6).*

M—Markala, 1951 September 1.
D—Dakar, 1952 February 25.
P—Paris, 1952 February 25.

Ordinates: Observed intensity as percentage of uneclipsed intensity.
Abscissae: Time in arbitrary units. The times of optical contact are marked with arrows.

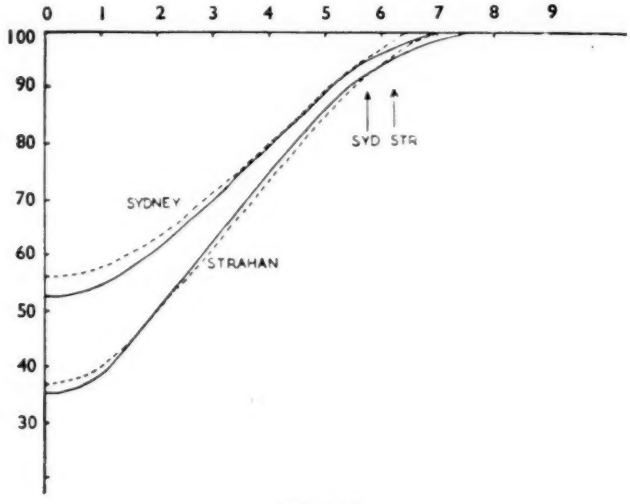

FIG. 10 *b*.

— — — *50 cm eclipse curves obtained for quiet Sun by Christiansen, Yabsley and Mills.*
——— *60 cm results that would have been obtained for the circularly symmetrical distribution of " brightness " derived by Stanier's interferometric method.*

Ordinates: Observed intensity as percentage of uneclipsed intensity.
Abscissae: Time in arbitrary units. The times of optical contact are marked with arrows.

intensity. This region was associated with flares and the formation of a new sunspot group, and produced a strong and prolonged geomagnetic disturbance.

The results at 1·4 metres showed a gradual narrowing of the distribution by about 20 per cent during the seven-month period of the observations. At 3·7 metres the distribution in 1952 was found to give appreciably less radiation from far out in the corona than that obtained by Machin in 1950, and at 7·9 metres the 1952 distribution shape was slightly wider than for 1951. These variations may possibly be associated with the sunspot cycle; it would be important to make regular distribution observations over a complete cycle.

6.3. *Comparison of results with eclipse measurements.*—Although it is difficult to deduce a unique distribution of the emission from eclipse observations, it is clear that the eclipse results can be used to check the distribution deduced by other methods.

Recent measurements at 1·78 metres by Denisse *et al.* (**6**) and at 1·18 metres by Laffineur *et al.* (**5**) during the eclipses of 1951 September 1 and 1952 February 25 coincided with quiet solar conditions, and by interpolation between the two wave-lengths a comparison with the distributions at 1·4 metres is possible. Fig. 10 *a* shows the eclipse curves that would have resulted for the elliptical distribution measured on 1952 May 30, together with the actual eclipse results obtained at Paris (P), Dakar (D) and Markala (M) at 1·78 metres. The full eclipse curve for 1·18 metres (1952 February 25, Khartoum) is not given but the percentage radiation remaining at totality is plotted. These results show that the distribution derived by interferometric means at 1·4 metres is consistent with the eclipse measurements.

It is convenient here also to compare the distribution derived at 60 cm by Stanier with the eclipse results (1948 November 1) obtained at 50 cm by Christiansen, Yabsley and Mills (**7**). They deduced three eclipse curves for the quiet Sun obtained at three widely separated sites, and two of these curves are shown (Fig. 10 *b*) with those deduced assuming the distribution to be that derived by Stanier. The agreement is seen to be very good. At the total eclipse of 1952 February 25, Laffineur (**5**) measured the percentage of the total radiation remaining at totality for a wave-length of 55 cm to be (19 ± 1) per cent.

The agreement between these recent observations and the figure of 29 per cent derived from Stanier's 1949 results is not as good as with the earlier eclipse observations; it is possible that the explanation is a decrease in the effective size of the Sun between 1949 and 1952, similar to the decrease observed at 1·4 m between 1951 and 1952.

Acknowledgments.—This work was carried out at the Cavendish Laboratory as part of a programme of radio research supported by the Department of Scientific and Industrial Research. The author is indebted to Mr M. Ryle, F.R.S., for his invaluable help and encouragement, and to his colleagues who assisted in making the observations. The work was carried out during the tenure of an E. Oliver Ashe Overseas Scholarship (Kimberley, South Africa).

Cavendish Laboratory,
University of Cambridge:
1953 *March* 21.

References

(1) Sander, K. F., *Nature*, **159,** 506, 1947.
(2) Dicke, R. H. and Beringer, R., *Ap. J.*, **103,** 375, 1946.
(3) Covington, A. E., *Nature*, **159,** 405, 1947.
(4) Piddington, J. H. and Hindman, J. V., *Austr. J. Sci. Res.* A, **2,** 524, 1949.
(5) Laffineur, M. *et al.*, *C.R. Acad. Sci.* (*Paris*), **228,** 1636, 1949; *ibid.*, **234,** 1528, 1952.
(6) Denisse, J-F. *et al.*, *C.R. Acad. Sci.* (*Paris*), **233,** 917, 1951; *ibid.*, **234,** 1597, 1952.
(7) Christiansen, W. N., Yabsley, D. E. and Mills, B. Y., *Austr. J. Sci. Res.* A, **2,** 506, 1949.
(8) Minnett, J. C. and Labrum, N. R., *Austr. J. Sci. Res.* A, **3,** 60, 1950.
(9) McCready, L. L., Pawsey, J. L. and Payne-Scott, R., *Proc. Roy. Soc.* A, **190,** 357, 1947.
(10) Stanier, H. M., *Nature*, **165,** 354, 1950.
(11) Machin, K. E., *Nature*, **167,** 889, 1951.
(12) Smerd, S. F., *Austr. J. Sci. Res.* A, **3,** 34, 1950.
(13) Ryle, M., *Proc. Roy. Soc.* A, **211,** 351, 1952.
(14) Ryle, M., Smith, F. G. and Elsmore, B. E., *M.N.*, **110,** 508, 1950.
(15) Fraunhofer Institute *Sonnenzirkular*.
(16) von Klüber, H., *The Observatory*, **72,** 207, 1952.

MOTIONS IN THE SUN AT THE PHOTOSPHERIC LEVEL

III. The Evershed effect in sunspots of different sizes

T. D. Kinman

(Communicated by the Director, University Observatory, Oxford)

(Received 1953 September 22)

Summary

Velocity fields are derived from the sight-line velocities at 315 points in the spectra of one large and three small sunspots, using Evershed's positive-on-negative method of measurement. Corrections for scattered light derived graphically from observations at the solar limb are applied to these velocities and also (since the scattering is mainly instrumental and therefore constant) to the previously determined velocities for Mt. Wilson No. 9987. The velocities in the small spots are also corrected for obliteration.

The motion in the new large spot confirms the previous result of a purely radial horizontal flow reaching a maximum velocity in the penumbra and extending into the photosphere. A comparison of the velocity fields of all the spots shows (1) that the maximum radial velocity increases linearly with the umbral radius, and (2) that the time to reach maximum velocity is independent of the size of the umbra and equal to about 13×10^3 seconds. On a simple model of a sunspot this leads to the conclusion that the heat absorbed per gram of material in flowing from the umbra to the photosphere is the same for all spots.

Introduction.—Motion in a sunspot at the photospheric level may be found from the Doppler displacements of the absorption lines in its spectrum. Using this method, Evershed (**1**) discovered radial velocities of the order of 2 km sec^{-1} in the penumbrae of sunspots. Recently, observations were made at Oxford* to determine the complete velocity field of a single, large and regular sunspot. The purely radial flow discovered by Evershed was confirmed and it was found that the velocity increased from about 1 km sec^{-1} at the edge of the umbra to a maximum of about 2 km sec^{-1} at the centre of the penumbra and then decreased to zero well out in the photosphere. The flow was steady and laminar. These observations, together with the general appearance of the spot, suggest a simple model in which cool material rises in the umbra and then spreads out radially in a thin layer which is gradually warmed up from beneath. On this model the velocity field in the penumbra will depend on :

(*a*) conditions deep down in the spot (presumably depending on the magnetic field) which determine the flux of material issuing from the umbra and also its temperature, i.e. the initial conditions of the material entering the penumbral layer; and

(*b*) conditions near the surface which determine the rate at which energy is supplied to the moving penumbral layer.

* Motions in the Sun at the photospheric level. II. The Evershed effect in sunspot Mt. Wilson No. 9987, T. D. Kinman (**3**). This paper is hereafter referred to as Paper II.

It was shown in Paper II that the rate at which energy is absorbed by the penumbral layer is a function of the radial distance from the centre of the umbra and the velocity field may be expected to vary with the size of the sunspot in consequence. It is therefore of interest to make further measurements of these Evershed velocities, both to confirm existing results and to determine the variation of the velocity field with spots of different sizes.

A discussion of the errors encountered in these velocity determinations in Paper II showed that the major systematic error is due to scattered light. The error from this cause was estimated to be 10 per cent. An accurate determination of the scattering correction and its application are therefore essential if true Evershed velocities are to be found. This problem is therefore discussed in the first section of this paper. The determination of the corrected velocities in five sunspots of different sizes forms the second section, and the resulting velocity fields are compared in the third section. A short physical discussion of these results is given in the fourth and final section.

1. *Scattered light*

1.1. *The determination of the scattering function.*—The light scattered by the atmosphere and telescope may be determined by observations at the solar limb following each observation of the Evershed effect. The spectroscope slit is set radially just outside the limb so that the scattered light from about 10″ out to 120″ from the limb may be photographed at the required wave-length. At distances nearer to the limb, obliteration and the vertical apparatus function of the spectroscope would invalidate the observations. The absolute intensity of the light is found from an equal exposure 40″ inside the limb through calibrated N.P.L. filters which in this wave-length region cut down the light by a factor of 0·0191. The characteristic curve for each plate is found from a spectrum of the centre of the disk taken through a Zeiss step-wedge. Another spectrum of the centre of the disk is taken through filters in order to determine any non-uniformity in illumination along the slit.

Microphotometer tracings of these spectra are made perpendicular to the dispersion at wave-lengths λ 5880 and λ 5960, thereby bracketing the region used for velocity measurement. The spectra taken to verify the uniformity of illumination are similar and the small non-uniformity shown is probably largely due to vignetting in the spectroscope. The correction for non-uniformity is applied both to the scattered light and to the wedge spectra. The scattered light is then found by the usual methods and expressed as a percentage of the surface brightness 40″ inside the limb. The surface brightness at this point is found in terms of the surface brightness $I(0, 0)$ at the centre of the disk by interpolating the mean of the five standard observations of limb-darkening (**12**). No systematic difference is found between the scattered-light curves at the two wave-lengths measured. The scattered light expressed as a percentage of $I(0, 0)$ is plotted against distance from the limb in Fig. 1 for three days. The full curves *a*, *b* and *c* are the scattered-light curves for 1952 May 23, 1952 June 27 and 1952 June 28 respectively. Since these curves are so similar, the scattered-light correction is evaluated from a mean of the three curves, which is shown dashed in Fig. 1. The relative constancy of the curves observed on different days suggests that the scattering may be caused primarily by the telescope.

Consider an annulus of radii s and $s+\delta s$. Let the light which is scattered from an element of the annulus at position angle θ and of area $s\,\delta s\,\delta\theta$ on to its centre be $U(s).B(s,\theta).s\,\delta s\,\delta\theta$, where $B(s,\theta)$ is the surface brightness of the element and $U(s)$ is the scattering function. The light coming from the annular zone between s_1 and s_2 ($s_1>s_2$) will therefore be

$$\int_0^{2\pi} d\theta \int_{s_2}^{s_1} s\,.\,U(s).B(s,\theta).ds=\bar{s}(s_1-s_2)U(\bar{s})\int_0^{2\pi} B(\bar{s},\theta)\,d\theta, \qquad (1)$$

where $U(\bar{s})$ is the value of the scattering function in an annular zone of mean radius $\bar{s}$. Let the area out to $s=120''$ be divided into eight such annuli (as shown in Table I) and let the unknown mean values of the scattering functions corresponding to each annulus be U_1, U_2, U_3, . . . U_8. These annular zones are then drawn to scale on a sheet of Kodatrace.

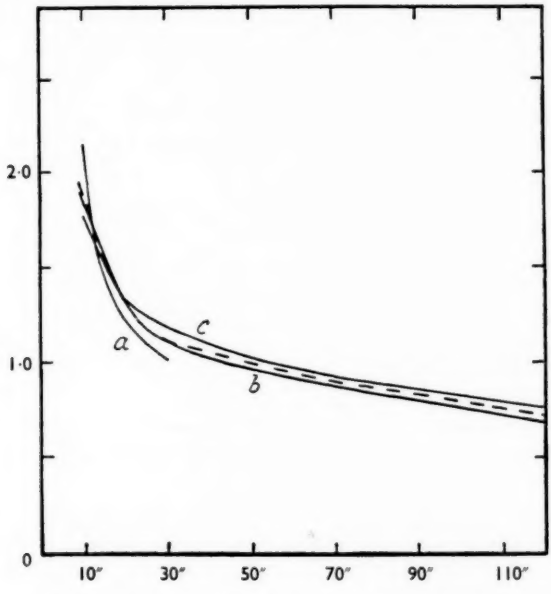

FIG. 1.—*The scattered light at the solar limb on three days.*
Ordinate : Scattered light as a percentage of I(o, o).
Abscissa : Distance from the limb in seconds of arc.

a 1952 *May* 23.
b 1952 *June* 27.
c 1952 *June* 28.
– – – *Mean of a, b and c.*

The region of the disk which is within 120″ of the limb is also drawn to scale and is divided into curved strips parallel to the limb. A mean surface brightness B_n, derived from limb-darkening, is then assigned to each strip. To find the scattered light at a point x'' from the limb, the annular scattering zones are centred at this point on the drawing of the solar limb (Fig. 2). Then if σ_{pn} is the area which is common to the annulus to which U_p refers

and the limb zone to which B_n refers, the measured surface brightness of the scattered light $I(x)$ is given by

$$I(x) = U_1(\Sigma_n \sigma_{1n} B_n) + U_2(\Sigma_n \sigma_{2n} B_n) + \ldots U_8(\Sigma_n \sigma_{8n} B_n) + Q, \qquad (2)$$

where Q is the small amount of light which is scattered from distances greater than 120″. Q may therefore be put equal to the surface brightness of the scattered light at 120″ from the limb or $0{\cdot}0072I(0, 0)$.

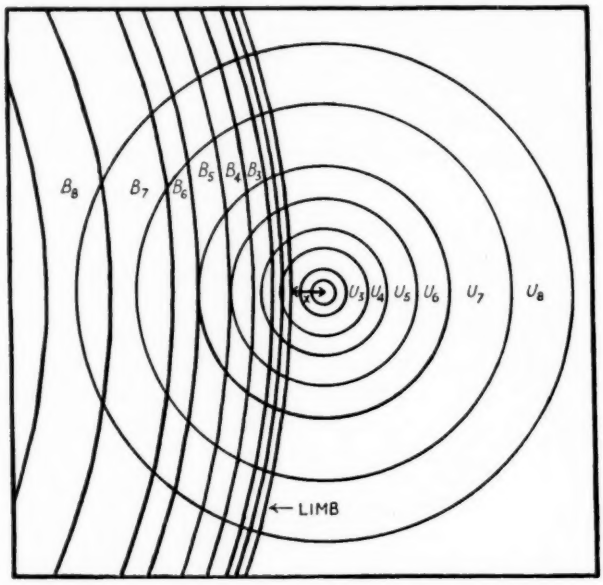

FIG. 2.—*The graphical method of finding the scattering function.*

The areas σ_{pn} may be measured with a planimeter and therefore all quantities in equation (2) are known except the values of the scattering functions U_p. In the region in which $I(x)$ is known, the coefficients of U_1 and U_2 are zero and therefore by taking $I(x)$ at six values of x we can obtain six equations to find the remaining six values of the scattering function U_3, $U_4 \ldots U_8$. In order to reduce the calculation involved, approximate solutions are first found by the two-Sun method described below (which becomes more accurate towards the limb) and these are then corrected by trial and error to give the best solution of the six equations.

The surface brightness of the scattered light at 120″ from the limb is $0{\cdot}0072I(0, 0)$. If we now imagine that there are two such limbs, one on either side of the point, then there will be twice this amount of scattered light or $0{\cdot}0144I(0, 0)$ at this point (**4**). This is approximately equal to the surface brightness of the light scattered from the region beyond 120″ having the mean surface brightness of the Sun ($0{\cdot}814I(0, 0)$). The surface brightness of the light scattered from a region of unit surface brightness beyond 120″ is obtained by dividing by $0{\cdot}814I(0, 0)$ and equals 0·0177.

Zanstra (**13**), in discussing the observations of Redman and Shirley on a star image (**9**), has shown that within 5″–10″ $U(s)$ follows an exponential law and that for the longer-range scattering an inverse power function holds. Now the kind of power function and the ranges over which both it and the exponential function hold are likely to vary with the conditions. An exponential function of the form $U(s)=\alpha e^{-\beta s}$ is therefore fitted to the observed values of $U(s)$ for the inner zones U_3, U_4 and U_5 using least squares. Similarly an inverse power function $U(s)=A(B+s^2)^{-1}$ is used for the outer zones U_6, U_7 and U_8. The resulting scattering functions are given in Fig. 3 and it may be seen that the curves fit within the errors of the observations. The exponential function may therefore be extrapolated to give the scattering function and hence the scattered light within 10″. The contributions of all zones from 0″ to 120″ are given in Table I and adding to them the 0·0177 surface brightness which is due to light scattered from outside 120″, the total surface brightness of the light scattered from all distances from regions of unit surface brightness is 0·0896.

TABLE I

The light scattered from each zone

Scattering function	Range	Light scattered from each zone		
U_1	0″ –0″·5		Extrapolation from the exponential formula	0·0001
	0″·5–1″·0			0·0003
	1″·0–2″·0			0·0010
	2″·0–3″·0			0·0016
	3″·0–4″·0			0·0019
	4″·0–5″·0			0·0021
U_2	5″–10″			0·0124
U_3	10″–20″	0·0168	Exponential formula	0·0202
U_4	20″–30″	0·0137		0·0103
U_5	30″–45″	0·0044		0·0058
U_6	45″–60″	0·0032	Inverse power formula	0·0030
U_7	60″–90″	0·0069		0·0071
U_8	90″–120″	0·0075		0·0065
	>120″	0·0177		0·0177
		Graphical method		
		Total :		0·0896

1.2. *The correction of the observed velocities for scattered light.*—In order to determine the scattered light at any point in or near a sunspot, a scale drawing of the spot is made assuming that the umbra and penumbra are circular. The error in the scattered-light correction introduced by this assumption is not greater than one per cent in the case of the most irregular spots discussed here. For the present purpose the true intensity profile of a spot may be represented by a step function where the intensities in the umbra, penumbra and photosphere are in the ratios 0·3 : 0·8 : 1·0. Then using the annular zones of the scattering function marked on a sheet of Kodatrace, the total scattered light at any radial distance from the centre of the umbra is found graphically.

The scattered light at any point comes predominantly from the photosphere and even inside a spot is not greatly reduced from the value of 0·0896 photospheric surface brightness which obtains at large distances from the spot.

The greatest reduction (which is here relevant) occurs at the edge of the umbra in the case of the larger spots. Here the surface brightness of the scattered light is 0·0765 of that of the photosphere and is made up as follows:

From the umbra	: 0·0056	photospheric surface brightness
,, ,, penumbra	: 0·0209	,, ,, ,,
,, ,, photosphere	: 0·0500	,, ,, ,,
Total surface brightness of scattered light	: 0·0765	photospheric surface brightness

These are maximum values for the contributions from the umbra and penumbra. For points farther out or for smaller spots, these contributions are smaller.

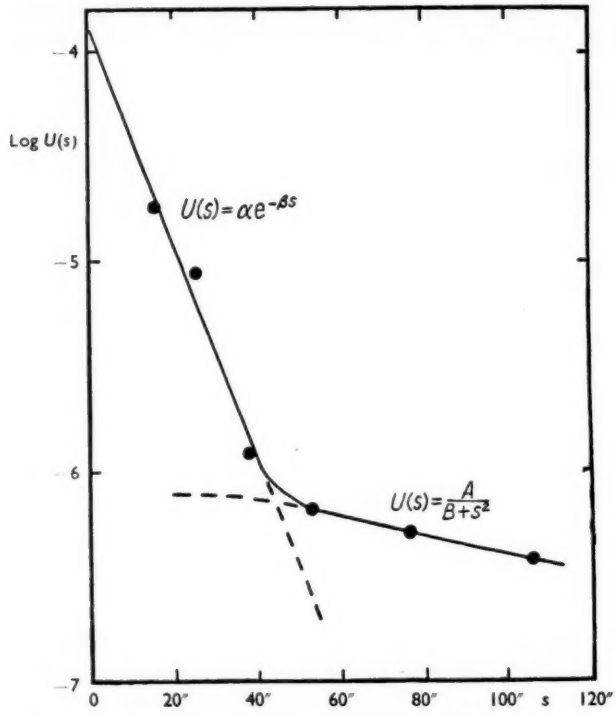

FIG. 3.—*The logarithm of the scattering function U(s) as a function of s in seconds of arc.*

The velocity corresponding to the umbral and far photospheric light is zero, but the near photospheric and penumbral light comes from regions in which there is a velocity shift. However, these velocity shifts will be both positive and negative and it may therefore be assumed that all the scattered light has zero velocity.

Consider a point at a radial distance r from the centre of the sunspot. Let the true surface brightness be $I(r)$ and the surface brightness of the scattered light be $I_{sc}(r)$ at this point. From the known scattering function, the loss of

the true surface brightness by scattering is $0{\cdot}090I(r)$ and the gain in the surface brightness from the scattered light of zero velocity is $I_{sc}(r)$, which can be calculated. The observed intensity will therefore be

$$I_{obs}(r) = 0{\cdot}910I(r) + I_{sc}(r).$$

Let the true sight-line velocity at any point be $V(r)$; then from Miss Hart's observations on blended spectra (**2**) the observed velocity is linearly dependent on the intensity of the scattered light, and therefore

$$V(r) = \left(1 + \frac{I_{sc}(r)}{0{\cdot}910I(r)}\right) . V_{obs}(r),$$

where $V_{obs}(r)$ is the observed sight-line velocity. Now it is shown in Paper II that the true radial, tangential and vertical velocity components $u(r)$, $v(r)$ and $w(r)$ at any radial distance r in a sunspot are related to the true sight-line velocity $V(r)$ by a linear relation

$$V(r) = A\,.\,u(r) + B\,.\,v(r) + C\,.\,w(r),$$

where A, B and C are coefficients which depend only on the azimuthal (but not radial) position in the spot and on the position of the spot on the disk. These true component velocities may therefore be obtained from the component velocities derived from the sight-line velocity $V_{obs}(r)$ by multiplying by the factor

$$\left(1 + \frac{I_{sc}(r)}{0{\cdot}910I(r)}\right).$$

Since no measurements have been made of the intensity distribution in these sunspots, it is assumed that the variation of the true surface brightness $I(r)$ across the penumbra is that given by Richardson (**10**). The correction factor may thus be evaluated and the true velocities found for the sunspots under discussion. Now since $I_{sc}(r)$ cannot exceed $0{\cdot}090$ and the present observations are confined to the penumbra and photosphere, the correction factor cannot exceed $1{\cdot}13$ and will in general be somewhat less. Even an error of as much as 10 per cent in the scattering function would therefore lead to an error of only 1 or 2 per cent in the corrected velocities.

2. *The determination of the velocity components in five sunspots*

2.1. *The selection of observations and their measurement.*—In the early summer and autumn of 1952, a total of seventy spectra of eleven sunspots were obtained using the Oxford telescope (**5**) and spectroscope (**6**). Since this was a time of sunspot minimum, it was imperative to use every opportunity of taking spectra and later to make a selection from what was obtained.

The dispersion (at λ 5935) is $1{\cdot}5$ A/mm and the image scale is $10''{\cdot}3$/mm. The slit height and width were $9{\cdot}4$ mm and $0{\cdot}040$ mm respectively and Ilford Rapid Process Panchromatic emulsion and Kodak Press Contrast developer were used for all spectra.

The spectra were obtained using the Guiding Plate and filar micrometer previously described.* By means of this, known points on the image of the sunspot may be guided on to the slit until an exposure is made at the instant of best seeing. The exact position in each spot corresponding to each spectrum

* Motions in the Sun at the photospheric level. I. Methods, H. H. Plaskett (**7**). This paper is hereafter referred to as Paper I.

is found later by comparing the spot features visible on the spectrum with a Greenwich photograph * of the spot.

The spectra are taken in the region of λ 5900, where atmospheric lines are plentiful, in order that these lines may be used as standards. In the previous measurements described in Paper II, fifteen solar and twenty-two atmospheric lines were used. The measurement of this number of lines is very laborious and the number is therefore reduced in the present measurements to six solar lines (numbers 1, 4, 6, 7, 8 and 9 in Table IV, Paper II) and seven atmospheric lines (numbers 1, 4, 6, 9, 10, 11 and 13 in Table III, Paper II). Since the rejected lines are those which are faint and difficult to measure, the resulting loss in accuracy should be quite small. An analysis of thirteen points using (*a*) six solar lines and (*b*) fourteen solar lines showed r.m.s. errors of a single line of $\pm 0{\cdot}32$ and $\pm 0{\cdot}36$ km sec^{-1} respectively, and r.m.s. errors of the mean of $\pm 0{\cdot}13$ and $\pm 0{\cdot}10$ km sec^{-1} respectively. It is seen that the loss of accuracy is small.

The spectra are selected for measurement by the following criteria :

(1) The angle subtended at the centre of the Sun by the spot and the observer should be about 45°. This is the best position on the disk to observe a horizontal velocity field (Paper II).

(2) The spectra should show streaks due to granules, high contrast and sharply defined spot features as evidence of good seeing.

(3) The spot should be isolated and regular in appearance.

(4) The spot should be stable. It must be remembered however that the lifetime of small spots (umbral radius ~5″) is generally only two or three days.

Seventeen spectra of four of these spots are thereby chosen for measurement. Of these, three are of a small spot which is possibly a remnant of the group Mt. Wilson No. 10928, four are of a small spot Mt. Wilson No. 10955, five are of a large spot Mt. Wilson No. 10957 and five are of a small spot Mt. Wilson No. 11051. In addition, corrected velocities may be found from the fourteen spectra of Mt. Wilson No. 9987 (which were discussed in Paper II) assuming the scattered light to be the same for these as for the present spectra.

The spectra are measured on the Evershed positive-on-negative micrometer described in Paper I. Nine independent settings are made on each line and since the machine is self-recording there is no prepossession in making the settings. Two positive spectra of the centre of the disk (one red right and the other red left) are used and both direct and reverse measures are made at each point in the spectrum so that any systematic error which might arise from measuring in one direction only is eliminated. Using the method described in Paper II, the sight-line velocities (corrected for the motion of the Sun and of the observer) and the sunspot polar coordinates (r, ϕ) can be found for the measured points. In this system of coordinates with origin at the centre of the spot, r is the horizontal radius from the centre of the umbra and ϕ is the position angle measured counter-clockwise from the direction of solar rotation.

2.2. *Mt. Wilson No.* 10957.—Five spectra of this large sunspot (umbral diameter 20″ and heliographic coordinates $B = -9° 11'$, $L = 72° 00'$) were

* Positive copies of these photographs were kindly supplied to us by Mr H. W. Newton with the permission of the Astronomer Royal.

obtained with moderate seeing on 1952 June 27. The slit passed along an E.–W. line through five different parts of the spot: the centre of the umbra, the North and South edges of the umbra and 15″ North and South of the centre of the umbra. An exposure of 2·5 seconds was used.

The spectra are measured in the spot and its neighbourhood at intervals of 0·3 mm with a spectrum height limited to the same size. The sight-line velocities and coordinates (r, ϕ) are thus found at 98 points in the spot.

Reduction of sight-line velocities to velocity components in the spot.—Motion in a sunspot is conveniently considered in terms of the cylindrical velocity components $u=\dot{r}$, $v=r\dot{\phi}$ and $w=\dot{z}$ which are the radial, tangential and vertical velocity components respectively. It is shown in Paper II that these are related to the corrected sight-line velocity V by the linear relation

$$V=u(\cos\phi\cos\gamma_1+\sin\phi\cos\gamma_2)+v(\cos\phi\cos\gamma_2-\sin\phi\cos\gamma_1)+w\cos\gamma_3,$$

where $\cos\gamma_i$ is a direction cosine which depends upon the position of the points of measurement on the disk. Since this relation is linear, u, v and w may be found by least squares from a group of points in an annular zone about the umbra in which the motion is assumed to be constant.

Two preliminary solutions for u are made. In the first the zones are of constant perpendicular distance from the edge of the umbra and ϕ is measured between this perpendicular and the direction of solar rotation. In the second the zones are of constant distance from the edge of the umbra measured radially from the centre of gravity of the umbra and ϕ is measured between this radius and the direction of solar rotation. There is little difference between the r.m.s. errors of the two solutions and so the second system of coordinates (r^*, ϕ) is adopted since this is used for the earlier spot Mt. Wilson No. 9987.

A least squares solution for the three components u, v and w is now made. It is found that the motion is predominantly radial and that the tangential component is erratic and of the same order as its r.m.s. error. The vertical component is small and comparable with its r.m.s. error in the penumbra but increases to about $+0{\cdot}5$ km sec^{-1} in the photosphere.

Now it may be shown that any departure from cylindrical symmetry in a purely radial flow will produce a spurious vertical component in a solution which assumes cylindrical symmetry. Let the coefficients of u and w be denoted by A and C respectively in the equation of condition. The coefficient C is independent of ϕ and is therefore constant if the spot is taken to be plane. The greatest departure from cylindrical symmetry in the appearance of the spot is that between the Eastern and Western halves. It is therefore seen that for two points E. and W., in the Eastern and Western halves, for which $\phi_E=\pi-\phi_W$, we have $A_E=-A_W$. If in fact the radial flow is asymmetrical, having values u_E and u_W at E. and W., the sight-line components are A_Eu_E and $-A_Eu_W$ respectively. Consequently, if cylindrical symmetry is assumed, a solution for u and w gives

$$A_Eu_E=A_Eu+C_W,$$

$$-A_Eu_W=-A_Eu+C_W,$$

from which

$$w=\frac{A_E(u_E-u_W)}{2C} \quad \text{and} \quad u=\frac{u_E+u_W}{2}.$$

Thus for n such pairs of points, the solution will give components

$$w = \frac{1}{n}\sum_n \left(\frac{A_E(u_E - u_W)}{2C}\right)_n \qquad \text{and} \qquad u = \frac{1}{n}\sum_n \left(\frac{u_E + u_W}{2}\right)_n .$$

Actually the measured points are not in pairs 180° apart, but if there are nearly as many points with the coefficient A positive as negative, an East–West asymmetry in the radial motion gives rise to a spurious vertical motion. The radial component obtained is the arithmetic mean of the actual irregular radial components. Since the present spot shows a distinct East–West asymmetry, an asymmetrical flow may be expected and hence a spurious vertical component.

Finally a solution is made for the radial component u alone. The results are given in Fig. 4 (*a*) for points in (1) the Eastern half and (2) the Western half of the spot. The considerable East–West asymmetry in radial flow is very apparent. Now we may consider the residuals $(u - \bar{u})$, where $\bar{u}$ is the mean velocity of both halves of the spot at a given radial distance. These residuals may be interpreted either as radial or vertical components. In either case the residuals reach their maximum values in two fairly restricted regions outside the Eastern and Western penumbrae, one of which (the Eastern) corresponds to a place where both the penumbra and umbra are very irregular. Now vertical motion would be expected to show some cylindrical symmetry and not to occur in localized regions in the spot. The hypothesis of irregular radial flow is therefore more likely and agrees with the irregular outline of the spot.

TABLE II

Sunspot, Mt. Wilson No. 10957

(*a*) *Radial velocity in km sec*$^{-1}$ (*Eastern half of spot*)

r^*	n	u_1	u_2	σ
0·17	6	+1·36	+1·51	±0·19
0·53	9	+2·16	+2·40	±0·20
0·89	7	+2·09	+2·31	±0·26
1·27	10	+2·38	+2·61	±0·16
1·66	6	+2·66	+2·93	±0·21
2·10	5	+2·26	+2·49	±0·10
2·66	9	+1·74	+1·92	±0·25

(*b*) *Radial velocity in km sec*$^{-1}$ (*Western half of spot*)

r^*	n	u_1	u_2	σ
0·17	7	+0·41	+0·46	±0·20
0·53	7	+1·16	+1·29	±0·15
0·89	8	+1·48	+1·63	±0·32
1·27	7	+0·90	+0·99	±0·25
1·66	7	+0·12	+0·13	±0·25
2·07	5	+0·07	+0·08	±0·21
2·63	5	−0·66	−0·73	±0·27

r^* is measured in units of ten thousand kilometres from the edge of the umbra.

The radial velocities determined in the Eastern and Western halves of the spot are therefore treated separately, and they are given in Tables II (*a*) and II (*b*). In both these tables the first two columns give r^*, the mean radial distance of the zone from the edge of the umbra and n, the number of points within it.

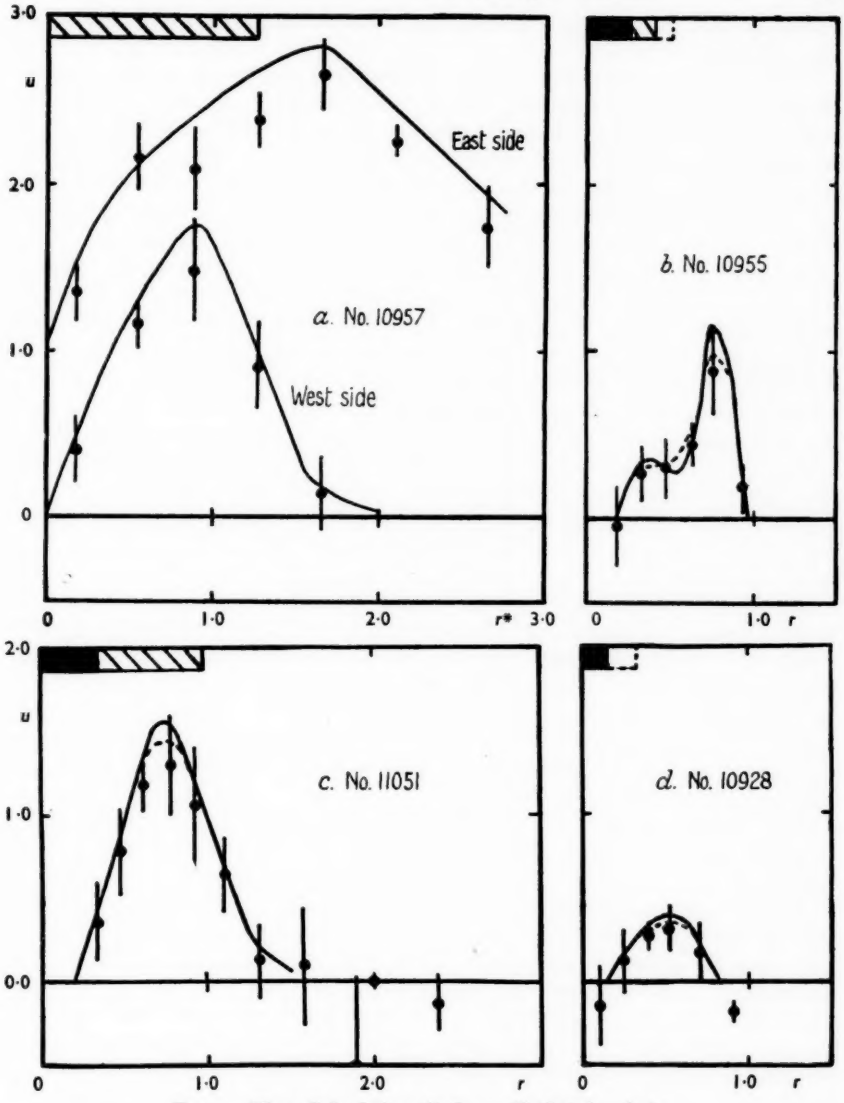

FIG. 4.—*The radial velocity u (in km sec^{-1}) plotted against :*

(a) the radial distance from the edge of the umbra (r) in No. 10957. The uncorrected velocities are shown by small filled circles and the r.m.s. errors of the mean by vertical lines. The velocities corrected for scattered light are shown by the full curve. No correction for obliteration is applied.*

(b), (c) and (d) the radial distance from the centre of the umbra (r) in Nos. 10955, 11051 and 10928 respectively. The uncorrected velocities are shown by small filled circles and the r.m.s. errors of the mean by vertical lines. The velocities corrected for scattered light are shown by a dashed curve and the velocities also corrected for obliteration by a full curve.

Abscissae : r and r are in units of ten thousand kilometres.*

The positions of the umbra and penumbra are indicated in the top left-hand corner a each graph. The estimated edges of the penumbra (for b and d) are shown dashed.

The third and fifth columns give u_1 the radial velocity and σ its r.m.s. error from the mean.

The correction for scattered light discussed in Section 1 is now applied, and the final corrected velocity u_2 is given in the fourth column of Tables II (*a*) and II (*b*). As is shown in Paper II, the correction for obliteration in large spots is negligible and therefore no correction is applied for it here. These results are given in Fig. 4 (*a*) for the two halves of the spot. The uncorrected velocities are shown by small filled circles and the r.m.s. errors of the mean by vertical lines. The velocities corrected for scattered light are shown by a smooth curve.

2.3. *Mt. Wilson Nos.* 10928, 10955 *and* 11051.—These three small sunspots (of projected umbral diameters about 4″, 6″ and 8″ respectively) were observed with moderate seeing. Under these conditions, with a tremor disk of about the same size as the umbrae, it is useless to try to set any particular feature of the spot on the slit: the best that can be done is to set the umbra as centrally on the slit as possible. A more exact position may be deduced later by comparing the spectrum obtained with the Greenwich photograph of the spot. Three spectra of No. 10928 ($B=-9°\,44'$; $L=231°\,31'$) were obtained on 1952 May 23 with an exposure of 3 seconds, four spectra of No. 10955 ($B=16°\,37'$; $L=108°\,26'$) on 1952 June 28 with an exposure of 2·5 seconds, and five spectra of No. 11051 ($B=13°\,58'$; $L=148°\,50'$) on 1952 November 8 with an exposure of 5 seconds.

In the case of the smaller spots Nos. 10928 and 10955 the spectrum height to be measured is limited to 0·1 mm and measurements are made at this interval inside the spot and at 0·2 mm intervals outside it. In the case of the somewhat larger spot No. 11051, however, the spectrum height is limited to 0·2 mm and the spectrum is measured at this interval in and near the spot and at an average interval of 0·4 mm well outside it. In this way the sight-line velocities and the spot coordinates (r, ϕ) are found at 57 points in No. 10928, 64 points in No. 10955 and 96 points in No. 11051.

The velocity field determined for the large spot No. 10957 confirms the previous result (Paper II) that the motion in a sunspot is wholly radial and horizontal with modified cylindrical symmetry about the edge of the umbra. In all three of the small spots the edge of the umbra is ill-defined, and since in this case the difference between r and r^* is small, it is sufficient to group the measured points in zones of r rather than r^*. The measured sight-line velocities in these spots are therefore grouped in zones of r and solutions are made for the radial component u alone. The results of these three solutions are given in Table III. In this table, the first column gives the mean radius r of the zone from the centre of the umbra, the second the number of points n in the zone, the third the radial velocity u in km sec^{-1} for the zone and the sixth the r.m.s. error σ of the mean of this velocity.

The scattered-light correction is now applied to these velocities. In the case of No. 11051, although (judging from the greater exposure times needed) the atmospheric scattering must have been greater, the scattered light recorded within 12″ and beyond 65″ from the limb was actually less than for the summer plates. It is concluded therefore that the observation must have been invalidated, probably by a mistake in setting the limb on the slit. The scattering correction derived for the summer observations is used for the velocities in No. 11051 which are therefore likely to be undercorrected.

The error in the correction can hardly exceed 50 per cent, however, which corresponds to a maximum error of 0·07 km sec^{-1} in the velocity curve, which is within the errors of the observations. The radial velocity (u_2) corrected for scattered light is given in the fourth column of Table III for the three spots.

TABLE III

The radial velocity in km sec^{-1} in three sunspots

Mt. Wilson No. 10928

r	n	u_1	u_2	u_3	σ
0·11	13	−0·14	−0·19	−0·19	±0·24
0·26	10	+0·12	+0·13	+0·17	±0·19
0·40	11	+0·27	+0·30	+0·33	±0·08
0·54	9	+0·32	+0·35	+0·39	±0·14
0·73	7	+0·17	+0·19	+0·23	±0·17
0·92	7	−0·18	−0·20	−0·20	±0·06

Mt. Wilson No. 10955

r	n	u_1	u_2	u_3	σ
0·19	14	−0·05	−0·06	−0·06	±0·24
0·34	15	+0·27	+0·30	+0·35	±0·17
0·48	13	+0·29	+0·32	+0·28	±0·14
0·63	10	+0·44	+0·49	+0·49	±0·13
0·76	6	+0·88	+0·97	+1·17	±0·25
0·95	6	+0·18	+0·20	+0·20	±0·15

Mt. Wilson No. 11051

r	n	u_1	u_2	u_3	σ
0·34	9	+0·37	+0·42	+0·42	±0·24
0·48	9	+0·78	+0·88	+0·89	±0·26
0·62	9	+1·19	+1·33	+1·41	±0·17
0·78	10	+1·30	+1·46	+1·56	±0·30
0·93	10	+1·05	+1·16	+1·20	±0·37
1·10	8	+0·64	+0·70	+0·70	±0·23
1·32	10	+0·13	+0·14	+0·20	±0·22
1·58	11	+0·10	+0·11	+0·11	±0·36
1·90	8	−0·42	−0·46	−0·46	±0·45
2·38	12	−0·13	−0·14	−0·14	±0·17

r is measured in units of ten thousand kilometres from the centre of the umbra.

Unlike large spots, the velocities in small spots will be considerably affected by bad seeing. An examination of the detail visible on the spectra suggests that an upper limit to the range over which obliteration occurs is 5″. A correction for obliteration over this range, using Rayleigh's method (**8**), is therefore applied, and the finally corrected velocities (u_3) are given in the fifth column of Table III. These results are also given in Figs. 4 (*b*), 4 (*c*) and 4 (*d*). The radial velocity in km sec^{-1} is plotted against radial distance from the centre of the umbra in units of ten thousand kilometres. The uncorrected velocities are shown by small filled circles and the vertical lines denote the r.m.s. error of the mean velocity. The velocities corrected for scattered light are shown by a dashed curve and the velocities also corrected for obliteration by a full curve.

2.4. *Mt. Wilson No.* 9987.—Since the scattered light is primarily caused by the apparatus, the correction for it obtained in Section 1 may also be applied to the velocities in sunspot No. 9987 which are discussed in Paper II. The resulting radial velocities are given in Table IV. The first two columns give r^*, the distance from the edge of the umbra, and n, the number of points in each zone. The third and fourth columns give u_1 and u_2, the radial velocity in km sec^{-1} before and after correction for scattered light, while the last column gives σ, the r.m.s. error of the mean velocity. As shown in Paper II, the correction for obliteration in large spots is negligible and no correction is applied for it here.

TABLE IV

Sunspot Mt. Wilson No. 9987

The radial velocity in km sec^{-1}

r^*	n	u_1	u_2	σ
−0·1	8	+1·05	+1·18	±0·06
0·1	9	+1·30	+1·45	±0·12
0·3	9	+1·84	+2·05	±0·06
0·5	12	+1·90	+2·11	±0·04
0·7	17	+1·92	+2·13	±0·04
0·9	16	+1·67	+1·84	±0·03
1·0	15	+1·79	+1·97	±0·05
1·2	18	+1·19	+1·31	±0·04
1·4	10	+1·20	+1·32	±0·08
1·6	9	+0·78	+0·86	±0·08
1·7	12	+0·68	+0·75	±0·02
2·0	18	+0·45	+0·50	±0·02
2·4	13	+0·17	+0·19	±0·03
2·8	14	+0·05	+0·06	±0·01
3·4	22	+0·10	+0·11	±0·01
4·3	21	+0·15	+0·17	±0·01

r^* is measured in units of ten thousand kilometres from the edge of the umbra.

3. *Observed regularities in the velocity fields of five sunspots.*—In order to compare these velocity fields, the radial velocities of the five spots must all be known in terms of the same distance-variable. The velocities in the three small spots are only known as a function of r (the radial distance from the centre of the umbra) since the edges of their umbrae appear too diffuse to be well determined. In the following discussion therefore this parameter is used for all the spots. For the larger spots r may be found by adding the mean umbral radius to the known values of r^*.

A comparison of the velocity curves in Fig. 4 shows that the radial velocity is greater for the larger spots than for the smaller. In Fig. 5 the maximum velocity u_{max}—to choose a representative point—is plotted against the umbral radius a and the r.m.s. errors of the mean velocity are shown by vertical lines. These quantities are also tabulated for the five spots in the second and third columns of Table V. It is seen that, within the errors of the observations, u_{max} increases linearly with a. The following linear relation between them is found by least squares:

$$u_{max} = (1{\cdot}7 \pm 0{\cdot}2)a + 0{\cdot}56 \pm 0{\cdot}17.$$

Here, as in Fig. 5, u_{max} is in km sec^{-1} and a is in units of ten thousand kilometres. The errors of the coefficients are the r.m.s. errors of the mean.*

It may also be seen from Fig. 4 that the maximum velocity occurs within the penumbra for the larger spots Nos. 9987, 10957 and 11051 (umbral radii 10·5, 10·0 and 3·5 thousand kilometres respectively) and outside the penumbra for the two smaller spots Nos. 10955 and 10928 (umbral radii 2·5 and 1·7 thousand kilometres respectively.) The poor definition of the penumbrae for these latter spots suggests that their penumbral widths may have been underestimated. The mean ratio of penumbral to umbral radii for spots of this size (derived from 90 spots in the *Greenwich Heliographic Results*) is 2·0,

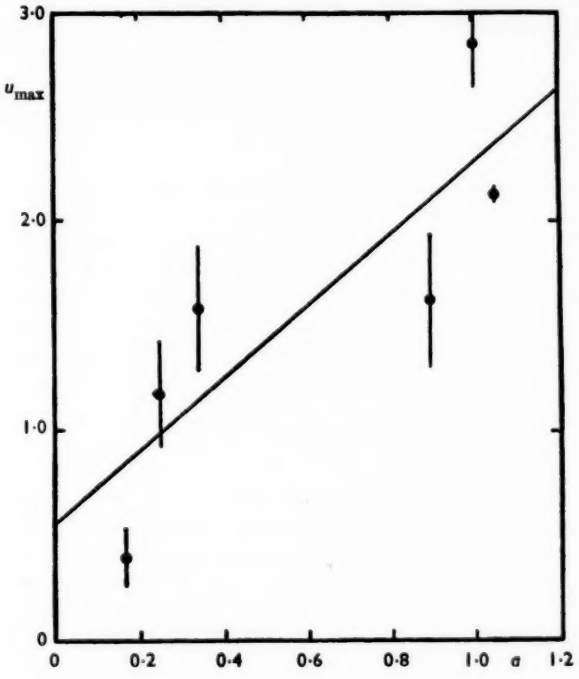

FIG. 5.—*The maximum velocity u_{max} as a function of umbral radius.*
Ordinate : u_{max} is in km sec^{-1}.
Abscissa : a is in units of ten thousand kilometres.

and the outer edge of the penumbra based on this value is shown dotted in Fig. 4. The velocity maximum, however, lies well beyond either the estimated or measured limits of the penumbrae of these small spots. It is interesting to note in this connection that Evershed, in observing spots of intermediate size (umbral radius 5 to 6 thousand kilometres), judged that the velocity maximum occurred at the outer edge of the penumbra, which is in satisfactory agreement

* R. Michard (*Ann. d'Ap.*, **14**, 101, 1951) using Abetti's observations (*Pub. R. Oss. Arcetri*, **50**, 47, 1932) also finds an increase of Evershed effect with spot size. Abetti's observations (uncorrected for scattered light or obliteration) refer, however, to the edge of the penumbra and not to the velocity maximum.

with these observations. There is no doubt, however, that in all the present observations (unlike most of Evershed's estimates from the appearance of the lines), the velocity field continues beyond the outer edge of the penumbra.

TABLE V

The maximum velocity u_{max} and the time $t_{max\,u}$ to attain it as a function of the umbral radius a

Mt. Wilson number	a	u_{max}	$t_{max\,u}$
10928	0·17	0·39 ± 0·14	12·0 ± 3·0
10955	0·24	1·17 ± 0·25	15·4 ± < 3·0
11051	0·35	1·58 ± 0·30	10·6 ± < 3·0
10957 (West)	0·90	1·62 ± 0·32	12·9 ± < 3·0
10957 (East)	1·00	2·85 ± 0·21	17·9 ± 6·0
9987	1·05	2·13 ± 0·04	9·2 ± < 3·0

The umbral radius (a) is measured in units of ten thousand kilometres. The maximum velocity (u_{max}) is in km sec^{-1} and the time ($t_{max\,u}$) to attain it is in thousands of seconds. The errors are the r.m.s. errors of the mean.

Now although the radial velocities in large spots are greater, the distance which the material travels before attaining maximum velocity is also greater than in small spots. This suggests that the time to reach maximum velocity may be comparable in differently sized spots. The radial velocity u is known as a function of distance r and therefore the time taken by the material to flow a given distance may be found. It is necessary to choose some identifiable point r_0 as origin. For convenience this is taken as the radial distance at which the increasing radial velocity equals 0·1 km sec^{-1}. The time $t(r)$ to travel a distance r is then given by

$$t(r) = \int_{r_0}^{r} \frac{dr}{u} \tag{3}$$

and can be found by numerical integration. The time to reach maximum velocity ($t_{max\,u}$) is plotted in Fig. 6 against umbral radius. These quantities are also tabulated for the five spots in the second and fourth columns of Table V. It is seen that although $t_{max\,u}$ ranges from $9{\cdot}2 \times 10^3$ sec for No. 9987 to 18×10^3 sec for the East side of No. 10957, there is no systematic variation of $t_{max\,u}$ with umbral size. The largest errors occur for No. 10957 East ($\pm 6 \times 10^3$ sec) where there is uncertainty in extrapolating to 0·1 km sec^{-1} and in No. 10928 ($\pm 3 \times 10^3$ sec) where the fractional error in velocity is greatest. These errors are shown by full vertical lines in Fig. 6. It may be concluded therefore that within the errors of the observed velocities the time for the material to reach its maximum velocity is constant for spots of different sizes and equals about 13×10^3 seconds.

The motions in these five spots thus appear to obey the following empirical laws:

(1) The maximum radial velocity attained increases linearly with umbral size.

(2) The time to reach maximum velocity is independent of umbral size and is equal to about 13×10^3 seconds.

These laws are based on a very small, though probably sufficiently representative sample of the spots at a time of sunspot minimum. It is clearly essential (in spite of the labour required to measure each velocity field) that a more

extensive sample should be obtained both to confirm these laws and to determine the dispersion accurately.

4. *A physical discussion.*—In order to make a physical examination of the observed velocity fields, the following simple model of a sunspot (proposed in Paper II) is adopted. There is a steady laminar flow of cool material from the umbra radially and horizontally outwards in a thin layer. This moving layer is gradually warmed by the hotter layers beneath it. In this section we shall examine $q(t)$, the heat absorption per unit mass, as a function of time in the moving layer. It would be expected that the $q(t)$ curves should be the same for different spots if a gram of umbral material always had the same initial temperature and was subsequently heated by photospheric and sub-photospheric material, the temperature of which was independent of spot size.

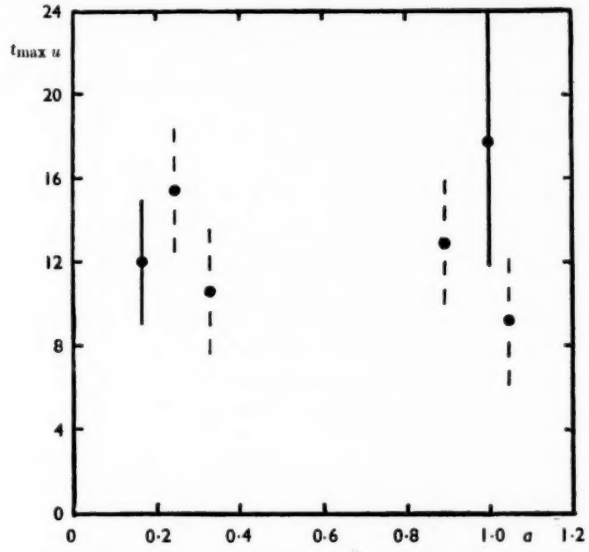

FIG. 6.—*The time to reach maximum velocity, $t_{\max u}$ as a function of umbral radius a.*

Ordinate : $t_{\max u}$ is in thousands of seconds.
Abscissa : a is in units of ten thousand kilometres.

In this model the penumbra may be considered as an ideal monatomic gas with constant specific heat for the range of temperatures encountered (4000 deg. K – 6000 deg. K). Radiation pressure is negligible compared with the gas pressure at this level of the atmosphere. The gravitational potential energy of the material is constant since the flow is horizontal, and viscous forces are ignored for the sake of mathematical simplicity. The mechanical and heat energies alone need be considered in finding the energy absorbed by the moving penumbral layer.

4.1. *Energy absorption by the moving penumbral layer.*—The first law of thermodynamics may be written in terms of Lagrangian time derivatives

$$\frac{Dq}{Dt} = \frac{De}{Dt} + p\frac{D(1/\rho)}{Dt}, \qquad (4)$$

where e, p and ρ are the internal energy, pressure and density per unit mass respectively. In a steady state, $\partial/\partial t$ terms are zero and for an ideal gas (4) may be written

$$\frac{Dq}{Dt} = \frac{u}{\gamma - 1}\left(\frac{1}{\rho}\frac{dp}{dr} - \frac{c_p(\gamma-1)}{\rho}T\frac{d\rho}{dr}\right), \tag{5}$$

where u and T are the radial velocity and temperature, c_p is the specific heat at constant pressure and γ is the ratio of the specific heats. Euler's equations of motion for a steady horizontal outflow with cylindrical symmetry give

$$u\left(u\frac{du}{dr} + \frac{1}{\rho}\frac{dp}{dr}\right) = 0, \tag{6}$$

while the equation of continuity for a radial horizontal outflow is

$$\frac{1}{\rho}\frac{d\rho}{dr} + \frac{1}{u}\frac{du}{dr} + \frac{1}{r} = 0. \tag{7}$$

The parameters p and ρ are unobservable and must therefore be eliminated from equation (5) for $\frac{Dq}{Dt}$. From (5), $\frac{1}{\rho}\frac{dp}{dr}$ is eliminated by (6) and $\frac{1}{\rho}\frac{d\rho}{dr}$ by (7) to obtain

$$\frac{Dq}{Dt} = \left(c_pT - \frac{u^2}{\gamma-1}\right)\frac{du}{dr} + \frac{c_pTu}{r}, \tag{8}$$

which is an expression for the heat absorbed per second per unit mass in terms of the velocity, velocity gradient and temperature at a radial distance r from the centre of the umbra. I am indebted to Dr J. B. Sykes for pointing out that the expression for Dq/Dt which is given in Paper II may be simplified as above by the elimination of the temperature gradient. All the parameters on the right-hand side of (8) are known except the temperature T of the moving layer. A first approximation to this may be found from the intensity profile of a large spot (at effective wave-length λ 6450) given by Richardson (**10**). The temperature $T(r)$ corresponding to a surface brightness $I(r)$ (in terms of the photosphere as unity) is then

$$T(r) = 5740(I(r))^{1/4} \text{ deg. K.} \tag{9}$$

Dq/Dt may therefore be calculated in the region of the observed velocity fields. The time taken to reach any point is known from equation (3) and consequently Dq/Dt may be found as a function of t. It is then integrated numerically so that $q(t)$, the amount of energy absorbed per gram at time t, may be plotted as a function of t.

The $q(t)$ curves for the five spots are shown in Fig. 7. The position of the outer edge of the penumbra is marked on each curve by a short vertical line, except for No. 10928, where $t=0$ occurs outside the spot. It may be seen from Fig. 7 that there is a marked similarity between the $q(t)$ curves of five very differently sized spots. Thus the time to absorb maximum energy, though it varies from 10^4 sec for No. 9987 (umbral radius $10{\cdot}5 \times 10^3$ km) to 2×10^4 sec for the East side of No. 10957 (umbral radius $10{\cdot}0 \times 10^3$ km), shows no systematic run with umbral size. The likely error in t for No. 10957 is known to be of the order of 6×10^3 sec, and consequently some of the differences must arise from errors in the observed velocities. In the second place, q_{max}, the maximum

energy absorbed, although it ranges from 20×10^{11} erg g^{-1} to 44×10^{11} erg g^{-1}, shows no systematic variation with spot size. We may calculate the likely error in $q_{\max}$ since from (8) we have

$$\frac{Dq}{Dt} = u\frac{dq}{dr} = \left(c_p T - \frac{u^2}{\gamma - 1}\right)\frac{du}{dr} + \frac{c_p T u}{r},$$

and therefore

$$\frac{dq}{dr} = c_p T \frac{d}{dr}\ln(ur) - \frac{u}{\gamma - 1}\frac{du}{dr}. \tag{10}$$

Now since T is only likely to vary between 4000 and 6000 deg. K we may assume with sufficient accuracy for this purpose that it is constant, and integrate to obtain

$$q(r) - q(r_0) = q(r) \simeq c_p \overline{T} \ln\left(\frac{ur}{0{\cdot}1 r_0}\right) - \frac{(u^2 - 0{\cdot}01)}{2(\gamma - 1)}. \tag{11}$$

The probable error Δq in q arising from errors Δu in u and Δr_0 in r_0 is therefore

$$\Delta q = \left[\left(\frac{c_p \overline{T}}{u} - \frac{u}{\gamma - 1}\right)^2 (\Delta u)^2 + \left(\frac{c_p \overline{T}}{r_0}\right)^2 (\Delta r_0)^2\right]^{1/2}, \tag{12}$$

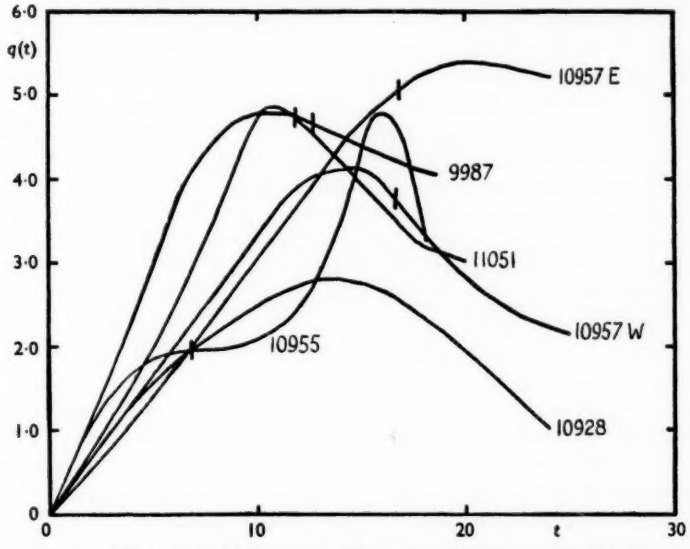

FIG. 7.—*The heat absorbed per gram $q(t)$ as a function of time t for five spots.*
Ordinate : $q(t)$ is in units of 10^{12} erg g^{-1}.
Abscissa : t is in thousands of seconds.
The short vertical line shows the position of the outer edge of the penumbra (absent for 10928).

since the error in r is relatively small. For No. 10957 (East) and No. 10928, the errors in $q_{\max}$ amount to 4×10^{11} and 6×10^{11} erg g^{-1} respectively, and therefore a large part of the scatter in $q_{\max}$ in Fig. 7 must arise from this cause. We therefore conclude that the observed $q(t)$ curves are independent of umbral size within the errors of the observations.

It is of interest to compare $q_{\max}$ (which averages 35×10^{11} erg g^{-1}) with the changes of internal and kinetic energy in a gram of material. The change in internal energy in going from the umbra to the photosphere $c_v(T_{\text{phot}} - T_{\text{umb}})$

equals $2{\cdot}25 \times 10^{11}$ erg g^{-1}, and the kinetic energy of material with a velocity of 2 km sec^{-1} is 2×10^{10} erg g^{-1}. It is seen that these are much smaller than q_{max}, so that a large amount of the energy absorbed must appear in forms other than internal and kinetic energy—probably in the performance of external work and ultimately as radiant energy.

We now see why the time to reach maximum velocity is independent of umbral size. The dominant term in equation (8) for Dq/Dt is $c_p T(du/dr)$ except in the close neighbourhood of the velocity maximum, and it follows that $q_{max}(t)$ will occur $(Dq/Dt = 0)$ very shortly after the velocity maximum $(du/dr = 0)$. Therefore since $q(t)$ is the same for all spots, so must be the time to reach maximum velocity. Consequently maximum velocity occurs at increasing distances beyond the penumbra with decreasing size of spot—as is seen in Fig. 4.

4.2. *The temperature in the moving layer.*—While a time-dependence of heat absorption which does not vary with umbral size appears to account for the observed radial flows, it remains unexplained how for small spots there can be a net gain of energy per unit mass well outside the penumbra. Now by the second law of thermodynamics, heat must flow down a temperature gradient unless work is being done on the system. Therefore, for the moving matter outside the penumbra to experience such a net gain, its temperature must be less than that of a stationary mass of gas in thermal equilibrium which is at the same level in the undisturbed photosphere. If this be so, it would be expected that between the penumbra of a small spot and the bright region farther out (where Dq/Dt is negative) there should be a region where the surface brightness is less than that of the undisturbed photosphere. There are however no observations to support this.

The explanation may be found in the small optical thickness of the moving layer. For a spot of umbral radius a, vertical umbral velocity u_u and penumbral velocity u_p at a radius r, the thickness of the layer given by continuity is

$$h = \frac{u_u a^2}{2u_p r}. \tag{13}$$

Now u_u/u_p must be less than 0·1 and outside the spot a/r is less than 0·5, therefore, for a small spot where a is 2000 km, the layer cannot be thicker than 50 km. Now the observed surface brightness is due to the sum of the radiation contributed by the moving layer and by the deeper-lying stationary layers. The proportion of total radiation coming from a layer 50 km thick centred on $\tau = 0{\cdot}3$ in a Strömgren atmosphere (**11**) varies from 7 to 15 per cent at $\mu = 1{\cdot}00$ and 0·50 respectively, where $\cos^{-1}\mu$ is the angle from the centre of the disk subtended at the centre of the Sun. The layer cannot be cooler than the temperature of the umbra at the same level, so that the maximum effect will be to lower the surface brightness at these points to from 95 to 90 per cent of that of the undisturbed photosphere. The effect would be greater nearer the limb, but here it would tend to be disguised by the presence of faculae. It would be of interest to try to observe this slight darkening (effectively a weak extension of the penumbra), which should be visible outside the penumbrae of very small spots.

In consequence of this, the surface brightness of the penumbra indicates the temperature of the underlying rather than the moving layer. The smaller

extent of the penumbra in small spots thus follows from the reduced cooling effect of the small umbra on the underlying layers in these spots.

If, however, the observed surface brightness does not refer to the moving layer, we have made an error in evaluating (8) by assuming that the temperature T of the moving layer can be deduced from the observed surface brightness. Fortunately the effect of this error is not large because the dominant term in Dq/Dt is linear in T. The minimum possible temperature of the layer is that of the umbral material (4250 deg. K) and the maximum assumed temperature is that of the photosphere (5740 deg. K), so that the maximum possible effect is to overestimate Dq/Dt by a factor of 1·4; the actual error is likely to be much less.

Let us consider the consequence of such an error in the calculated Dq/Dt. If $q_{\max}$ is constant and Dq/Dt is too large the estimated time to reach $q_{\max}$ must be too short and this effect should be more marked for small spots than for large. Again the small umbral cooling in a small spot means that the underlying layers are warmer; Dq/Dt should therefore be greater and the time to reach maximum energy shorter than in a large spot. It can scarcely be claimed that these second-order effects are shown in Fig. 7. It is possible that they are disguised by the inevitably large errors in the observed velocities and by our assumptions about the temperature of the moving layer.

In order to reduce the complex problem of the physical constitution of a sunspot to manageable proportions, it is necessary to make calculations with a simple model such as that used in this paper. The validity of the model may be assessed from the extent to which it represents and predicts the observed properties of actual spots. The present model accounts for the observation that the time for the radial velocity to reach its maximum is independent of the umbral size. Further, it predicts that a bright ring should be found outside the penumbra; in the case of large spots the bright ring is adjacent to the penumbra, but for smaller spots is separated from the penumbra proper by a region less dark than the penumbra. Owing to the small optical thickness of the moving layer, however, these variations in surface brightness will be small.

Conclusion.—Observations of the velocity fields of sunspots of different sizes lead to the empirical rules first that the maximum radial velocity increases linearly with umbral size, and secondly that the time to reach maximum velocity is independent of umbral size. The proposed model of a sunspot accounts for the observed velocity fields and leads to the conclusion that the heat absorption per unit mass in moving from the umbra to the photosphere is the same function of time for all spots. The reason for the dependence of the maximum radial velocity on size, however, rests outside the scope of the physical discussion which is possible with the present model. Since the $q(t)$ curves are the same for all the spots, the velocity at any time can only depend on the initial values of u and r when the heat absorption process starts, values which are probably determined by conditions deep down in the umbra. From the continuity conditions expressed in equation (13) these initial values (u_p and r) are seen to depend upon the radius of the umbra and the upward velocity of the material within it; these are presumably determined by the magnetic field acting at a deeper level in the umbra and may be a function of the size of the spot.

Since from 50 to 100 velocity determinations are needed to find the velocity field even of a small spot, it has so far only been possible to measure the velocities in five spots. Further observations are required, particularly of small sunspots (in which the fractional error in velocity is greater than for large spots), in order to confirm and, if possible, extend the simple laws of radial outflow found from the present observations. New photometric observations are also desirable, particularly to test the prediction of a slight darkening which may occur outside the penumbrae of very small spots. Such observations are planned for the fairly immediate future, as well as observations (with higher dispersion and a large solar image) on the upflow in the umbrae of large and small spots.

I am deeply grateful to Professor H. H. Plaskett for suggesting this work to me and also for the very generous help which he has given at all times. In particular, the discussions in Sections 3 and 4 of this paper are largely due to him. I am also indebted to Miss A. B. Hart for several helpful discussions.

University Observatory,
Oxford:
1953 *September* 19.

References

(1) J. Evershed, *Kodaikanal Obs. Bull.*, **2**, 63, 1909.
(2) A. B. Hart, *M.N.*, **114**, No. 1; *Comm. Univ. Obs., Oxford*, No. 43.
(3) T. D. Kinman, *M.N.*, **112**, 425, 1952; *Comm. Univ. Obs., Oxford*, No. 35.
(4) E. Pettit and S. B. Nicholson, *Ap. J.*, **71**, 153, 1930.
(5) H. H. Plaskett, *M.N.*, **99**, 289, 1939; *Comm. Univ. Obs., Oxford*, No. 14.
(6) H. H. Plaskett, *M.N.*, **112**, 177, 1952; *Comm. Univ. Obs., Oxford*, No. 33.
(7) H. H. Plaskett, *M.N.*, **112**, 414, 1952; *Comm. Univ. Obs., Oxford*, No. 34.
(8) Lord Rayleigh, *Scientific Papers*, Vol. I, p. 135, Cambridge, 1899.
(9) R. O. Redman and E. G. Shirley, *M.N.*, **98**, 613, 1938.
(10) R. S. Richardson, *Ap. J.*, **78**, 359, 1933.
(11) B. Strömgren, *Pub. og. Meddel. Kobenh. Obs.*, No. 138, 1944.
(12) J. B. Sykes, *M.N.*, **113**, 198, 1953; *Comm. Univ. Obs., Oxford*, No. 38.
(13) H. Zanstra, *M.N.*, **103**, 265, 1943.

CINEMATOGRAPHY OF PARTIAL SOLAR ECLIPSES

II. Observations at the eclipse of 1948 November 1, at Mombasa

R. d'E. Atkinson and J. D. Pope

(Communicated by the Astronomer Royal)

(Received 1953 August 20)

Summary

The first paper in this series gave the purpose and general principles of the method. The present paper describes the apparatus and the actual work at Mombasa, where it was tried out for the first time. The optical and electrical details are given at some length, since the method is new and the result was satisfactory. The analysis of the data obtained will appear in a subsequent paper.

The purpose of the expedition which went to Mombasa from the Royal Greenwich Observatory, for the eclipse of 1948 November 1, was to obtain a timed cinematographic record of the change in position angle shown by the thin solar crescent near mid-eclipse. This was to be done with a fixed camera, so that the diurnal motion could give the zero of position angles. The general principles of the method have already been set forth*, and the present paper describes the apparatus in more detail than was then done, and gives an account of the actual work at Mombasa, together with a brief summary of the observational material secured; in all essentials this material came well up to expectations. The analysis of it will be the subject of a later paper.

1. *Optical apparatus.*—The principal optical items, which were assembled on a primitive optical bench, were a "Vinten K" 35 mm cine camera (with its lens removed); a visual telescope lens of roughly 1 metre focal length, well corrected for spherical aberration and coma; and an unsilvered glass mirror which was in fact one face of a new Hilger spectrograph prism. This mirror, which was mounted in front of the lens, served the double purpose of greatly reducing the light at the earliest possible point, and of directing the beam through the lens and into the camera at any desired time, while both the latter remained fixed. The reflecting face measured 10 cm × 5 cm, which was not as large as would, in principle, have been ideal; but the lens was always used with a stop, and even the largest aperture employed was fairly well filled. To give a further reduction in light-intensity, and also to eliminate the secondary spectrum, either one or two Wratten 58 (green) filters were used; these were in the form of a gelatine film 5 cm square, mounted between two squares of "selected" glass, the complete filter being 4 mm thick; a brass holder was attached to the camera front so that one or both of these filters could be readily slipped into it, as near to the focal plane as possible.

It is perhaps worth stressing that for the particular task that is here involved a well-designed simple lens used with a filter is likely to prove superior to even the most complicated and highly corrected apochromat; and at all events it cannot prove inferior. When the diameter of the field is little more than a degree,

* R. d'E. Atkinson, *M.N.*, **113**, 18, 1953. This paper is hereafter referred to as Paper I.

and when only moderate apertures ($f/18$ or narrower) are required, a good achromat which obeys the sine condition will show the Airy disk and the first diffraction ring over the whole field; for photographic work (especially with fully exposed images) it is still highly desirable to eliminate the secondary spectrum with a suitable filter, but once that has been done there is no further improvement which could be attained by any complication of lens design, while any actual lens, if designed for a larger field, may have made sacrifices which leave it permanently inferior to the simple one, within the restricted field of the latter.

The optical bench which supported the prism, lens, and camera was fabricated out of 5-cm angle-iron, with brass plates bolted to the upper face near both ends to serve as base-plates. A short length of tubing (telescope tube) was also bolted to the central region to act as a mount for the lens cell (Fig. 1). The

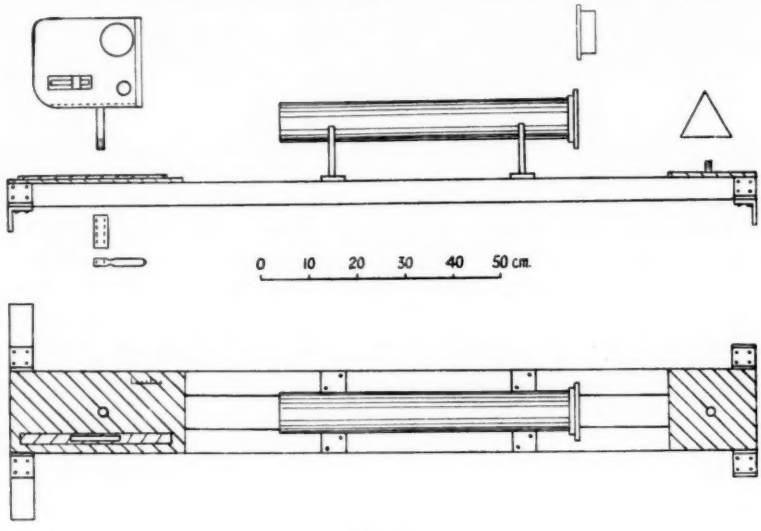

FIG. 1.

brass plate at the camera end was 9 mm thick, and was slotted so that a stout bolt which had been attached to the underside of the camera could pass through it; a clamp could be screwed up on this from below to lock the camera in place. The underside of this make of camera has a shallow longitudinal keyway machined in it, running through from front to back; a strip of brass was cut to fit this and was permanently pinned in place on the base-plate as soon as the camera had been squared on to the lens; when the clamp was slackened, the camera could then be slid forwards or backwards on the base-plate, for focusing, and always remained properly squared on. The base-plate was engraved with a millimetre scale, and under the best conditions the correct focus setting could be determined to about half a millimetre, at the widest stop used. As already mentioned (Paper I, pp. 26, 27), there was no need to cover in the space (about 28 cm long) between the end of the tube and the front of the camera, and for the purpose of setting the moving solar image accurately on the camera front, and inserting the filter, it was much more convenient to leave this space open. The camera and lens were carefully squared on to each other in the workshop at Greenwich.

The prism mounting was of a simple altazimuth type. The 5 mm thick brass plate at the prism end of the bench was made the base-plate for a turn-table, and this carried the bearings of a horizontal axis, the gunmetal trunnions of which were integral with a stout gunmetal hoop which passed behind the prism and formed the basis of the actual prism holder (Fig. 2). The two axes of motion intersected in the centre of that reflecting face which was actually used; the other face, and the back, of the prism were disregarded, and most of the incident light passed through the prism and escaped in harmless directions. To hold the prism, two triangular plates of brass were cut to fit its ends; one was rigidly attached to the hoop, close to one trunnion, while the second was pressed against the second end of the prism by a fairly strong spring inside the second trunnion. Small leaf-springs, attached to the edges of the brass triangles, pressed lightly on very small areas of the prism faces, to keep the triangles in register with the prism ends. The prism was thus firmly held, while at the same time there was no danger of stresses due to differential expansion in hot sunlight.

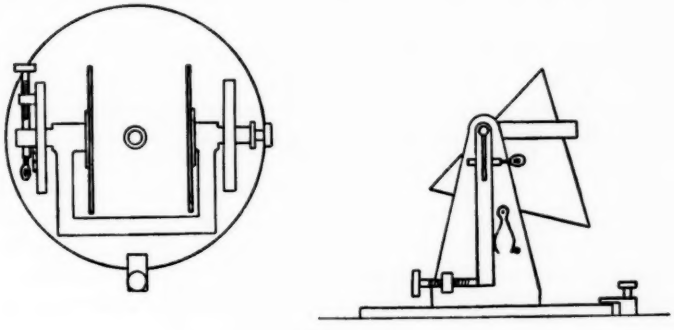

FIG. 2.

The turn-table could be clamped both by a stout nut on its centre bearing and by a rim clamp; it was not provided with any explicit slow motion, but its large diameter and smooth motion allowed it to be set very closely to any desired position. The hoop and trunnions could be clamped to a slow-motion arm controlled by a screw and a strong leaf-spring; this one possibility of slow motion was found to be enough even though the geometry was such that motion of the prism in either one of its coordinates separately caused a slanting movement of the image, and indeed even clamping the turn-table deflected it slightly. It was realized that an equatorial type of mounting would be more convenient, since the final adjustment could then be made in one coordinate only; but the extra complication could not be contemplated in the time available, and it was also feared that such an arrangement might be less rigid. Extreme stability, once the prism has been finally set for the eclipse run, is essential, and it is believed that this condition was well met.

Three cardboard stops were provided for the lens, with apertures $f/36$, $f/25$ and $f/18$; they could be slid into a sheet-metal mounting on the front of the cell, and as their outer faces were white the beam of light from the prism could readily be seen on them; as soon as this beam was adjusted to be central on the aperture, the image was normally picked up on the camera front.

As already explained (Paper I, p. 23), it was intended to arrange the camera so that the image should move parallel to the long edge of the frame, as a result of the diurnal motion. When the Sun transits south of the zenith, it is always possible (and often necessary) to arrange that the image shall approach the "window" from the right; the area to the right of the window was therefore painted white, and a horizontal line was drawn on it at the height of the frame centre, with short cross-lines at the positions where the "following" (unobscured) limb of the Sun should be at the last few whole and half minutes before switch-on time. The whole-minute marks were numbered, and the observer's task at the time of the eclipse was thus to adjust the prism so that the moving image was at the right height (as judged by the horizontal line), and with the east limb tangential to successive marks at the appropriate times; when he was satisfied, he would clamp the prism, check on another mark or two as the image moved past them, insert the green filter, and wait for switch-on time. The procedure was tried out at Greenwich, and the slight inconvenience due to the fact that any one adjustment of the prism made the image move obliquely was soon found to be insignificant.

In the field, the setting operation was rehearsed repeatedly, especially near the right time of day ($07^h 20^m$), and both observers soon found no difficulty in getting the image satisfactorily "on" during the early part of a run-up, and even in then deliberately throwing it off in both coordinates and re-setting at a later stage of the *same* run-up. The adjustment is not really very critical, since only the convenience and not the accuracy of the subsequent reductions depends on it; no error in height which leaves the image still fully within the frame will do any harm beyond introducing a slight slant into the diurnal direction, and a small longitudinal error will at worst also lose a short stretch at the start or finish, and not even that if it is known and allowed for by switching on a little late or early.

What naturally could not be tested in advance was the question whether the crescent would give any more trouble than the full disk. To guard against entire failure to find it, provision was made for approximate marking of the correct prism settings, in both coordinates, during final rehearsals. This precaution might have been found helpful if the eclipse weather had been poor, but in the actual eclipse conditions it proved entirely superfluous; the patch of light from the prism was still quite visible on the lens stop, and the crescent was sufficiently in focus on the camera front to lose no brilliance from this cause, so that setting the crescent was as easy as setting the full disk.

Even if, by mischance, the observer were single-handed at the time of the eclipse, so that during the last half hour he had to receive time signals, etc., as well as to set the prism, he would in general find it quite practicable to keep the image somewhere in view all the time, by making a quick readjustment of the prism every five or ten minutes; indeed, if the Sun is visible he will probably do this in any case, and will thus arrange that the image is already conveniently placed at the time (about six or seven minutes before mid-eclipse) when the final setting is due to be made.

Two complete sets of apparatus were made up on the above lines; Fig. 1 shows the smaller, in which the lens had a focal length of 935 mm. The second bench was longer, and carried a wider telescope tube, as the focal length of the lens was 1132 mm, but it was otherwise identical. Either bench could easily be carried and put in place on the pier by one man if necessary.

The benches were originally designed for use in a horizontal position, and they had been partly completed at Greenwich before it was found that in the actual circumstances of the Mombasa eclipse this position would result in a very large angle of incidence at the reflecting face, if the azimuth were so chosen that the diurnal motion of the image would be parallel to the long side of the frame. There were practical objections to laying the camera on its side, as well as some doubt how well the film would run then; but it appeared that the benches could be used, without alteration, in a slanting position, provided the piers were suitably constructed. A length of 5-cm angle-iron was therefore provided, and fitted with two rag-bolts, for grouting into the pier, and the side elevation of the pier as subsequently constructed at Mombasa is shown in Fig. 3, with this iron in position at A. In use, two small strips of lead were placed in the angle, so that the cross-member at the camera end of the bench would be supported only at two points near its ends, and a thin wedge of hardwood was placed under the lower

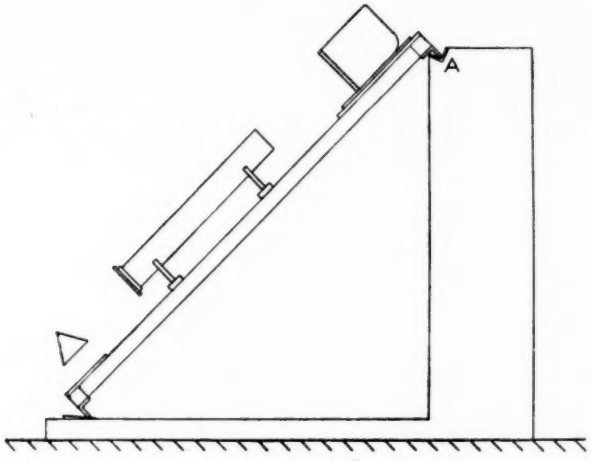

FIG. 3.

end of the bench and adjusted to give the exact tilt required. The result was a three-point support which appeared very stable. It was verified at Greenwich that the arrangement would permit a wide range of tilts, and it was computed (Paper I, p. 25) that at a tilt of 45° the angle of incidence would be reasonably small; a final decision as to the tilt (and the resulting azimuth) was left until the site should be selected.

2. *Electrical apparatus.*—For timing the exposures it was decided to use pen-recording tape chronographs, with one pen directly responding to the motion of the camera shutter, and one indicating the time. A plain rubbing contact was arranged, inside the camera, consisting of a light spring rubbing on the edge of a disk which was attached to a spindle rotating at the same speed as the shutter; 180° of the disk was metal and 180° an insulator, so that the periods of "make" and "break" were closely equal. The disk was phased so that contact was made when the shutter aperture was passing the middle of the frame, and the instant of this contact was taken to be the instant of exposure for the whole photograph. The shutter aperture used was the narrowest available, namely 10°, and the

exposure time was thus $1/(36f)$ if f was the number of frames per second. As f was about 18, this time was about $\frac{1}{650}$ sec; the total time required for the aperture to pass over all relevant parts of the frame was perhaps three times this, but this was still several times smaller than the uncertainty with which one could hope to determine the moment of mid-eclipse under the best possible conditions. It was verified that even in the most unfavourable case the diurnal motion itself caused a still smaller error; it will not displace one cusp with respect to the other by as much as 0'·1 of position angle, if the shutter opening passes over the whole crescent at the rate that was here involved.

Two new chronographs were specially made in the Observatory workshop at the Abinger station. They used modified telegraph relays which required a current of 12 milliamp, and the pens consisted of standard silver tubing of 0·5 mm external diameter and 0·2 mm bore, about 7 cm long in all, mounted on the armatures; a full response was obtained even with signals as short as 5 milliseconds. Ordinary Stephens' red ink, with the addition of a few drops of formalin and glycerin, was fed to the pens through PVC tubing. The phase difference between the two pens was adjustable by a screw, and to set this the standard Observatory practice was employed of feeding the same signal to both pens and adjusting until they indicated zero time difference. This adjustment was checked, as a routine, every time the chronograph was used for any purpose. The tape speed was 10 cm/sec, and times were nominally read to the nearest $\frac{1}{200}$ sec.

The simple rubbing contact was found more satisfactory than a cam-operated one which was first tried, and examination of the tapes showed that it was in fact very reliable. The actual motion of the pen was considerably more sluggish at the start of the "break" than at the start of the "make", but allowing for this the current was evidently flowing for half the time, pretty closely. A systematic delay of $\frac{1}{100}$ sec (which would not be serious) can hardly be present; if the "make" were always $\frac{1}{100}$ sec late, and the "break" were punctual (as it must have been, within very close limits), the time the current was on would be $\frac{\frac{1}{36}-\frac{1}{100}}{\frac{1}{36}+\frac{1}{100}}$ of the time it was off, i.e. the two times would be as 8:17; an error of this magnitude would be conspicuous. A lag in response of the pen itself, both on make and on break, is of course possible, but would be the same whether the signal came from the camera or the chronometer; as between the two pens, it would be taken up by the zero adjustment.

The second pen was arranged to record either radio time signals or seconds impulses from a contact chronometer, the intention being to use the direct signal if reception was good enough, and if not to turn over to the chronometer; the same pair of pens could then be used, before and after the eclipse, to compare the chronometer with those portions of the special eclipse signal, or of any other, which might be well enough received. Operation of the pens from the camera or chronometer contacts was by means of a simple battery circuit, with a condenser across the contacts to minimize sparking; operation from the radio receiver output involved the use of an amplifier, which was made in one unit with a noise suppressor and the necessary change-over switches, to enable either pen to be connected to the radio, the chronometer or the camera as desired. The principle of the unit was as follows.

The output of the radio receiver was a 1000-cycle tone, and this was fed directly to a resistance-capacitor and diode rectifying circuit, biased to cut off

all signals of less than 6 volts amplitude; this eliminated all atmospheric noise of moderate intensity. The output of this circuit was fed to the grid of a triode, which was again negatively biased to cut off at low amplitudes; it delivered about 12 milliamp (mean) d.c. when the voltage fed to the grid reached 9 volts, i.e. when the total signal strength was 15 volts or more. The impedance of this output circuit was different from that of the simple battery and contact ones, but it was calculated that the time constants, with the chronograph impedance included, differed by only a few milliseconds. Two complete chronographs were taken; in one the tape was driven by a 230-volt a.c. motor, and the other had an independent clockwork-driven tape-puller.

It was hoped that the Rugby 16 kc/s (GBR) signal would be receivable, but, as this was doubtful, preparations were also made for short-wave reception. The Post Office Engineering Branch selected MIK, 9725 kc/s, as the most suitable of the available short-wave transmitters, and agreed to transmit a signal from Greenwich, both on GBR and on MIK, continuously from 04^h05^m to 04^h35^m and from 05^h00^m to 05^h05^m U.T. on the morning of November 1, and also on the previous day for a final "dress rehearsal"; the present opportunity is taken of again acknowledging with thanks their willing cooperation in this respect. The time of mid-eclipse was about 04^h28^m, and the transmission periods were chosen so as to allow some freedom in tuning-up and recording the chronometer errors, as well as a later check on chronometer rates, in case a chronometer had to be used.

For short-wave reception a rhombic aerial having a major axis of 94·5 metres and a minor axis of 55 metres was arranged; the portable tubular wooden masts for this were the largest single item in the expedition's equipment. The long-wave receiver could be connected either to a frame aerial or to an inverted L erected across the minor axis of the rhombic aerial.

The camera motors required 24 volts d.c., and two 24-volt lead-acid accumulators were provided. There were also two small petrol-driven generators, each of which could deliver either 12 volts d.c., for charging, or 230 volts a.c., which could be used (if no mains supply was available) for radio receivers, chronograph motor, lighting, soldering, etc. Two vibrator-packs were taken, as a stand-by H.T. supply for the radios, in case the generators failed or were otherwise occupied.

Although the first shutter opening, at the start of the eclipse run, is unmistakably identifiable on the chronograph tape, so that the entire series (3000 or so) of contacts can be counted from this without ambiguity, the arrangement as described above does not provide any check on this count; there is, for example, no ready way of identifying on the tape the point where the film runs out, if, as was intended, this point is actually reached. Moreover, although the first exposure should also be identifiable on the film, it would not be so if the observer forgot to run off a few blank frames after loading the camera, to take up the loop which is normally fogged in loading; if that happened, there would thus be no zero for the timing system at all. It was therefore thought advisable to incorporate a positive checking device. The cameras had originally been designed for rough timing work, with an arrangement for projecting the dial and hands of a watch on to a small area at one corner of the picture. It was decided to use this projection system, without the watch, to project a small patch of light on the corner whenever a hand-operated shutter was open (keeping it normally closed), and to attach a contact to the mechanism of this shutter so that the camera pen

would throw during the time the shutter was open. This involved losing the contact times of those photographs which were taken during the operation, but the camera ran so uniformly that the times could be readily interpolated. The shutter was similar to those used in cheap box-cameras, and was arranged to open for about $\frac{1}{8}$ sec, so that only two or three contact times should ideally be lost each time. This shutter gave a little trouble in the field, as it sometimes stuck open; however, this was watched for on the tape, and a second operation freed it, still without any appreciable loss of contact times. At the eclipse itself, the observers did not in fact make an error, and the first frame of the eclipse run was clearly recognizable on the film; the identification marks, which were imprinted several times during the 3-minute run, were thus not required, but they checked with the counts from the first exposure.

Almost every item of equipment, except the masts for the rhombic aerial, was prepared in duplicate, and there was also a certain amount of camp gear (especially buckets, large bottles and an ice-box) and a full supply of tools, radio spares and workshop spares (bolts, shims, sheet-metal, iron strap, etc.). The complete equipment was packed in a "Container" 3·5 m × 2·0 m, 2·6 m high, of standard Admiralty pattern, which had windows and a door and could be used as an office and laboratory (and probably also as a darkroom if necessary) in the field. The container left England, by sea, on September 8, and the observers followed by air and arrived in Mombasa on October 5.

3. *Work at Mombasa.*—On arrival at Mombasa, contact was made with the Resident Naval Officer, Lt. Cdr. Johnson, who had been advised in advance and had undertaken to give any help in his power. His assistance, and the willing cooperation of his staff, were of the greatest value throughout all stages of the work. He reported that there was room for a site in the precincts of the Coast Defence Battery (King's African Rifles) which was on a level and commanding promontory within the area of the town itself, and that he understood the Commanding Officer, Major C. F. Rouse, was prepared to give permission for its use if it was considered suitable. The situation was ideal in every respect, except that it could not fully provide for the four radio masts in the necessary rhombic array; however, a survey with a prismatic compass and tape, before the arrival of the apparatus, showed that the rhomb could just be set up, with its long diagonal at a bearing of 323° (Rugby = 334° and Washington = 312°), if two of the masts were outside the precincts and if a rather long lead-in from the end of the long diagonal was accepted. There was an excellent site for the camera itself, with the container close by, on open ground about 40 metres from an abrupt drop to the sea; and the whole situation, including its obvious freedom from the risk of interference by man or beast, and the availability of mains a.c., was so suitable that no other site was considered. The two observers were thereupon very kindly offered living quarters on the premises, and were made temporary members of the Officers' Mess; the hospitality and kindness of all the officers of the station contributed greatly, both directly and indirectly, to the success of the undertaking.

On the arrival of the container, the R.N.O. arranged for its transport from ship to site, and provided a travelling crane to lift it from the lorry. It had suffered slight structural damage in transit, but none of the apparatus was affected, and it admirably fulfilled its intended purpose of serving as a laboratory and office. A more suitable darkroom was arranged in an ammunition cellar kindly provided

by the Commanding Officer, and a regular supply of ice made it possible to keep a stock of cold water, as well as of developing and fixing solutions, always on hand here, and also to store unused film properly.

An azimuth line was laid out without waiting for the masts, radio and chronometers to be brought into action, by utilizing the fact that at that latitude and season there were periods, about a couple of hours from sunrise and sunset, when the Sun's apparent motion was vertical, so that its azimuth was independent of the time. A tilt of 45° for the optical bench was definitely decided on, and a pier was laid out in the corresponding azimuth of about 224°. It was constructed of light coral blocks (the standard local building material) by a local stone-mason, and was rendered all over with cement after the angle-iron had been grouted in (Fig. 3). Since the final azimuth of the camera would be determined purely by the lie of this angle-iron, which was only about 45 cm long and somewhat difficult to set in any direction with precision, the height of the pier was made sufficient to permit a slightly steeper tilt than the intended 45°, to allow for final adjustment in tilt by means of the wedge, if the azimuth itself proved incorrect. After the cement had set, the camera assembly was placed in position on the pier, and the theodolite was sited 2 to 3 metres from the prism end and adjusted until it was in line with the lens centre and the centre of the camera frame; the azimuth of this line was determined, and was found to be about a degree off the intended value; a correction to the 45° tilt was then computed and the bench was always set at this corrected tilt by means of the wedge; the tilt was measured by a field clinometer which read to the nearest minute.

The above adjustments are considerably less easy and reliable than the ones which are possible when a horizontal camera position can be accepted; in that case, one can set up a theodolite (focused for infinity) so that it looks straight into the camera lens, and can sight directly on the centre of the frame, getting both the fore-and-aft tilt and the azimuth correct with high accuracy, even if the theodolite is slightly out of line with the bench; the cross tilt can also be adjusted with a carpenter's level. In the slanting position the theodolite must be placed very exactly in line with the lens cell and the camera front, and must be sighted on them alternately, both its focus and its dip being changed each time; the cross tilt of the camera cannot readily be checked at all. However, the subsequent measurement of the eclipse film showed that the correction applied to the tilt was sufficiently appropriate; the image of the Sun's south limb moved parallel to the long edge of the frame within about $\frac{1}{3}$ degree, which is a satisfactorily small slant.

While these adjustments were in progress the second observer (J. D. P.) erected the radio masts and the short-wave and long-wave antennae, charged the batteries, studied the quality of reception of the various signals, and rated the chronometers. It was found, as had been feared, that GBR was unsatisfactory; the noise level was such that one could just read morse, but could not record a signal clear of serious noise-interference. For satisfactory tape recording, with a relay which tends either to throw fully or not to respond at all, a high degree of freedom from noise is essential, and it was decided to rely on the short waves; suitable stations gave such clear signals that it seemed highly probable the camera could be recorded directly against the signal, when the time came, but of course chronometer rating was continued as well.

The question as to the best use, if any, to make of the nearly complete set of duplicate equipment which had been brought had been left open; but one

possibility had always been that if the weather seemed likely to involve broken cloud, two stations some miles apart would offer a better insurance than one station with double equipment. (As is, unfortunately, not uncommon, available meteorological reports made no distinction between a 50 per cent chance of a clear sky and a 100 per cent chance of 4/8 cloud, and the question could not be decided in England.) Even the local meteorological information was not very convincing, but the chance of broken cloud did on the whole seem very appreciable, and it was decided that two stations should be used if each observer could be provided with a suitable assistant. Fortunately, two members of R.N.O.'s staff, Mr J. E. Wheal and Mr C. G. Wragg, were anxious to help and appeared thoroughly competent to do so, and a second site was therefore looked for. A situation on the far side of the eclipse track would of course have provided an interesting check, if both stations had obtained good results; communications were, however, difficult and the two stations would have been practically isolated from each other. For a first attempt, the maximum chance of getting at least one satisfactory record was all that it seemed wise to aim for, and a site within easy reach was thought essential.

A very suitable one was found on the edge of the airfield at Port Reitz, about 10 km away, and the Officer Commanding kindly gave his permission for a pier to be erected there, close to a small hut, which he also placed at the expedition's disposal. A similar pier to that at Mombasa, but somewhat larger so as to accommodate the larger bench, was therefore erected here, in the appropriate azimuth, and a small aerial was run up to an existing mast; a few days before the eclipse all the necessary equipment, including one set of batteries and one generator, was brought to this station and placed in the hut. Focus tests were repeated (the films being developed at the main station) and all apparatus was wired up and rehearsed. The observer (R. d'E. A.) did not remain at Port Reitz overnight, but returned to Mombasa each time, carrying the chronometer with him, and chronometer errors were constantly determined as before.

The one important item which could not be duplicated at any second station was the rhombic aerial, and there was thus little hope that Greenwich signals could be recorded at Port Reitz with satisfactory clearness. The chronometer did not show serious discontinuities as a result of its trips over a road which was rough in places, but it was decided to arrange a radio check on it in the following manner. The local Cable and Wireless station was approached, and agreed to broadcast some ordinary morse signals for half an hour or so at the time of the eclipse; at pre-arranged times, the Mombasa eclipse station was to receive these against MIK, while the Port Reitz station received them against its chronometer. During the actual eclipse run, the Port Reitz station would record the camera against its chronometer, and these chronometer times could thus be tied to MIK by means of the local signal, both before and after. The necessary suppressor-amplifier unit for the Port Reitz station was constructed by J. D. P. in the field.

In addition to rehearsals to familiarize the observers with the procedure, a number of trial runs were taken with live film to determine the focus settings, the rheostat settings for the camera motors, and the stops and filters for various states of the sky, as well as to check that the minute-marks on the camera had been correctly placed, and that the computed azimuth was going to be correct. This latter point was verified by noting the time of day when the image ran horizontally, comparing the times for different days, and extrapolating to the eclipse date. Much of this work had naturally to be done with the Sun at approximately the

right elevation (20°–25°), and its heating effect was then not very great; nevertheless a light shield was constructed for each camera, of sheet metal and strap iron, to keep direct sunlight from the bench, camera, and lens. The prism was often exposed to sunlight for some time before a run began. Focus tests during the heat of the day did not show any systematic difference from the others, except of course that whenever the second filter was used the setting had to be increased by about half the filter thickness. At the eclipse itself, one filter and a stop of *f* 25 were expected to be satisfactory, and in fact were so.

Some trouble was experienced in developing the test films; even the cellar was fairly hot, and reticulation almost always appeared. Various temperatures for the developer, washing water, and fixing bath were tried, but all had necessarily to be considerably cooler than the air to which the wet film was intermittently exposed in processing, and no satisfactory arrangement was ever found. However, this did not prevent a reliable estimate of the best focus, still less of the best stop and filter combination, and it had never been intended to develop the eclipse films themselves before returning to England.

On October 31 a full dress rehearsal, with complete rolls of film, was run through at the proper time; there was some cloud, but it did not actually interfere with the programme. The developed films appeared satisfactory. On November 1 there was a heavy thunder-shower at the Port Reitz station until about $04^{h}00^{m}$ U.T., but the observers (R. d'E. A., assisted by Mr Wheal) were then able to set the bench in position and proceed in general as planned; one chronograph pen clogged up ten minutes before switch-on time, but this was successfully cleared and reconnected before the final prism setting was due. The image was correctly located and the camera switched on at the intended time. The camera speed was nearly correct and the film ran out at approximately the intended time. The chronograph record was satisfactory, except for sticking of the hand-operated shutter when this was used. The local station was audible, but was not successfully recorded on the tape. On developing the film in England it was found that the images were correctly placed, and fully exposed, with the background completely clear, but quite unexpectedly they were double, and the film was not considered worth measuring. The doubling was not of the kind sometimes seen with a badly wrong focus setting, but was always in the direction of motion of the film, and is thought to have been caused by a phasing fault in the camera. This was not observed in rehearsals, but it was subsequently verified that it was in all cases nearly possible; the widest shutter opening for which the mechanism was designed was 180°, and the pressure plate released for nearly all of the remaining 180°, so that a 10° exposure took place before the pressure plate had fully locked the film in place.

At the Mombasa station (J. D. P., assisted by Mr Wragg) the programme ran without any mishap. The images were correctly located, and the camera was switched on at the correct time; it ran slightly fast, so that the film ran out after 172 seconds instead of 190 as planned, but the loss due to this is hardly significant since the stretch that was observed was observed with correspondingly increased weight. The chronograph record was satisfactory, and the direct radio signals were clearly recorded with only a very occasional disturbance due to atmospherics. On developing the film in England it was found to be very satisfactory, with well-defined images throughout; although the crescent is only 9 mm long, a considerable amount of obviously real detail appears at the cusps when they reach mountains on

the lunar limb. A selection of 6 of the 3 100 pictures is shown in Plate 10, with the approximate U.T. of each. There was, as had been expected, no trace of general sky fog and thus no indication at all where the edge of the frame had been (except when the identification mark was imprinted near one corner), and the direction of diurnal motion had therefore to be obtained with reference to the line joining two of the perforations; it was, as stated above, within about $\frac{1}{3}$ degree of being parallel to this line. It is evident from Plate 10 that the south (right-hand) limb of the Sun was unobscured throughout, and that a very large swing in position angle was obtained. There was a trace of haze near one cusp in the early part of the run; it may be seen on the first exposure of Plate 10, but it did not seem ever to get very close to the cusp.

The analysis of the results has been completed, and will appear in a later paper.

Royal Observatory,
Greenwich, S.E.10:
1953 *July* 15.

Royal Greenwich Observatory,
Abinger Common,
Surrey.

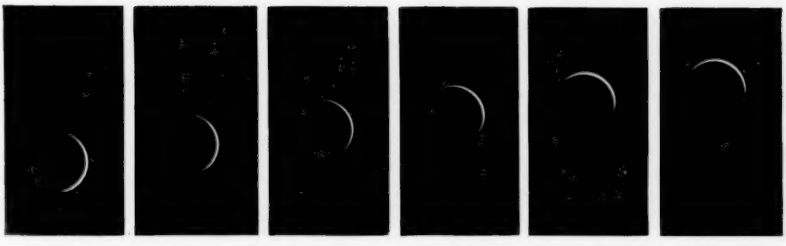

04 : 26 : 20 04 : 26 : 54 04 : 27 : 28 04 : 28 : 02 04 : 28 : 36 04 : 29 : 10

(Approximate U.T. instants of exposure.)
There are about 620 exposures between each of these six and the next.

ON THE MAGNETIC OSCILLATIONS OF A GRAVITATING LIQUID STAR

C. Plumpton and V. C. A. Ferraro

(Received 1953 August 21)*

Summary

The oscillations of a gravitating liquid star in the presence of a central magnetic pole are considered, and it is shown that the reduction in the periods of the various modes of oscillation derived in an earlier paper, in which gravitational forces were neglected, is not as great as was expected.

The results are discussed in relation to the oscillation theory of magnetic variable stars.

1. *Introduction.*—The problem of the oscillations of a conducting spherical mass of gas in the presence of a permanent magnetic field is of interest in connection with the variable magnetic fields of stars such as HD 125248. Several attempts have been made to discuss its solution, but so far a number of simplifying assumptions have had to be made to render the problem tractable. Schwarzschild (**1**) considered the *small* oscillations of a star, the material of which was supposed infinitely conducting and incompressible, in the presence of a uniform magnetic field. He did not take into account the gravitational forces arising during the oscillations. Ferraro and Memory (**2**) made the same assumptions as Schwarzschild except that they took explicit account of the increase of the magnetic field with depth. Miss Gjellestad (**3**) in an earlier incomplete investigation first took account of the gravitational forces, and Cowling (**4**) gave a more detailed discussion of the problem in which he took account not only of the gravitational and electromagnetic forces, but also of the compressibility of the stellar gas.

Cowling showed that in problems of astrophysical interest the gravitational restoring forces far exceed the electromagnetic forces, *except* when the oscillations are mainly horizontal. In an earlier investigation (**5**) Cowling had demonstrated the existence of *gravitational* oscillations of this type but in (**4**) he points out that they do not cover all possible oscillations. He drew attention to the fact that such a solution as he considered could not be fitted to the boundary of the star so as to ensure the continuity of the magnetic field there, and on this account his subsequent discussion of the problem is, to some extent, incomplete.

In this paper, which is a sequel to (**2**), we firstly draw attention to the fact that the *nature* of the oscillations of a magnetic star depends essentially on the form of the permanent stellar magnetic field. Secondly we show that for a uniform liquid star, magnetic oscillations exist in which the motion is very nearly horizontal and in which the function of the gravitational forces is merely to suppress the radial oscillations of the star. Thirdly it is shown that the neglect of the gravitational forces in (**2**) is not as important as might have been expected.

2. *Small oscillations of a magnetic liquid star.*—As is legitimate in this case, we shall assume the conductivity of the material to be infinite, so that, if **E** and **H**

* Received in original form 1953 June 11.

denote the electric and magnetic fields at any point and $\mathbf{v}$ the velocity of the gas, we have very nearly

$$\mathbf{E} = -\mathbf{v} \wedge \mathbf{H}, \tag{1}$$

where electromagnetic units are used. Maxwell's second circuital relation then gives

$$\frac{\partial \mathbf{H}}{\partial t} = \operatorname{curl}(\mathbf{v} \wedge \mathbf{H}). \tag{2}$$

Let $\mathbf{H}_0$ denote the permanent stellar magnetic field and $\mathbf{h}$ the small variations from this during the oscillations of the star, so that $\mathbf{H} = \mathbf{H}_0 + \mathbf{h}$; let $\boldsymbol{\xi}$ denote the displacement of an element of the liquid from its equilibrium position, so that $\mathbf{v} = \partial \boldsymbol{\xi}/\partial t$. Then, following Cowling (**4**), we can integrate (2) to give

$$\mathbf{h} = \operatorname{curl}(\boldsymbol{\xi} \wedge \mathbf{H}_0) \tag{3}$$

to the first order of small quantities.

The equation of motion of an element of the liquid is

$$\frac{d\mathbf{v}}{dt} = \frac{1}{\rho}\mathbf{j} \wedge \mathbf{H} - \operatorname{grad}\left(\frac{p}{\rho} + \Omega\right), \tag{4}$$

where p is the pressure and ρ the density, Ω is the gravitational potential and $\mathbf{j}$ the electric current, given by

$$\operatorname{curl} \mathbf{H} = 4\pi\mathbf{j};$$

or, if the permanent field $\mathbf{H}_0$ is derived from a potential function, by

$$\operatorname{curl} \mathbf{h} = 4\pi\mathbf{j}. \tag{5}$$

Eliminating the last term in (4) and using (5) we find, to the first order of small quantities,

$$\frac{\partial \operatorname{curl} \mathbf{v}}{\partial t} = \operatorname{curl}\left\{\frac{1}{4\pi\rho}[(\operatorname{curl} \mathbf{h}) \wedge \mathbf{H}_0]\right\}.$$

Use of (3) and $\mathbf{v} = \partial \boldsymbol{\xi}/\partial t$ leads finally to the following equation for the displacement:

$$4\pi \operatorname{curl} \frac{\partial^2 \boldsymbol{\xi}}{\partial t^2} = \operatorname{curl}\{[\operatorname{curl} \operatorname{curl}(\boldsymbol{\xi} \wedge \mathbf{H}_0)] \wedge \mathbf{H}_0/\rho\}. \tag{6}$$

Thus, the nature of the solution depends essentially on the form of the permanent field $\mathbf{H}_0$.

3. *Solution for a liquid star.*—The equation of continuity requires further that

$$\operatorname{div} \mathbf{v} = 0$$

or

$$\operatorname{div} \boldsymbol{\xi} = 0. \tag{7}$$

Assuming further that the motion is confined to meridian planes and that the permanent field is due to a central magnetic pole of strength m, the solution proceeds much as in (**2**). Thus, (7) implies the existence of a stream function ψ such that the radial and transverse resolutes are respectively given by

$$\xi_r = -\frac{1}{r^2 \sin\theta}\frac{\partial \psi}{\partial \theta}, \quad \xi_\theta = \frac{1}{r \sin\theta}\frac{\partial \psi}{\partial r}, \tag{8}$$

where (r, θ, ϕ) are spherical polar coordinates with origin at the centre of the sphere. Likewise, the equation

$$\operatorname{div} \mathbf{h} = 0$$

implies the existence of a stream function u such that the radial and transverse resolutes of the magnetic field variations are given by

$$h_r = -\frac{1}{r^2 \sin\theta}\frac{\partial u}{\partial \theta}, \quad h_\theta = \frac{1}{r\sin\theta}\frac{\partial u}{\partial r}. \tag{9}$$

If the period of oscillation is $2\pi/\lambda$, the equation for ψ is, from (6), or from (23) of (**2**),

$$-4\pi\rho\lambda^2\psi = m^2\frac{\partial}{\partial r}\left\{\frac{1}{r^2}\Delta\left(\frac{1}{r^2}\frac{\partial\psi}{\partial r}\right)\right\}, \tag{10}$$

where

$$\Delta = \frac{\partial^2}{\partial r^2} + \frac{(1-\mu^2)}{r^2}\frac{\partial^2}{\partial\mu^2}, \tag{11}$$

and $\mu = \cos\theta$. The magnetic field variations are then obtained from the function u, where

$$i\lambda u = (m/r^2)\frac{\partial\psi}{\partial r}. \tag{12}$$

We can reduce (10) to a non-dimensional form by writing

$$r = \eta x, \quad \eta^6 = m^2/(4\pi\rho\lambda^2); \tag{13}$$

the solution of the resulting equation, which need not be given here, is then (*cf.* Section 8 of (**2**))

$$\psi = \frac{i}{\lambda a^2}\sum_1^\infty (1-\mu^2)^{1\,2} F_n(x) P_n^{\,1}(\mu), \tag{14}$$

where

$$F_n(x) = AF_n^{(1)}(x) + BF_n^{(2)}(x), \tag{15}$$

A, B are arbitrary constants, and the functions $F_n^{(1)}$, $F_n^{(2)}$ are given by (49) of (**2**). The factor $i/\lambda a^2$ is introduced in (14) to make F_n identical with its definition in (**2**).

4. *The variations of the gravitational potential.*—The gravitational potential of a nearly spherical homogeneous liquid whose surface is of the form

$$r = a(1 + \Sigma\epsilon_n P_n(\mu)), \tag{16}$$

in which ϵ_n is small, is given (**6**) approximately by

$$\Omega = -\frac{4\pi G\rho a^3}{3}\left(\frac{3a^2 - r^2}{2a^3} + \Sigma\frac{3r^n\epsilon_n P_n}{(2n+1)a^{n+1}}\right),$$

where G is the constant of gravitation. At the surface this becomes

$$\Omega = -\frac{4\pi G\rho a^2}{3}\left(1 - 2\Sigma\frac{(n-1)\epsilon_n P_n}{(2n+1)}\right),$$

so that the variation of Ω from its equilibrium value $-4\pi G\rho a^2/3$ is

$$\Omega' = \frac{8\pi G\rho a^2}{3}\Sigma\frac{(n-1)\epsilon_n P_n}{(2n+1)}. \tag{17}$$

By (8),

$$\xi_r = -\frac{1}{r^2\sin\theta}\frac{\partial\psi}{\partial\theta} = \frac{1}{r^2}\frac{\partial\psi}{\partial\mu};$$

hence, by (14), at the surface its value is

$$(\xi_r)_s = \left(\frac{i}{\lambda a^2}\right)\Sigma n(n+1)F_n(x_1)P_n(\mu), \tag{18}$$

where $x=x_1$ is the equation of the surface of the star in equilibrium. But $(\xi_r)_s=r-a$, where a is the equilibrium radius of the star; whence

$$\epsilon_n=\{in(n+1)F_n(x_1)\}/(\lambda a^3). \tag{19}$$

Substituting in (17) we find finally

$$\Omega'=\frac{8\pi G\rho i}{3a\lambda}\Sigma\frac{(n-1)n(n+1)}{(2n+1)}F_n(x_1)P_n(\mu). \tag{20}$$

5. *The pressure variations.*—The pressure variation p' from the equilibrium pressure can be determined by replacing p' by $p'+\rho\Omega'$ in (46) of (**2**); using (20) this gives

$$p'=\sum_1^\infty\left\{\left[\frac{i\rho\lambda}{\eta}G_n(x_1)-\frac{8\pi G\rho^2 i}{3\lambda a}\frac{(n-1)n(n+1)}{2n+1}F_n(x_1)\right]P_n(\mu)\right\}, \tag{21}$$

where

$$G_n(x)=AG_n^{(1)}+BG_n^{(2)},$$

in which A and B are the same as the constants entering in (15) and $G_n^{(1)}$ and $G_n^{(2)}$ are given by (50) of (**2**).

6. *The period equation.*—The boundary conditions to be satisfied are that at the surface of the star, $x=x_1$, $p'=0$, and that the magnetic field should be continuous in crossing the surface. The first gives, using (21),

$$G_n(x_1)=\frac{8\pi G\rho\eta}{3(2n+1)\lambda^2 a}(n-1)n(n+1)F_n(x_1),$$

which may be expressed in the form

$$G_n(x_1)=K(n-1)n(n+1)F_n(x_1)/(2n+1)x_1^7 \tag{22}$$

by using the relation (58) of (**2**), namely $\lambda=(H_s/a)(x_1^6/4\pi\rho)^{1/2}$, and writing

$$K=\frac{32\pi^2G\rho^2a^2}{3H_s^2}. \tag{23}$$

The continuity of the magnetic field leads to the same condition as in (**2**), namely,

$$H_n(x_1)=0, \tag{24}$$

where

$$H_n(x_1)=AH_n^{(1)}(x_1)+BH_n^{(2)}(x_1)$$

and $H_n^{(1)}$, $H_n^{(2)}$ are defined by (56) of (**2**). Elimination of the ratio A/B from (22) and (24) gives the period equation

$$G_n^{(1)}(x_1)H_n^{(2)}(x_1)-G_n^{(2)}(x_1)H_n^{(1)}(x_1)$$
$$=\frac{K(n-1)n(n+1)}{(2n+1)x_1^7}[F_n^{(1)}(x_1)H_n^{(2)}(x_1)-F_n^{(2)}(x_1)H_n^{(1)}(x_1)]; \tag{25}$$

and the period is $2\pi/\lambda$, where

$$\lambda=\frac{H_s}{a}\left(\frac{x_1^6}{4\pi\rho}\right)^{1/2}.$$

7. *The first harmonic* ($n=1$).—In this case the second term in (25) vanishes identically, so that the periods are the same as found by Ferraro and Memory in (**2**). This result was to be expected since when $n=1$ the equation for the surface represents a sphere shifted bodily by the amount $a\epsilon_1$ in the direction of the axis $\theta=0$. Thus no gravitational forces are brought into play.

8. ***The second harmonic*** ($n=2$).—The nature of the roots of (25) depends on the magnitude of the numerical constant K given by (23), and so on the relative magnitude of the magnetic and gravitational restoring forces. For Babcock's star, in which $H_s \sim 10^4$ gauss, $\rho \sim 1$, $a \sim 1{\cdot}6R_\odot$ ($R_\odot$ = radius of the Sun), we find $K \sim 10^9$. Thus, unless x_1^7 is comparable with K, the roots of (25) will be approximately given by those of

$$F_2^{(1)}H_2^{(2)} - F_2^{(2)}H_2^{(1)} = 0 \qquad (26)$$

provided such roots exist. We find that the first root of (26) is very nearly $x_1 = 2{\cdot}4$, so that $x_1^7/K \sim 5 \times 10^{-7}$ and very small. Thus the approximation made in deriving (26) is valid; moreover the absence of the gravitational constant G in this equation shows that the oscillations are essentially magnetic.

From (22) we see that $F_2(x_1) \sim 0$, and hence that ψ and ξ_r both vanish to a high degree of approximation at the surface. Thus, the surface of the star is very nearly a stream surface and the motion is horizontal there. The equation of the stream lines for the fundamental mode is

$$\{F_2^{(1)}(x) - 0{\cdot}38F_2^{(2)}(x)\}\sin^2\theta\cos\theta = \text{const.},$$

very nearly, and the stream lines are as shown in Fig. 1. The position of the stagnation points is given by the condition $\xi_r = 0 = \xi_\theta$. But by (8) and (14)

$$\xi_r \propto (3\mu^2 - 1)F_2(x) \quad \text{and} \quad \xi_\theta \propto \mu(1-\mu^2)^{1/2}F'_2(x),$$

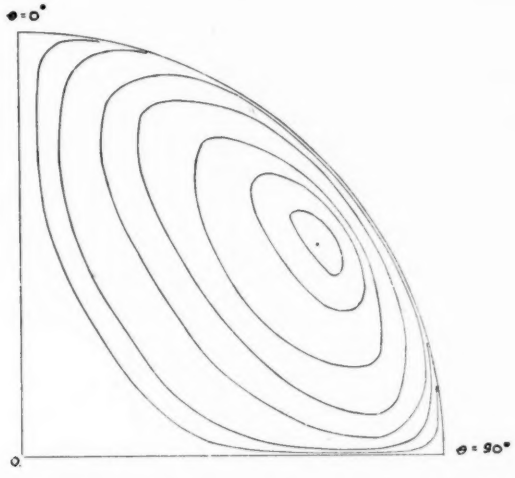

FIG. 1.—*Stream lines for the fundamental mode of the second harmonic vibration (only one quadrant in a meridian plane is shown.)*

so that its position is given by the first root of

$$F'_2(x) = 0 \quad \text{and} \quad \mu = 1/\sqrt{3}.$$

This gives, very nearly, $x = 2{\cdot}05$, $\theta = 54^\circ 42'$. Thus, the stagnation points lie fairly close to the surface, as might have been expected.

9. ***Discussion.***—The fundamental mode of the second harmonic corresponds to a period of oscillation of about 280 days, as against 890 days found by Ferraro and Memory (**2**). Whilst this period is very nearly three times smaller it is

clear that no great reduction in the period is to be expected by allowing for mechanical forces. This result may seem at first surprising since, as Cowling points out in (**4**), mechanical forces tend to produce rapid oscillations. The explanation of the paradox in this case is to be sought in the fact that if we consider the magnetic field variations of a star as due to forced oscillations excited by mechanical vibrations, it may not be possible to have continuity of the magnetic field at the surface. In this case finite forces would arise at the surface due to the action of the magnetic field on the current sheet—a point to which Cowling has himself drawn attention. The oscillations are therefore essentially of magnetic type.

This makes it clear that we can neglect neither the gravitational nor the magnetic restoring forces, especially as the nature of the oscillations is determined by the permanent stellar magnetic field.

Whilst the difficulty of obtaining a smaller period (of the order of 9 days, as required by observations of Babcock's star) remains, it must be remembered that we have here considered a very specialized model. It remains to be seen whether better agreement can be reached when the hypothesis of incompressibility is removed. We hope to consider this problem in a later communication.

Queen Mary College,
London, E.1:
1953 *August* 20.

References

(**1**) M. Schwarzschild, *Ann. d'Astrophys.*, **12**, 148, 1949.
(**2**) V. C. A. Ferraro and D. J. Memory, *M.N.*, **112**, 361, 1952.
(**3**) Miss G. Gjellestad, Rep. No. 1, 1st Th. Astrophys., Oslo, 1950.
(**4**) T. G. Cowling, *M.N.*, **112**, 527, 1952.
(**5**) T. G. Cowling, *M.N.*, **101**, 367, 1941.
(**6**) H. Jeffreys, *The Earth*, 3rd edn., p. 137, Cambridge, 1952.

SOLAR RADIO EMISSIONS AT 4-METRES WAVE-LENGTH DURING 1947–50 INCLUSIVE AND THEIR RELATION TO SOLAR ACTIVITY*

J. S. Hey

Summary

Bursts at 4·1 metres wave-length of solar radio emission of duration exceeding $\frac{1}{4}$ minute and intensity greater than 2×10^{-21} watt m^{-2} $(c/s)^{-1}$ are analysed with respect to solar flares in order to determine (1) time differences between flares and radio bursts and (2) the distribution on the solar disk of flares with associated radio bursts.

There is a tendency for the onsets of the bursts to lag behind the onsets of the flares; the records of radio intensity, with rapid and spasmodic fluctuations in amplitude, make it difficult to determine onset precisely, but the median lag of bursts behind the flares is about a minute or two. The median lag of the maxima of the bursts behind the flares is also about a minute. It is pointed out, however, that both for onsets and maxima the dispersion of the distribution of time differences between flares and bursts is such that a very appreciable proportion of the radio bursts precede the flares. The analysis of time differences is extended to ionospheric phenomena associated with flares. The distributions all show considerable dispersion, and it appears that there are secondary controlling factors both in the solar phenomena and in the ionosphere with varying influence on any individual occurrence.

The analysis of the occurrence of radio bursts with respect to solar longitude from central meridian helps to confirm the previous tentative conclusion that there is a greater chance of radio bursts in association with flares on the eastern half of the visible solar disk than for flares on the western half. The asymmetry occurs in the observations for each year and the statistical significance becomes increasingly evident.

* The full text of this paper is published in *Report No.* 372, *R.R.D.E.* (*now R.R.E.*), Ministry of Supply, Malvern, Worcs.: 1952 October. Acknowledgment is made to Chief Scientist, Ministry of Supply, for permission to publish this summary.

CONTENTS

PAGE

Meeting of 1953 May 8:
Fellows elected ... 527
Presents announced ... 527

Additional Meeting of 1953 July 22:
Acknowledgments ... 528
Presents announced ... 528
Associated meetings ... 528

Meeting of 1953 October 9:
Death of Dr Edwin Hubble ... 529
Fellows elected ... 529
Presents announced ... 529

C. S. Beals and J. B. Oke, On the relation between distance and intensity for interstellar calcium and sodium lines ... 530

D. G. Ewart, The constants of the velocity ellipsoid from the radial velocities of 820 stars ... 553

R. Wilson, The ionized helium series originating from the fifth quantum level ... 557

P. Swings, A. McKellar and K. N. Rao, Spectra of the late N-type stars in the ultra-violet, violet and blue-green regions ... 571

J. H. Piddington and R. D. Davies, Thermal radio emission from the Sun and the source of coronal heating ... 582

P. A. O'Brien, The distribution of radiation across the solar disk at metre wavelengths ... 597

T. D. Kinman, Motions in the Sun at the photospheric level. III. The Evershed effect in sunspots of different sizes ... 613

R. d'E. Atkinson and J. D. Pope, Cinematography of partial solar eclipses. II. Observations at the eclipse of 1948 November 1 ... 635

C. Plumpton and V. C. A. Ferraro, On the magnetic oscillations of a gravitating liquid star ... 647

Summary of paper in *Report No.* 372, *R.R.D.E.* (*now R.R.E.*), Ministry of Supply, Malvern, Worcs., 1952 October:

J. S. Hey, Solar radio emissions at 4-metres wave-length during 1947–50 inclusive and their relation to solar activity ... 653

Printed in London by Taylor & Francis, Ltd., 1954 May